ALMA MATER STUDIORUM
UNIVERSITÀ DI BOLOGNA

DOTTORATO DI RICERCA IN

SCIENZE BIOTECNOLOGICHE, BIOCOMPUTAZIONALI, FARMACEUTICHE E FARMACOLOGICHE

Ciclo 36

Settore Concorsuale: 03/D2 - TECNOLOGIA, SOCIOECONOMIA E NORMATIVA DEI MEDICINALI

Settore Scientifico Disciplinare: CHIM/09 - FARMACEUTICO TECNOLOGICO APPLICATIVO

ALTERNATIVE STRATEGIES TO IMPROVE INTRANASAL AND NOSE-TO-BRAIN DRUG DELIVERY

Presentata da: Elisa Corazza

Coordinatore Dottorato

Maria Laura Bolognesi

Supervisore

Barbara Luppi

Esame finale anno 2024

Abstract

The nasal route is an appealing option for drug administration due to features like increased patient compliance, avoidance of the first-pass effect, fast onset of action, and direct access to the central nervous system. Despite advantages, challenges include limited nasal tissue surface, mucus and epithelial barriers, as well as mucociliary clearance. This Ph.D. project aimed to overcome these shortcomings by investigating strategies capable of enhancing drug permeation through the nasal mucosa. Two main approaches were considered. One method involved adding molecular enhancers to increase membrane apparent permeability, specifically highlighting postbiotics as potential natural and eco-friendly excipients for nasal drug delivery. The other approach intended to counter mucociliary clearance using mucoadhesive agents and “smart” polymers, thus extending the residence time and favoring complete drug absorption. Parallel to this, the usefulness and applicability of different *in vitro* tools in the pre-clinical assessment of drug permeability were considered. Great attention was paid to the ready-to-use PermeaPad® biomimetic membrane, which was implemented with a layer of reconstituted mucin to mimic the composition of the nasal mucosa. This membrane was employed, together with tissue-based models and a primary cell-based system, to establish the ability and the mechanism of diffusion improvement by liquid and semisolid formulations.

Keywords

Nasal route; Permeation; Molecular enhancer; Postbiotic; Mucoadhesion; *In vitro* model

Table of contents

Table of contents

Table of contents

Table of contents

PART I: INTRODUCTION

1. Anatomy and physiology of the human nasal cavity

Due to its structure and anatomical features, the nose is the organ dedicated to air filtration, humidification, and temperature control, together with olfaction [1]. Specifically, the human nasal cavity covers a surface area of 160 cm^2, it extends from the nostrils, at the anterior opening, to the nasopharynx backward, for a length of 120-140 mm [2,3]. Its total volume is about 15-20 mL and is symmetrically divided into two chambers by the nasal septum [4,5]. The lumen of each nasal passage is characterized by a continuous mucus layer that lies upon a vascularized and innervated mucous membrane of 0.3 – 5 mm thickness, which features a layered architecture: the nasal epithelium on the surface facing the lumen of the nasal cavity, and the underlying lamina propria [3,6]. Function, cell types, as well as the degree of vascularization and innervation, depend on the region of the nasal passage considered: nasal vestibule, respiratory region, or olfactory region (**Figure PI 1.1**) [6].

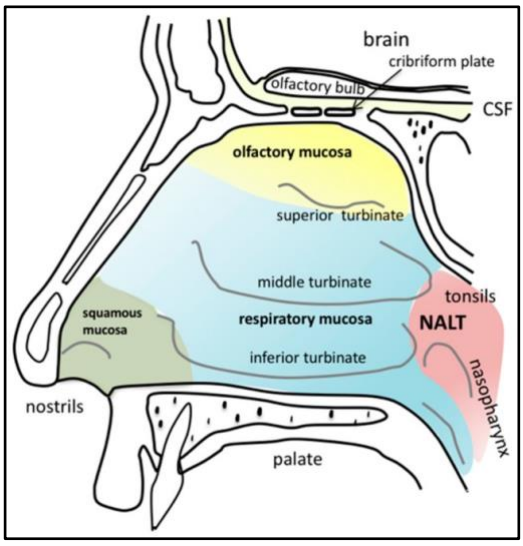

Figure PI 1.1 Anatomy of the human nasal cavity: main nasal regions and their covering epithelium. From S. Gänger *et al.*, 2018 [8].

1.1. Nasal vestibule

The vestibule is the first region the air encounters once inhaled and is limited to the small dilatation (0.6 cm^2) immediately inside the nostrils before the main chamber [4,6,7]. Its first-line protective function against potentially harmful atmospheric agents is due to the presence of a stratified squamous epithelium, which is similar to that of the skin but less keratinized (**Figure PI 1.2**) [4,6–8]. Indeed, the basal cells located in the lamina propria are covered by several layers of squamous cells, that became flatter and flatter by getting closer

to the luminal surface [6]. Moreover, at this site, the membrane is just slightly vascularized and contains nasal hairs, sweat, and sebaceous glands [6–9].

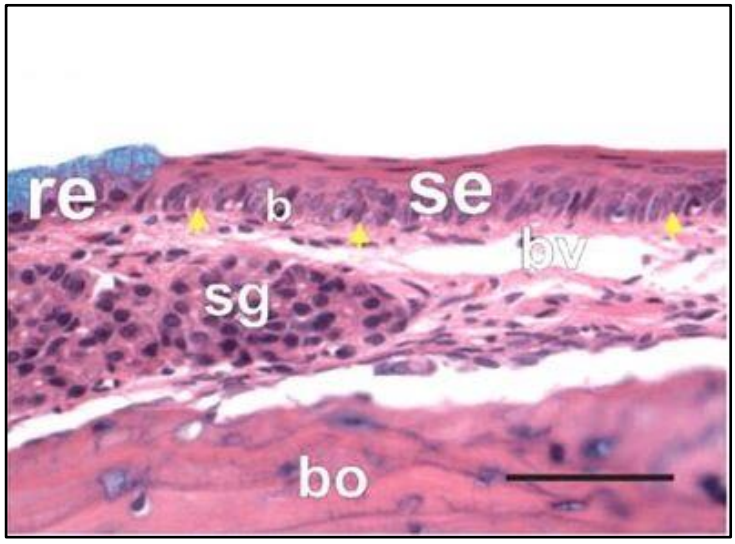

Figure PI 1.2 The stratified squamous epithelium (se). Tissue section stained with hematoxylin-eosin and alcian blue (barr dimension 50 µm). Abbreviations: respiratory epithelium (re), basal cells (b), subepithelial glands (sg), blood vessels (bv), bone (bo). The limit between the surface epithelium and the lamina propria underneath is highlighted by the yellow arrowheads. From J.R. Harkema *et al.*, 2006 [6].

1.2. Respiratory region

Moving backward to the nasopharynx, a narrow area lined by a transitional epithelium, that is made of non-ciliated columnar cells possessing microvilli and basal cells, defines the limit between the nasal vestibule and the respiratory area [6]. This is the largest nasal region (130 cm^2) accounting for 80-90% of the total surface and is specifically restricted to the lateral walls of the nasal cavity, and the three projecting nasal turbinates: inferior, middle, and superior [4,7]. The mucous membrane of this area consists of a ciliated respiratory epithelium containing different cell types (**Figure PI 1.3**): goblet cells, ciliated cells, intermediate cells, basal cells, serous glands, seromucous glands, and interepithelial glands [4,8]. Basal cells serve as progenitors for the columnar ciliated cells that make up the respiratory epithelium, while seromucous glands together with goblet cells are responsible for the production and release of both nasal secretions and mucus [8]. Concerning blood supply and neural innervation, the respiratory region is highly vascularized by branches of the ophthalmic and maxillary arteries and is innervated by the trigeminal nerve [7]. The anatomical architecture of the respiratory region reflects the main functions that are exerted here, that is, warming and filtering the inhaled air [8]. In fact, within the respiratory region, the air's low flow rate coupled with its turbulent movement determined by the turbinates'

shape get it closer to the vascularized walls promoting its warming and humidification [4,10]. Furthermore, inhaled particles (dust, pollutants, microorganisms) with 5-10 μm diameter deposit on the mucus and are entrapped in the viscoelastic gel, which is propelled by the cilia toward the nasopharynx to be eliminated through the digestive tract [11].

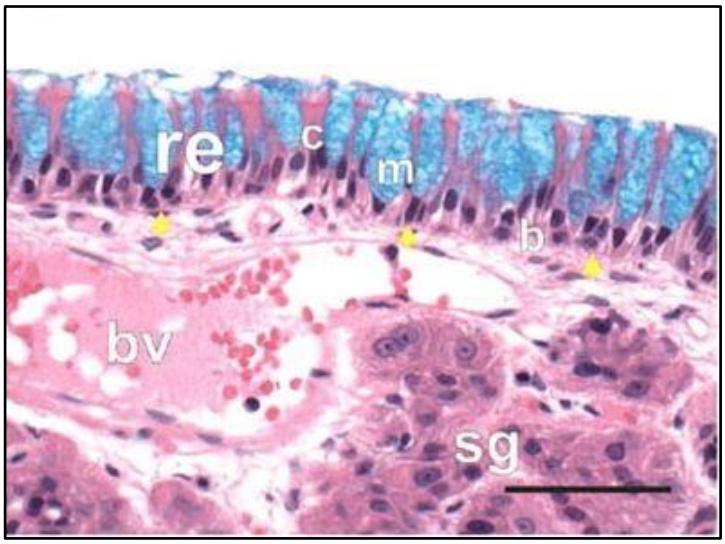

Figure PI 1.3 The respiratory epithelium (re). Tissue section stained with hematoxilyn-eosin and alcian blue (barr dimension 50 μm). Abbreviations: columnar ciliated cells (c), goblet mucous cells (m), basal cells (b), subepithelial glands (sg), blood vessels (bv). The limit between the surface epithelium and the lamina propria underneath is highlighted by the yellow arrowheads. From J.R. Harkema *et al.*, 2006 [6].

1.3. Olfactory region

The apical section of the nasal cavity, which accounts for almost 10% of the total surface area, is represented by the olfactory region, whose physiological role is the perception of odorants [5]. Indeed, the olfactory membrane is not only made of epithelial cells, secreting cells, and glands, but it also contains neuronal cells responsible for the sense of smell (**Figure PI 1.4**) [8]. Specifically, the superior turbinate and the uppermost part of the nasal septum are lined by a ciliated pseudostratified epithelium, but unlike the respiratory mucosa, most of the cilia are of the non-motile type [12]. Along with epithelial cells, olfactory sensory neurons (OSN) are found: unmyelinated, bipolar cells, whose axons project on the one hand toward the olfactory bulb and on the other hand to the mucous surface [1]. The structure, as well as the physiology of OSN, is supported by olfactory ensheathing cells, which are involved in both the maintenance of the electrophysiology and outgrowth of neurons, sustentacular cells, which contribute to neurons' structural stability, and lastly, globose and horizontal basal cells, which represent a reservoir of stem cells [8]. Here, the mucus is produced by Bowman's glands and the lamina propria is vascularized from the

sphenopalatine, anterior and posterior arteries and, besides the olfactory nerves, its innervation is also provided by the trigeminal nerve [7].

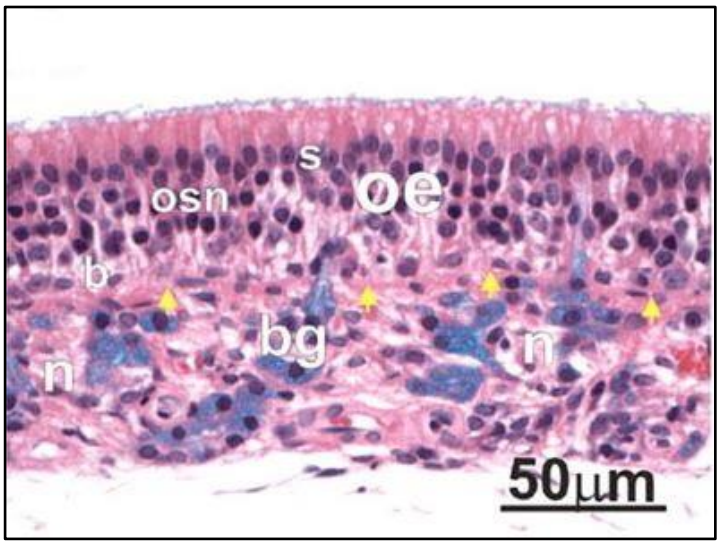

Figure PI 1.4 The olfactory epithelium (oe). Tissue section stained with hematoxilyn-eosin and alcian blue. Abbreviations: sustentacular cells (s), cell bodies of olfactory sensory neurons (osn), basal cells (b), Bowman's glands (bg), nerve bundles (n). The limit between the surface epithelium and the lamina propria underneath is highlighted by the yellow arrowheads. From J.R. Harkema *et al.*, 2006 [6].

1.4. Nasal-associated lymphoid tissue

The nose is also home to the primary site for nasal immunity induction against pathogens and inhaled antigens, known as nasal-associated lymphoid tissue (NALT) [3]. This is distributed in the nasal cavity as discrete focal aggregates in which B cells, T cells, macrophages, and dendritic cells-enriched areas can be found [3,6]. Moreover, the NALT is overlaid by the lymphoepithelium, which comprises both ciliated and non-ciliated cells, together with some intraepithelial lymphocytic cells [6].

2. Nasal drug delivery

The most common and convenient route of drug administration has always been the oral one, but the reduced absorption at the gastrointestinal level coupled with other drawbacks hamper the systemic delivery of active pharmaceutical ingredients (APIs) [4,13]. As a result, the research put a lot of effort into looking for alternative ways of drug delivery [13]. The nasal route of administration is considered a non-invasive drug delivery strategy with unique advantages that grabbed scientists' attention, as demonstrated by the growing trend of publications in the field [14].

2.1. Local administration

Drug administration via the nose has been conventionally exploited to treat conditions that primarily affect the nasal cavity or nearby areas, such as asthma, allergic rhinitis, and local inflammations, as well as to ease nasal congestion [4,9,15]. The standard of care for the aforementioned conditions includes decongestants, antihistamines, corticosteroids, antibiotics, or saline solutions, and are usually administered as liquid formulations in the form of nasal sprays/aerosol pumps [2,16]. The local application of medications or substances directly to the nasal passages allows for precise targeting of the affected area obtaining a rapid onset of action, and reduced exposure of the rest of the body to the API leading to fewer adverse effects, and lower doses than systemic administration [4,9,15,16].

2.2. Systemic administration

Even though the potential advantages of the nasal route as an alternative delivery strategy for drugs with systemic effects had already been well understood, we should wait until 1979 to read about the first serious demonstration of the feasibility of intranasal systemic delivery [17]. From that moment, the intranasal administration was placed at the forefront of drug delivery, seminars were dedicated to this new subject, and comprehensive reviews were written aiming to highlight challenges and future perspectives in the field [13]. The reason for such an interest in the nasal passage is due to some of its anatomical, physiological, and histological features [4]. As already mentioned, the nasal mucosa is extremely vascularized: the oxygenated blood, coming from the external and internal carotid systems, flows through a dense bed of fenestrated capillaries near the turbinates, while the venous return occurs through the sphenopalatine, facial, and ophthalmic veins and finally the internal jugular vein, which drains into the right heart chamber [18]. Since the packed distribution of blood vessels is characteristic of the turbinates, it is not surprising that systemic delivery of APIs occurs preferentially in the respiratory region [19]. Further, the high density of vessels and their leaky architecture contribute to rapid and complete drug absorption, leading to a faster onset of action [13]. Moreover, because of the direction the blood follows, a substance that is absorbed in the nasal cavity avoids both the liver's first-pass metabolism and the metabolism at the gastrointestinal level [4,13]. This has two direct consequences: the prevention of eventual irritation of the gastrointestinal mucosa as well as the accumulation of metabolites with potential side effects [4,9,13]. Besides what has been said so far, it must be noted that the direct connection of the nasal cavity with the external environment makes nasal administration a needle-free, painless, and non-invasive practice, all features that positively

contribute to the patient compliance and reduce the risk of injury or infection for blood-borne diseases such as human immunodeficiency virus (HIV) and hepatitis B virus (HBV) [9,13]. Due to its positive attributes and suitable characteristics, the nasal mucosa has emerged as a promising alternative to the oral and intravascular routes for both small molecules and biologics [4,15,19]. For some of them efficacy and safety of intranasal administration have already been demonstrated and therefore marked products are available, for some others, the feasibility and usefulness of nasal administration are still under investigation [15,19]. For instance, opioids, that are indicated for acute and chronic pain due to surgery, trauma, or cancer, are supposed to rapidly reach the onset of action and exhibit prolonged duration [19]. However, when given orally, the extensive hepatic and intestinal metabolism to which they are subjected limits their bioavailability, and, in the case of parenteral administration, the presence of professional people is required. Consequently, the development of intranasal dosage forms for such therapeutic agents would make easier and faster the achievement of pain relief and would improve the life quality of the patient [15,19]. This is already possible for fentanyl, which is marked both in the form of aqueous solution (Instanyl®) and pectin-based mucoadhesive formulation (PecFent®), while is under clinical trial an intranasal formulation for morphine [19]. Similar drawbacks are also observed with cardiovascular drugs and, consequently, metoprolol tartrate, nifedipine, nitroglycerin, and carvedilol are under evaluation for intranasal therapy as well. Another example is that of treatments for migraine and cluster headaches, a group of analgesic drugs used to alleviate severe pain and throbbing, that are commonly administered orally. Their delivery was rethought for the nasal route because, besides being extensively metabolized, they may be affected by erratic absorption due to nausea, vomiting, and gastric stasis from which most migraine patients suffer. Nowadays, some of these analgesics, such as sumatriptan, zolmitriptan, and butorphanol are marked as nasal sprays, Imitrex®, Zomig®, and STADOL NS® respectively [15,19]. Likewise, antiemetic and motion sickness drugs, such as metoclopramide hydrochloride, ondansetron, and scopolamine are considered optimal candidates for nasal delivery [15]. Indeed, this ensures more consistent dosing than oral administration and, unlike parenteral administration, does not require invasive procedures, that would be hampered in acute emesis. Concerning biologics, that is to say, peptide-, protein- or nucleic acid-based drugs, they are extremely susceptible to enzymatic degradation and characterized by very low bioavailabilities, therefore they are mainly administered through parenteral route, regardless of patient discomfort and painful injections [15,19]. However, wanting to increase patient compliance and adherence to long-

term treatments with biomacromolecules, absorption through the nasal mucosa was seen as an attractive alternative for biologics as well [15]. Thus some protein/peptide-based drugs are on the market, such as salmon calcitonin (Miacalin®, Fortical®), desmopressin (Minirin®, DDAVP®, Stimate®), buserelin (Suprefact®, Profact Nasal®), nafarelin (Synarel®) and oxytocin (Syntocinon®), while others are under development, like insulin [19].

2.3. Nose-to-brain administration

Alongside the aforementioned advantageous features, the nasal route also exhibits an anatomical connection with the central nervous system (CNS) and thus it grabbed the attention as a potential alternative strategy to deliver drugs whose target is located in the brain.

Transport flows between various nasal spaces have been documented since the nineteenth century, even though the field received a significant boost later in the last decade when it became clear that viruses, as well as tracer materials, low molecular weight drugs, and some peptides, could reach the CNS through the nasal passages [20]. Moreover, the growing concern regarding neurological diseases raised the need to dig into the mechanisms involved in nose-to-brain (N2B) delivery [16]. In fact, CNS diseases like Parkinson's disease, Alzheimer's disease, epilepsy, migraine, brain injury, etc., are commonly treated through systemic drug administration, despite the effectiveness of neurotherapeutics being hampered by several obstacles, namely first-pass metabolism and the blood-brain-barrier (BBB) [21]. The latter acts as a physical barrier made of pericytes, astrocyte foot processes, and capillary endothelium which do not have fenestrations and, in particular, these endothelial cells are tightly connected by means of tight junctions which create a continuous wall that prevents the diffusion of substances from the bloodstream to the brain [14,16]. In addition, the CNS is further protected from pathogens, neurotoxic substances, or other potentially dangerous molecules by efflux protein transporters, which help minimize the brain's exposure to these agents by expelling them back into the bloodstream [16]. Therefore, the brain bioavailability of drugs is negatively affected by these defense mechanisms and the amount of API that successfully reaches the therapeutic target is further reduced by enzymatic degradation and excretion during systemic circulation [22]. Different attempts have been made to overcome the limit posed by the BBB, including injections performed intrathecally, intracerebroventricularly, or intraparenchymally, but these approaches are incompatible with multiple daily applications, extremely invasive, associated

with a high risk of infection and require the presence of trained professionals. Consequently, the nose, being home to the olfactory and trigeminal nerves, was seen as a unique opportunity to deliver therapeutics to the brain exploiting a very short way to the CNS [9]. Four distinct pathways have been identified from the nasal cavity to the brain (**Figure PI 2.1**): olfactory, respiratory, NALT, and systemic (see section 2.2) pathways [22].

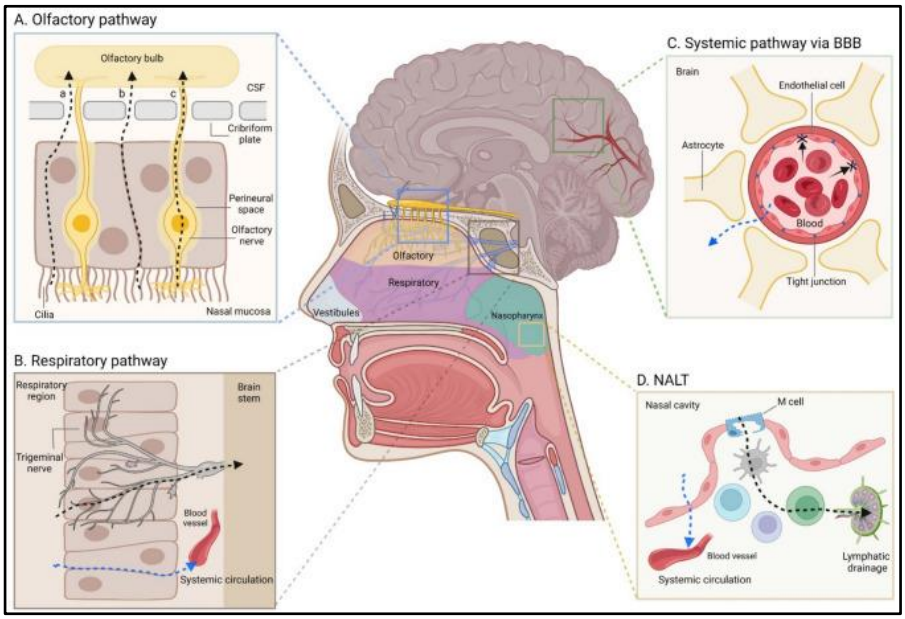

Figure PI 2.1 Nose-to-brain pathways A) Olfactory pathway, where a-c correspond to transcellular, paracellular, and intraneuronal mechanisms. B) Respiratory pathway. C) Systemic pathway. D) NALT pathway. Black and blue dotted arrows in the different panels stand for direct and indirect routes respectively. From S. Jeong *et al.*, 2023 [22].

Considering the olfactory region (**Figure PI 2.1A**), the ethmoid bone's cribriform plate is located between the nasal cavity and the brain, housing the olfactory bulbs and olfactory sensory neurons. Since these neuronal cells are involved in the olfactory transmission from the nasal cavity to the brain, this means that also drugs can be directly delivered to the CNS [22]. In fact, molecules are endocytosed (most of the time via a non-receptor mediated process) and transported along the axon until a synaptic cleft in the olfactory bulb is reached and the exocytosed substance can distribute throughout the CNS [8]. Apart from the intraneuronal route, which requires from 1.5 to 6h to take place, N2B drug absorption across the olfactory region can occur by other up-take mechanisms: by transcellular methods, including endocytosis and diffusion across the sustentacular cells, or paracellular methods through the junctions and clefts between the olfactory epithelial cells [12,16,22]. In these two scenarios, when the API reaches the lamina propria can be absorbed by local blood or lymphatic vessels, or alternatively can utilize the perineural spaces located between olfactory ensheathing cells and olfactory nerve fibroblasts to travel alongside the olfactory

nerves to reach the olfactory bulbs. Following their passage through the cribriform plate, these substances can theoretically access the cerebrospinal fluid and disperse throughout various regions of the brain [16]. The intraneuronal route is also possible across the trigeminal nerve within the respiratory region as each of its three branches is connected to the brain stem and olfactory bulb (**Figure PI 2.1B**) [22]. In this case, it is reported that the drug transport occurs in 17 - 56h and that the internalized molecule is released at a synaptic cleft in the brain stem [8]. Lastly, it is worth mentioning the NALT, which is mainly known as an immune organ, but it can also be involved in N2B delivery as the lymphoid tissue ultimately leads to cervical lymph nodes (**Figure PI 2.1D**) [22]. Various examples can be given concerning small molecules or biologics that have been tried to be delivered through N2B. Among these selegiline [23] and rasagiline [24], two monoamine oxidase B inhibitors used for treating Parkinson's disease, were formulated for intranasal delivery achieving a remarkable improvement in brain bioavailability compared to systemic administration. Tacrine hydrochloride, an FDA-approved (U.S. Food and Drug Administration) drug for Alzheimer's disease, was included in a microemulsion delivery system, which increased drug accumulation and selectivity in the brain [25]. Of note is the case of depression, for which in 2019 the FDA approved the first intranasal spray containing ketamine as an antidepressant. N2B strategy is of paramount interest also for tackling glioblastoma, a malignant brain tumor [14]. In fact, attempts were made to deliver small interfering RNA (siRNA) to the brain using chitosan nanoparticles, and after intranasal administration, the siRNA distribution was progressively detected in the nasal mucosa, in the olfactory bulb, and ultimately in the hindbrain [26].

2.4. Vaccine administration

A consistent number of microbial pathogens enter the body through a mucosal site, suggesting that the mucosal route of vaccination could help trigger a local immune response. This is also true for the nasal mucosa, which is the site of access for pathogens responsible for acute and chronic respiratory infections like *Streptococcus pneumoniae*, *Haemophilus influenzae*, *Mycoplasma pneumoniae*, *Mycobacterium tuberculosis*, influenza virus, parainfluenza viruses, and syncytial virus [27]. Most commercially available vaccines are administered parenterally (intradermal, subcutaneous, or intramuscular), but there is an intensive effort toward developing mucosal, including nasal, vaccines [19]. Besides its being the first site of contact with inhaled antigens, the nasal mucosa is also regarded as an optimal site for mucosal vaccination because of the presence of the NALT, that is the

lymphoid tissue located at the nasopharynx and consists of adenoid, palatine, lingual tonsils and the bilateral lymphoid bands [10]. Besides, mucosal vaccination shows a striking difference to injected vaccines, that is the ability to elicit both systemic and immune responses, as demonstrated by the enhanced levels of systemic immunoglobulin G (IgG) and nasal secretory immunoglobulin A (sIgA) [4,15,28]. This means that topical immunization offers a primary defense at the mucous membrane surface where the pathogen enters the body, while also providing secondary protection against the spread of the infection throughout the entire system [28]. Moreover, intranasal administration of vaccines does not require painful procedures or trained personnel, sterile products, or sterile dosing technique, thus being a particularly effective approach to achieve rapid mass immunization [14,15]. Examples of the effectiveness of intranasal vaccines in humans include those designed to protect against influenza A and B viruses, proteasome-influenza vaccines, adenovirus-vectored influenza vaccines, native group B meningococcal vaccines, attenuated respiratory syncytial virus vaccines, and parainfluenza 3 virus vaccines [3,4]. It is worth noting that nasal vaccination in humans is not limited to preventing upper respiratory infections alone. Following nasal immunization, sIgA can also be detected in other mucosal secretions [4]. This broader distribution of sIgA in various mucosal areas may be significant in countering viruses transmitted through different mucosal sites, such as HIV and HBV [3,4].

2.5. Shortcomings

Despite the advantages that have been highlighted while describing the different therapeutic effects that can be obtained through nasal administration, this delivery strategy is not free from shortcomings. These are related to both the features of the administration site and the physicochemical properties of the administered drug and they will be discussed in parallel in the following sections.

The prerequisite for drug absorption through the upper respiratory tract involves ensuring that the API reaches and adheres to the luminal surface of the epithelial membrane. Subsequently, the drug must be absorbed before it undergoes clearance or degradation, overcoming various obstacles that encompass the mucus layer, the nasal epithelium, the basement membrane, and the capillary endothelium (**Figure PI 2.2**) [29].

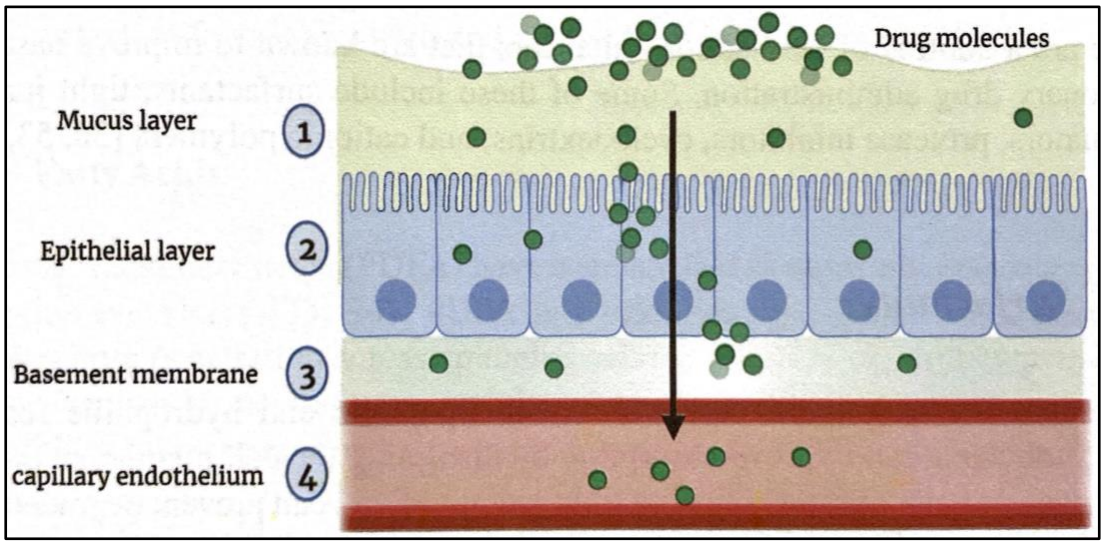

Figure PI 2.2 Barriers encountered by drugs during absorption across the nasal mucosa. From Amponsah, S.K., Adams, I. (2023). Drug Absorption via the Nasal Route: Opportunities and Challenges. In: Pathak, Y.V., Yadav, H.K.S. (eds) Nasal Drug Delivery; pp. 25 – 42 ISBN 978-3-031-23111-7.

2.5.1. Volume restriction

The primary drawback of nasal delivery lies in the limited applicable volume, which is only 25 – 200 μL per nostril at a time [18,30]. Indeed, the administration of higher volumes would cause direct loss of the drug due to runoff from the front or back of the nasal cavity [18]. This constraint renders nasal delivery unsuitable for drugs that necessitate high doses or that are poorly water-soluble [18,30].

2.5.2. Nasal pH

The pH of the human nasal cavity is reported to be slightly acidic, with values that range between 5.5 – 6.5 in adults, and 5.0 – 7 in infants [31]. It has been observed that alterations of the nasal pH due to pathological conditions or administration of therapeutic products lead to mucosa irritation [4]. Consequently, nasal formulations should be characterized by pH values as similar as possible to that of the administration site to avoid any damage (within 4.5 – 6.5) [31]. This can represent a limit for those APIs that show *p*Ka values lower than the physiological pH: since they are in the ionized form in the nasal cavity, their permeation across the mucosa will be hampered (further discussed in section 2.5.4) [4,31].

2.5.3. Mucus layer and mucociliary clearance

The first barrier that drugs face once administered in the nasal cavity is the mucus layer [29,32]. This consists of two components: the periciliary layer and the upper layer [29,31,32]. The periciliary layer is a thin, low-viscosity fluid, with a thickness just slightly shorter than an extended cilium's length, and it is covered by the more viscous upper layer, which ranges in depth from 0.5 to 5 μm [29,32]. In terms of composition, 90 – 95% of mucus is represented by water in which is possible to distinguish electrolytes, serum proteins, immunoglobulins, and lipids and 3% consists of mucins [19,32]. The latter are glycoproteins with a molecular weight that ranges between a few hundred Daltons to more than 1×10^7 Daltons [32], are the most abundant proteins in the mucus layer and can be of different types: membrane-bound mucins, that is to say those that are found at the apical side of epithelial cells, or secreted mucins, which can be monomeric non-gel forming or oligomeric gel-forming. Secreted mucins share a common framework comprising a repeating structure known as the PTS backbone, consisting of proline (P), threonine (T), and serine (S). These backbones are interspersed with regions rich in cysteine, which form coils due to interactions involving disulfide bonds. The PTS backbones also feature various amino sugar glycosylation modifications through O-linked bonding, including N-Acetylgalactosamine-galactose-N-Acetylglucosamine-Sialic acid (**Figure PI 2.3**). Differently, membrane-bound mucins are characterized by N-linked sulfate groups and SEA (sea-urchin sperm protein, enterokinase, and arginine) domains [8]. The viscoelastic mucus forms upon exocytosis of mucin granules, which further dissolve in nasal fluid enabling secreted mucins to produce an entangled network [8,32]. The adhesive behavior of mucus makes it effective at trapping particles, xenobiotics, and pathogens, which is necessary to protect the underlying epithelium from potentially harmful substances, but at the same time, it also hampers the absorption of therapeutic agents [19]. Indeed, APIs can be prevented or hindered from crossing the mucus layer by two main mechanisms. The first, indicated as interaction filtering, relies on the surface properties of the molecule, thus stopping all those substances that can make weak bonds (electrostatic and/or hydrophobic forces, hydrogen bonds) and/or specific binding interactions with the mucus components [33]. The second, named size filtering, depends on the size of the diffusing molecule and that of the mucus mash; in other words, it permits the passage of particles that are smaller than the gaps between the mucin fibers, while larger particles are blocked or prevented from passing through [33]. Generally speaking, this layer allows for the easy passage of small, neutral particles, whereas larger or charged particles may encounter greater difficulty in crossing it [19]. Moreover, because of the high water

content of the mucus layer, when it comes to small molecules, what really governs diffusion is lipophilicity [15,19].

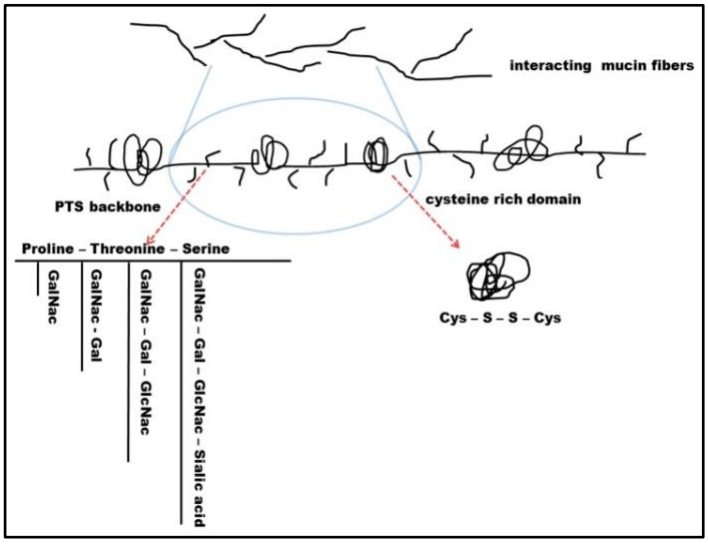

Figure PI 2.3 Structure of secreted mucin fibers. From S. Gänger *et al.*, 2018 [8].

The mucus is renewed every 10 – 15 minutes and, because of the beating of cilia, is also propelled from the nostrils to the nasopharynx and swallowed into the gastrointestinal tract at a speed of 5 – 6mm/min [4,9,29]. The mucus turns over coupled with its dynamics in the nasal cavity gives rise to the phenomenon of mucociliary clearance (MCC). Consequently, drugs that are applied nasally together with any exogenous substance absorbed at the mucus surface are rapidly cleared from the nasal cavity, resulting in a remarkable reduction in the residence time and thus in a weak absorption [4,9]. Because of the different distribution of ciliated cells, it can be noted a difference between an initial clearance phase lasting 15 to 20 minutes, during which approximately 50% of the administered dose is removed from the respiratory mucosa, and a subsequent slower phase that facilitates the removal of drug molecules deposited on the non-ciliated epithelium of the vestibule and the front segment of the nasal cavity [4,18]. Molecules that are particularly affected by MCC are hydrophilic ones which, being soluble in the mucus layer, are rapidly moved away from the absorption site, especially when they are affected by a slow rate of absorption (further discussed in section 2.5.4) [4,9,10,19].

2.5.4. Epithelial layer

Once passed through the mucus layer, drugs should overcome the nasal epithelium [15]. Similarly to other epithelia, cell-cell connections keep individual cells in very close proximity to each other preventing inhaled substances from penetrating deeper into the nasal mucosa

[8]. This barrier function is exerted by the junctional complex, which exhibits a hydrophilic character and comprises three regions: zonula occludens, zonula adherens, and macula adherence, in order from the apical side to the basolateral compartment of epithelial cells [15,20]. Drugs can overcome the nasal epithelium by exploiting two strategies: the transcellular or the paracellular route. If the transcellular mechanism is preferred, this means that the API crosses the epithelial cells either by passive diffusion driven by a concentration gradient or by active transport, which requires a receptor or membrane transporter-mediated process [12,18]. Alternatively, when the paracellular route is chosen, the therapeutic agent undergoes a slow and passive aqueous transport through the clefts and tight junctions between epithelial cells [12,18,19]. The physicochemical properties of the drug are of paramount importance in determining which pathway is adopted by the administered API [18]. It is generally observed that lipophilic drugs preferentially take the transcellular route because they can readily enter the lipid bilayer of the cell membrane through partitioning, whereas hydrophilic molecules can take one or the other route based on their molecular weight [15,18]. The typical range of diameters for tight junctions falls between 3.9 and 8.4 Å, thus they play a significant role in regulating molecular transport across the paracellular space [19]. Drugs characterized by molecular weights lower than 300 Da, reach the circulation fairly quickly, differently from those with weights higher than 1 kDa, which are absorbed very slowly. Apart from lipophilicity and molecular weight, the degree of ionization also affects drug absorption. In particular, it influences the diffusion across the lipid bilayer, which is facilitated for non-ionized molecules. This is a major hurdle for proteins because they seldom show a neutral charge at physiological pH [18].

2.5.5. Enzymatic metabolism

Even though the administration of drugs in the nasal cavity prevents molecules from undergoing the first-pass effect, this does not mean that they are completely safe from enzymatic degradation. Nasal metabolism is typically less potent than hepatic and intestinal metabolism, but it should not be disregarded [4]. In fact, metabolic enzymes have been detected in the nasal mucosa and they can contribute to the local degradation of the API, thus decreasing drug bioavailability. Biotransformation enzymes, such as carboxylesterases, aldehyde dehydrogenase, epoxide hydrolases, and glutathione S-transferase were identified, as well as cytochrome P450 isoenzyme, which is involved in the metabolism of cocaine, nicotine, alcohols, progesterone, and decongestants. The nasal mucosa is also home to proteolytic enzymes, such as aminopeptidases and proteases,

whose substrates are peptides and proteins [18,34]. In addition, similarly to the BBB, the nasal mucosa shows efflux transporters, among others the glycoprotein P, which is found on the apical surface of ciliated epithelial cells in both the respiratory and olfactory mucosa and prevents the influx of a wide range of hydrophobic and amphiphilic drugs [4], and the organic cation transporter, which is active towards antihistamines, opioids, and antibiotics [18].

2.5.6. Nasal blood flow

If a systemic effect is intended, the administered drug that has reached the lamina propria must enter the blood circulation [4]. This primarily occurs by diffusion, which implies the maintenance of a concentration gradient across the endothelium. Therefore, the rate of blood flow has a notable impact on the systemic absorption of drugs through the nasal route [4,9,18]. As the blood flow rate increases, the passage of drug molecules through the membrane and into the general circulation is enhanced. Similarly, nasal drug absorption is reduced by vasoconstriction, which decreases blood flow [4,18].

3. Improving nasal drug delivery

Enhancing the bioavailability of intranasally delivered drugs involves employing various synergistic approaches, whose primary goals are to enhance drug permeability and minimize excretion. These objectives can be accomplished by co-administering additional compounds together with the API or by refining the chemical attributes and pharmaceutical formulation of the drug [18]. Among the most common practical strategies to overcome the limit posed by both the administration site and the physicochemical properties of the therapeutic molecule are prodrugs, enzymatic inhibitors, absorption enhancers, mucoadhesive polymers, and novel formulations [4].

3.1. Prodrugs

A first attempt to solve issues related to drugs' reduced solubility, ineffective transmucosal absorption, and/or metabolic inactivation, is to chemically modify the molecules of interest and administer them in the form of prodrugs [4,35]. This term is used to describe those substances that require a metabolic transformation within the body to become active and manifest their pharmacological effects [4,18,35]. Examples of application of the prodrug strategy are providing a more hydrophilic or lipophilic character to the candidate drug. In the first case, to enable for instance the production of an aqueous nasal formulation with an

appropriate concentration, in the second case, to promote the absorption across the membrane [4,18]. Moreover, this approach has also been employed by some researchers to develop drugs that are more resistant to enzymatic metabolism [4].

3.2. Enzyme inhibitors

The use of enzyme inhibitors does not directly improve the absorption of the delivered drug, but rather it contributes to the molecule's stability by preventing its biotransformation. Consequently, the quantity of active drug available for absorption is expected to increase together with the efficacy of the treatment [35]. In this regard, bacitracin, boroleucin, amastatin, puromycin, and camostat, which are inhibitors of peptidases and proteases, have demonstrated their effectiveness in significantly enhancing the intranasal absorption of the luteinizing-hormone-releasing hormone, human growth hormone, encephalin, vasopressin, and desmopressin [36,37]. Similarly, inhibitors of the cytochrome P450 isoenzyme have been identified; indeed, fluvoxamine's contribution to the permeation enhancement of melatonin through both the respiratory and olfactory mucosa was proved [38].

3.3. Absorption enhancers

A more straightforward method compared to the aforementioned ones to enhance drug bioavailability is the incorporation of chemical permeation enhancers into the dosage form [39]. These are functional excipients added to the formulation because of their ability to enhance drugs' solubility [40] and/or transiently change the permeability of the epithelial cell layer, which can be achieved by increasing membrane fluidity or opening tight junctions [4,9,18]. Among the most common permeation enhancers investigated in the field of nasal delivery are cyclodextrins, tight junction modulators, cationic polymers, and surfactants [29,40].

3.3.1. Cyclodextrins

Cyclodextrins (CDs) are cyclic oligosaccharides formed through enzymatic action on starch, consisting of (α-1,4)-linked d-glucopyranose units [4,41,42]. They exhibit a distinctive toroidal configuration, where the outer section of the cone-shaped structure features hydroxyl groups, while the central cavity aligns with the carbon framework and glycoside oxygen of glucose [41]. This unique distribution of chemical groups imparts CDs with a hydrophobic interior cavity and a hydrophilic outer surface [4,41,42]. The most prevailing natural CDs in the pharmaceutical field include α-cyclodextrin, β-cyclodextrin, and γ-

cyclodextrin. Additionally, various derivatives of CDs have been synthesized, leading to the description of over 1500 distinct cyclodextrin derivatives to date. As a result of their chemical structure, CDs are primarily exploited for their ability to improve the apparent solubility and dissolution rate of lipophilic drugs [41]. Indeed, inclusion complexes can be formed upon the interaction (through weak bonds) between a poorly soluble molecule and the hydrophobic internal cavity of CDs, which improves the biopharmaceutical performance of BCS (Biopharmaceutical Classification System) Class II drugs, that will consequently display a behavior closer to that of substances belonging to BCS Class I. In addition, CDs play a role in the permeation process. This function is generally verified with lipophilic drugs and they are particularly active when the limiting step during absorption is the diffusion across the water layer that covers the epithelium. Specifically, most CDs enhance drug delivery by facilitating diffusion through aqueous barriers, but they cannot permeate across biological membranes because of their high molecular weight and low octanol/water partitioning coefficient [42]. An exception to this rule is represented by lipophilic CDs, like methylated β-cyclodextrin, which can permeate the mucosa and enhance drug delivery across biological membranes, including the nasal mucosa, due to its ability to remove the phospholipids and cholesterol from the cell surface [40,42]. Cyclodextrins find practical application in nasal drug delivery, as demonstrated by their use in developing an inclusion complex between dimethyl β-cyclodextrin and a fentanyl derivative (carfentanil) to enable the fast and safe administration of the opioid via the nasal cavity [43]. Nevertheless, despite their being extensively used in intranasal pharmaceutical formulations, cyclodextrins may exhibit some local and systemic side effects [4].

3.3.2. Tight junction modulators

The use of tight junction modulators represents an effective approach to enhance drug absorption through the paracellular pathway [29]. These compounds are capable of modifying the proteins found within these junctions, such as claudin and zonula occludens, leading to a weakening of cell-to-cell connections [9,29]. C-CPE and AT1002 are peptide-mimicking toxins capable of modulating the function of tight junctions. The former consists of the C-terminal fragment of an enterotoxin derived from *Clostridium perfringens*, it exerts its function by binding with claudins, and its activity was seen to successfully improve the paracellular absorption of pneumococcal vaccine. The second is an analog of *Vibrio cholera* toxin and acts on zonula occludens by reversibly binding with its receptor [44]. The primary challenge associated with tight junction modulators is their potential for toxicity.

Consequently, variants of peptide-mimicking toxins have been synthesized to reduce their harmful effects [29]. Alternatively, tight junction opening can be achieved by decreasing the concentration of endogenous calcium ions, which can be realized using calcium chelators such as ethylenediaminetetraacetic acid (EDTA), or through the use of anionic poly(acrylic acid) polymers like Carbopol®, which can sequester cations [44].

3.3.3. Cationic polymers

Cationic polymers are distinguished by their inherent positive charges present in the side chains and/or backbone of the polymer, and they have shown the ability to improve the absorption process through mucosal surfaces [45]. This is thought to be of particular interest for the intercellular transport of macromolecules and to occur because of a reduction in the transepithelial resistance, which, in turn, results in an elevated flux of extracellular markers [46]. Examples of polymers belonging to this class include natural ones like cationic gelatin, dextran, and chitosan, as well as synthetic ones such as poly(amido amine) (PAMAM), poly(L-lysine) (PLL), and polyethyleneimine (PEI) [45]. Miyamoto and co-workers explored the effect of the polycation poly-L-arginine (poly-L-Arg) as an absorption enhancer for the nasal administration of macromolecular therapeutics, using FITC-dextran of different molecular weights as an extracellular marker. This study demonstrated that poly-L-Arg of different mean molecular weights can promote the transmucosal delivery of FITC-dextrans with molecular weights up to 167.0 kDa [46]. Among the natural cationic polyelectrolytes, chitosan is the most frequently employed enhancer of absorption because of its advantageous qualities such as biocompatibility, biodegradability, and low toxicity [29,45]. Concerning the molecular structure, chitosan is a linear polysaccharide (units of 2-amino-2-deoxy-D-glucopyranose and 2-acetamido-2-deoxy-D-glucopyranose linked via β-(1,4) glycosidic bonds) resulting from the deacetylation of chitin, the main component of crustacean’s exoskeleton [41]. Chitosan's ability to enhance mucosal absorption is believed to result from a dual effect [40,45]. The protonated amino groups present in chitosan are likely to be engaged in electrostatic interactions with the negatively charged glycans of mucus, enhancing the contact time for the transport of the drug across the membrane [40,45]. In addition, chitosan drives the dehydration of epithelial cells with the consequent reversible opening of tight junctions [40]. Chitosan’s influence on cell-to-cell connections is further supported by the evidence that, in its presence, the spatial arrangement of proteins associated with tight junctions, such as zonula occludens-1 (ZO-1), and the cytoskeletal protein F-actin can be altered, impacting paracellular transport [45]. In the pharmaceutical

industry, chitosan serves as a valuable penetration enhancer for hydrophilic drugs that have limited absorption capabilities, and it is also exploited as a drug carrier. Enhancement of absorption through the nasal epithelium has been proved for calcitonin, insulin, and buserelin when chitosan is employed [41]. Despite its favorable features and usefulness in drug delivery, chitosan suffers from poor solubility in water at physiological pH, which strongly limits its application [29]. Anyway, to overcome the limited solubility of chitosan, various derivatives have been created, and one of the extensively examined chitosan analogs is N-trimethyl-chitosan. This derivative exhibits excellent solubility in aqueous solutions and maintains its charge over a wide pH spectrum (pH 1 – 9) [45].

3.3.4. Surfactants

Surfactants are surface-active compounds whose chemical structure includes two portions with opposite characteristics: at one side it is possible to distinguish the hydrophilic and water-soluble group, while at the other end is located the lipophilic and water-insoluble moiety. As a result, surfactants are characterized by an asymmetric and polar structure that gives these additives a peculiar amphiphilic nature [47]. Substances that fall into this group can be categorized based on the hydrophilic or lipophilic moiety. If the hydrophilic head is considered, this can be non-ionic or ionizable, and ionizable components can be further divided into cationic, anionic, or amphoteric categories. Regarding the hydrophobic region, most surfactants contain aliphatic chains, while some have polycyclic aromatic groups. Aliphatic surfactants can be also classified based on the length of their hydrocarbon chains, which can be short, medium, or long. Moreover, these chains may be saturated or unsaturated, branched or unbranched, and there may be more than one in the same molecule. Considering that moieties can be of different kinds, to understand which is the contribution of the two to the overall behavior of the molecule, surfactants are usually described by a hydrophilic-lipophilic balance (HLB) number, that is useful in choosing the suitable surface active molecule for a specific application (emulsifier, detergents, solubilizers), or the one possessing the best dispersion characteristics according to the experimental conditions [48]. Further on, the name of this varied group of molecules is derived from their ability to reduce surface tension when they adsorb at the interface between different states of matter, gases, liquids, and solids [47,48]. For instance, when they are found at the boundary between air and liquids, the reduction in surface tension enables substances to diffuse or even mix as an emulsion in water or other solvents. This detergent ability is proper to just the monomeric form of surfactants. When the surface-active

molecule is solubilized in water, the surface tension decreases in parallel with the increment in the surfactant concentration until a plateau is reached (**Figure PI 3.1**) [41]. The concentration of surfactant over which the surface tension remains constant is known as critical micelle concentration (CMC) and represents another specific attribute of the molecule [41,48]. When adding surfactants over their CMC, molecules do not distribute at the interphase, but rather they self-assemble into micelles of different shapes (cylindrical, spherical, hexagonal, laminar cubic, inverted cylindrical, or inverted spherical shape) depending on the kind of surfactant [41].

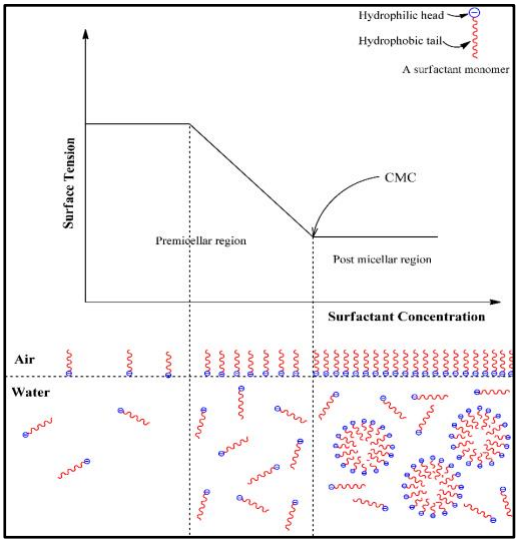

Figure PI 3.1 Surfactant's concentration influence on surface tension and the different distribution of surfactant molecules when added at a concentration below or above the critical micelle concentration (CMC). From S. Rai *et al.,* 2021 [49].

Because of their mechanism of action, these chemicals play a crucial role in the formulation and production of a wide range of industrial and consumer products, including cosmetics, detergents, and pharmaceuticals [47]. In pharmaceutical applications, surfactants serve various functions such as enhancing the solubility of drugs in aqueous solutions, acting as emulsion ingredients, serving as formulation vehicles, functioning as plasticizers in drug release systems for semi-solid forms, and boosting drug penetration or absorption. In particular, surfactants are the most commonly employed additives in intranasal formulations to enhance the permeability of drugs across the mucosal membrane [41]. Surfactants employed as enhancers for nasal absorption exert their function through various mechanisms, which encompass disturbing cell membranes, loosening tight junctions, and preventing enzymatic degradation, and they usually belong to one of the following groups: phospholipids, bile salts, fatty acid salts, non-ionic surfactants including alkyl glycosides [29].

3.3.4.1. Phospholipids

Phospholipids consist of phosphorus, a hydrophilic head, and a hydrophobic tail, all connected to an alcohol. Based on the specific type of alcohol in their structure, they can be categorized as glycerophospholipids and sphingomyelins. The formers have glycerol in their backbone, while the latter have sphingosine. Phospholipids used in the pharmaceutical field can be of either natural origin because they are the constituents of animal and plant cells, or synthetic [41]. Phospholipids' absorption-enhancing effect relies on their incorporation in the cell membranes [50] and, additionally, they are exploited for the ability to self-assemble to form colloidal structures, such as liposomes, emulsions, or lipid microspheres [41].

3.3.4.2. Bile salts

Bile salts are endogenous ionic amphiphilic compounds featuring a steroid structure whose physiological function is dissolving dietary lipids and liposoluble vitamins in the gastrointestinal tract. Bile salts such as deoxycholate, taurocholate, taurodeoxycholate, glycocholate, and glycodeoxycholate contribute to permeation enhancement through various mechanisms, promoting both paracellular and transcellular drug absorption [45,51]. Indeed, they can improve the transport of hydrophilic drugs by integrating into the cell membrane: once reached a specific concentration, they have the potential to form temporary micelles that comprise water molecules, thereby generating hydrophilic channels in the cell membrane. Alongside, bile salts can serve as junction modulators by either disrupting hemidesmosomes, which are assemblies of multiple proteins that ensure adhesion between basal epithelial cells and the underlying basement membrane, or binding to calcium ions located near tight junctions. Lastly, these additives can act as mucolytic agents and inhibit some mucosal membrane peptidases [51]. Despite their undeniable potential in fostering drug absorption, the clinical employment of bile salts is restricted due to their potential to cause irreversible mucosal damage and ciliotoxic effects [45], with dihydroxy bile salts having been reported to be more toxic compared to trihydroxy ones [51].

3.3.4.3. Fatty acid salts

Short-, medium-, or long-chain saturated and unsaturated fatty acids have also been used as excipients to improve both the overall stability of the formulation and enhance the permeation of APIs [52]. For some of these additives, the mechanism that stands behind the enhanced drug absorption has been elucidated. Sodium decanoate, a medium-chain fatty acid, serves as an absorption enhancer through a multifaceted process involving phospholipase-C mediated increase in intracellular calcium levels, which regulates tight junction proteins, coupled with detergent-induced membrane fluidization. Docosahexaenoic acid and eicosapentaenoic acid, both polyunsaturated fatty acids, play a significant role in altering epithelial permeability, impacting the integrity of the epithelial barrier, and changing the localization of tight junction proteins in lipid rafts fractions by altering the nearby lipid environment. Furthermore, their influence as modulators of tight junctions has also been noted [53].

3.3.4.4. Non-ionic surfactants

Non-ionic surfactants are widely used in the development of pharmaceutical formulations [41] and represent the most clinically advanced permeation enhancers in nasal drug delivery [39]. They are categorized into polyoxyethylene esters, poloxamers, and polyol esters, which encompass glycol, glycol ester, and sorbitan derivatives. Among these, sorbitan fatty acid esters (Spans) and their ethoxylated derivatives (Tweens) stand out as the most common [41]. Non-ionic surfactants are generally viewed as gentler tensides compared to ionic surfactants. This is due to their tendency not to alter membrane proteins and their less notable interaction with zwitterionic phospholipid bilayers. Nevertheless, it is important to note that the term "mild" does not directly imply safety, as this category of surfactants still includes some molecules that are effective at perturbing and solubilizing cell membrane constituents. Non-ionic surfactant excipients that induce cell perturbation include polysorbate 20, medium chain macrogol-8 glycerides, nonoxynol-9, D-α-tocopherol polyethylene glycol succinate (TPGS), macrogol 15 hydroxystearate (HS15), macrogol 35 castor oil, and sucrose laurate, to name a few examples [48].

Ying Li and co-workers explored the potential employment of laurate sucrose ester (SE), cremophor EL, and poloxamer 188 as permeation enhancers to further increase the intranasal absorption of sumatriptan succinate. What they found out was that all tested surfactants improved the absolute bioavailability of the drug compared to the control, with laurate SE showing the highest enhancing effect followed by cremophor EL and poloxamer

188 [54]. Another work examined the effect on cellular membranes of two non-ionic amphiphilic tenside groups and their mixture on human Caco-2 cell monolayers: the group of polyethylene glycol esters was represented by polysorbates 20, 60, 80, and Labrasol®, while the group of propylene glycol esters comprised Capryol 90®, Capryol PGMC®, Laurolycol 90®, and Laurolycol FCC®. The research pointed out that, in terms of cytotoxicity, polysorbates were the most toxic compounds and Labrasol® was the only surfactant with significant cytotoxicity above its CMC. However, when it comes to absorption-enhancing properties, polyethylene glycol esters alone or in blends could remarkably increase Lucifer yellow permeability below the IC_{50} concentration (i.e., the concentration of test substance reducing cell viability by 50% compared to the untreated control), and only polysorbate 20 and Labrasol® caused the redistribution of tight junctions [55].

Lastly, Alkylglycosides (AGs) represent a subset of non-ionic surfactants characterized by the attachment of groups like maltose, sucrose, or monosaccharides (e.g., glucose) to alkyl chains of different lengths. Among these, tetradecylmaltoside and N-lauryl-b-d-maltopyranoside stand out as the frequently employed types, because they have demonstrated potent properties for enhancing nasal absorption even at remarkably low concentrations. Although some AGs have displayed absorption-enhancing capabilities, they demonstrate substantial toxicity toward airway epithelial cells, likely due to their membrane-damaging effects [29].

3.3.5. Postbiotics

As it has been said so far, surfactants represent a relevant category of chemicals used in the pharmaceutical industry. However, the majority of commercialized surfactants are of synthetic origin, predominantly derived from petroleum, which contrasts with the current growing environmental awareness among consumers, which is amplifying the interest in biological compounds as potential alternatives to current products [56,57]. Furthermore, studies have indicated that chemical surfactants present in different formulations may pose risks, causing itching, irritation, and potential allergies through their interaction with lipids and proteins present in the cell membranes [58,59]. Consequently, discovering innovative approaches to substitute synthetic and petroleum-based products with renewable, biodegradable, and sustainable green strategies represents a new challenge aimed at fostering environmental and health maintenance [57]. As a result, pharmaceutical industries are now paying greater attention to the excipients they use, trying to include natural materials in their products. Among these, postbiotics are gaining growing consideration [60].

The International Scientific Association for Probiotics and Prebiotics (ISAPP) has recently revised the term "postbiotic," defining it as a combination of "biotic," that is to say relating to or originating from living organisms, and "post," a prefix indicating something occurring after, suggesting that this terminology has to be restricted to bio-products that do not contain living organisms [61]. In other words, postbiotics consist of the metabolic byproducts or bioactive compounds generated by living microorganisms during growth or fermentation, which exert beneficial effects independently of the presence of the living microorganisms [62]. The commonly used probiotic genera for postbiotic production are *Lactobacillus*, *Bifidobacterium*, yeast, *Bacillus*, and genetically modified organisms, with *Lactobacillus* and *Bifidobacterium* spp. as the most prominent because of their being identified as GRAS (Generally Recognized As Safe) microorganisms [62,63]. Different classification criteria have been proposed for postbiotics, but they are usually categorized based on the metabolites produced by the microorganism, namely short-chain fatty acids, exopolysaccharides, cell wall fragments, enzymes and proteins, cell-free supernatants, bacterial lysates, and other complex metabolites (**Figure PI 3.2**) [64].

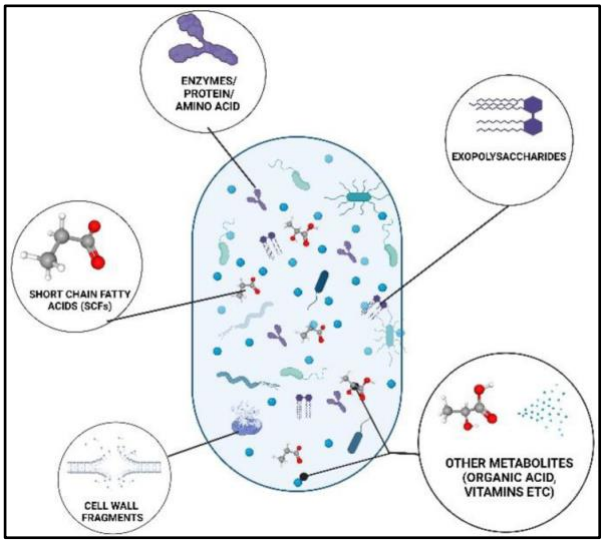

Figure PI 3.2 Postbiotics' classification based on the metabolites generated by the microbial cell. From P. Thorakkattu *et al.*, 2022 [64].

From 2013 onwards, there has been a notable increase in global research projects concerning postbiotics, resulting in their employment across various industrial sectors, including food, beverages, healthcare products, cosmetics, nutraceuticals, and more [60]. Focusing on the pharmaceutical field, postbiotics have been reported to exert antibacterial, anti-inflammatory, immunomodulatory, anti-proliferative, and antioxidant activities [64]. Moreover, evidence suggests that their application in the clinic would be beneficial for

treating acute/chronic diarrhea, immune dysfunction, allergic reactions, and neurodegenerative diseases among others [60]. Even though the current literature mainly covers evidence supporting postbiotics usefulness as therapeutic agents, the fact that these innovative biological products have a heterogeneous composition that comprises lipids, organic acids, and more complex molecules like biosurfactants, suggests that they might also show absorption-enhancing properties.

3.3.5.1. Microbial Biosurfactants

Microbial biosurfactants (BS) represent a promising solution to address the toxicity linked to frequent synthetic surfactant use. They also offer the opportunity to fulfill the need for improved biodegradability and chemical recyclability in new surfactants derived from renewable resources through an environmentally sustainable process [59].

Like chemical surfactants, BS are amphiphilic molecules able to reduce surface and interfacial tension, but their primary attribute is being bio-based molecules, because they are produced by microorganisms, such as yeast, bacteria, and some filamentous fungi [58,59]. BS are described as a heterogeneous group of compounds, which can be obtained using relatively simple and inexpensive procedures and substrates [56,57], they are physiologically produced during microbial growth as secondary metabolites [58], and their localization can be either anchored to the cell-surface or released in the extracellular medium [65]. BS are most frequently classified into low molecular weight and high molecular weight [66]. The former comprises different sub-categories like glycolipids (e.g. rhamnolipids) and lipopeptides (e.g. surfactin), which are mainly known for their superiority in lowering interfacial and surface tension [58,66]. BS belonging to this first group are characterized by a hydrophobic tail made of one or more fatty acid chains and a hydrophilic head represented by a peptide loop in the case of lipopeptides, or a sugar moiety in the case of glycolipids. Differently, high molecular weight biosurfactants, also named polymeric biosurfactants (e.g. emulsan, biodispersan, alasan) due to their complex chemical composition, are primarily used as emulsifying agents [58]. Most of the described microbial surfactants in the literature are of bacterial origin, with *Pseudomonas* spp., *Acinetobacter* spp., *Bacillus* spp., and *Arthrobacter* spp. being the most frequently reported genera known for producing biosurfactants, but because of the pathogenic characteristics of the producing organisms, the employment of these compounds is limited. Nevertheless, this obstacle has prompted the development of a new category of biosurfactants known as probiotic biosurfactants, which are derived from health-promoting bacteria. Lactic acid bacteria,

specifically, are recognized as a significant subset of GRAS bacteria, and they stand out as the main biosurfactant producers among probiotic organisms [65]. Even though BS share similar molecular structures and mechanisms of action with chemical surfactants, they exhibit numerous advantages over their synthetic counterparts, which encompass low toxicity, high biodegradability, cost-effective production with the possibility to exploit renewable raw materials, and improved stability at extreme conditions (temperature, pH, and salinity) [58,67]. Furthermore, due to their multifaceted nature as macromolecules with diverse functional groups, BS are highly versatile. Consequently, they have grabbed substantial interest from different industrial sectors, including environmental, oil, agriculture, textile, food, cosmetics, medicine, and pharmaceutics [58]. Specifically, in the pharmaceutical field BS have emerged as innovative bio-therapeutics and attempts have been made to exploit them in drug delivery. Indeed, BS produced by some probiotic strains showed antimicrobial activity against different microorganisms both Gram-positive and Gram-negative bacteria, thus appearing as a promising strategy to address the public health concern regarding antimicrobial resistance [65]. Moreover, BS have demonstrated antibiofilm activity through their ability to alter the physicochemical properties of surfaces, which can be of help in reducing microbial adhesion for example to medical implants used in orthopedic surgery [67]. A key application of BS in the pharmaceutical field could also be their activity as absorption enhancers. For instance, D.R. Perinelli et al. investigated whether rhamnolipids could improve the permeability of some macromolecules across Caco-2 and Calu-3 monolayers. They began by observing that rhamnolipids have a promising toxicological profile and are secreted by *P. aeruginosa* as factors that boost infiltration across epithelial barriers, thus suggesting a potential for enhanced performance as permeability enhancers. Indeed, their research illustrated that rhamnolipids have the potential to act as safe and efficient additives that improve the mucosal absorption of large molecules, and this effect appears to stem from their ability to modulate tight junctions [68]. Another work supporting the ability of BS to affect the rate and extent of permeation of some molecules is that published by L. Rodríguez-López et al. They aimed to assess whether a corn-steep liquor-derived BS extract influenced the permeation of a specific set of drugs through a diffusion system based on a silicon membrane. Out of the ten compounds analyzed, the presence of the BS notably enhanced the cumulative amount of permeated compound for five of them compared to the drug alone [69].

3.3.5.2. Cell-free supernatants

Cell-free supernatants (CFS) are liquid solutions comprising the residual metabolites produced during microbial growth and any unabsorbed nutrients from the cultivation medium [62,64]. The quantity and nature of the products primarily depend on the bacterial strain, the culturing medium type, and the treatment of bacteria post-propagation [63]. As a result, CFS from distinct microbial cultures demonstrate varying levels of activity and different chemical compositions [62]. Generally speaking, examples of soluble factors that have been identified in the CFS obtained from several bacterial strains include short-chain fatty acids (e.g. acetate, propionate, butyrate), enzymes (e.g. proteolytic enzymes, glutathione peroxidase), teichoic acids, peptidoglycan-derived muropeptides, endo- and exo-polysaccharides, cell surface proteins, vitamins (e.g. B-group vitamins), and organic acids (e.g. 3-phenylacetic acid and propionic) [64,70]. CFS are associated with anti-inflammatory ability, as was demonstrated for the postbiotic derived from *Lactobacillus casei* DG*,* which successfully attenuated the intestinal mucosa inflammatory response in an *ex-vivo* organ culture model of irritable bowel syndrome [71]. Because some microbial cells can secrete bacteriocins and/or organic acids, their CFS are also exploited as antimicrobial and antioxidant agents. This is the case of the CFS obtained from *Lactobacillus rhamnosus* SD11, which showed an inhibitory activity against *Staphylococcus aureus* and *Streptococcus mutans*, two pathogens involved in oral infections [72]. Not only CFS produced by *Lactobacillus* spp. have potential medical applications, but also those obtained from yeast. For example, the metabolic bio-products isolated from *Saccharomyces boulardii* (*Sb*) comprise motogenic factors that favor enterocyte migration, suggesting that *Sb*' CFS would be of extreme help in accelerating intestinal epithelial wound-healing in patients suffering from ulcerative colitis or Crohn's disease [73]. The multifunctional role of CFS is not the only attribute that encourages the employment of this class of postbiotics in the healthcare field; indeed, companies are also attracted by the evidence that these postbiotics seem to be a sustainable alternative [74]. First of all, CFS of probiotics are produced by naturally occurring microorganisms and are usually considered a waste in many pharmaceutical and food industries [72]; secondly, it has been observed that corn steep liquor, malt wastes, soybean meal, cotton seed, as well as wheat rice and fish waste can be a potential source of nutrient for the postbiotic producing cells [74]. Therefore their use would meet the current demand for more eco-friendly and biocompatible products obtained from renewable sources, minimizing waste accumulation [72]. At present time, most of the reports summarizing findings on CFS describe their use

as alternative green and natural therapeutic molecules for a wide range of clinical applications, but their potential role as excipients remains unexplored.

3.4. Mucoadhesive polymers

The inclusion of mucoadhesive polymers in a dosage form is an effective strategy to tackle issues related to the mucus gel layer and mucociliary clearance. In the specific case of nasal delivery, these excipients interact with the mucus produced by nasal submucosal glands, allowing the formulation to be longer retained in the nasal cavity, and leading to an increased concentration gradient of the drug across the epithelium [75].

Mucoadhesion is a complex process, that is described as the attractive bond established between a pharmaceutical dosage form and a mucosal membrane [76]. The complexity is due to the multimodal way through which the polymer-mucus interaction may occur, which is reflected in the description of six different theories that have been proposed to explain the phenomenon (**Figure PI 3.3**) [76,77].

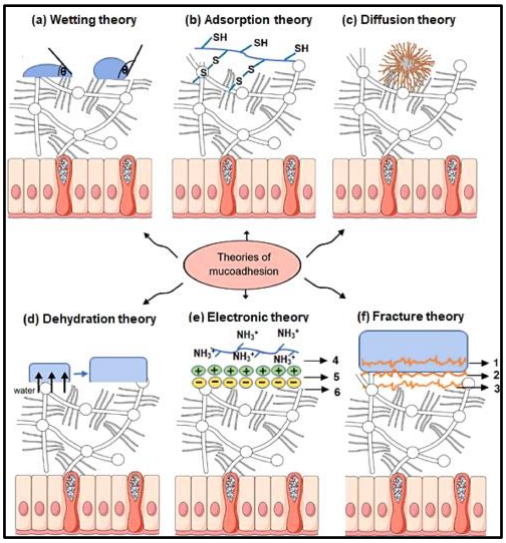

Figure PI 3.3 The six proposed theories to explain mucoadhesion. Figures (a) – (f) correspond to wetting, adsorption, diffusion, dehydration, electronic and fracture theory. Numbers 1 to 3 in figure (f) indicate the different levels at which the fracture takes place: hydrated layer, interface, and mucus layer, respectively. Numbers 4 to 6 in figure (e) stand for positively charged mucoadhesive polymer, electrical double layer, and negatively charged mucus, respectively. From S.P. Bandi *et al.,* 2021 [77].

The principles of wetting theory apply to liquid mucoadhesive formulations, wherein the mucoadhesive polymer can effectively spread on the mucus layer. Consequently, the better the spreading capability of the polymer, the stronger the adhesive interaction becomes. On the other hand, according to the adsorption theory, specific interactions like hydrogen bonds, van der Waals forces, and hydrophobic interactions between the polymer and mucus are responsible for adhesion. When specific interactions are not involved, mucoadhesion might

result from the creation of an interpenetration layer as described by the diffusion theory: adhesive macromolecules penetrate the mucus gel, and the soluble mucins diffuse into the dosage form. Other hypotheses consider that mucoadhesion may be ensured by a dehydration process of the mucus layer due to the gelation of the polymer (dehydration theory), or it can result from the development of an electrically charged double layer at the boundary between the mucoadhesive system and mucus due to electron transfer, allowing the generation of attractive forces within this double layer (electronic theory). Lastly, the fracture theory applies to solid and rigid mucoadhesive materials, whose adhesion efficacy is correlated to the force required for their separation from the mucosal membrane [76,77]. Nevertheless, none of the mentioned theories can singularly explain how the mucoadhesive phenomenon is ruled in the huge number of formulations that have been developed so far [76]. Therefore, it is reasonable that mucoadhesives work through a combination of different mechanisms: water absorption from the mucus layer occurs, causing the polymer to wet and swell; as the polymer swells, the dissociation of hydrogen bonds between the polymer chains takes place, resulting in increased polymer-water interaction (contact stage); finally, the polymer chains penetrate the mucus, establishing interactions with mucins, thereby stabilizing the adhesion (consolidation stage) (**Figure PI 3.4**) [75].

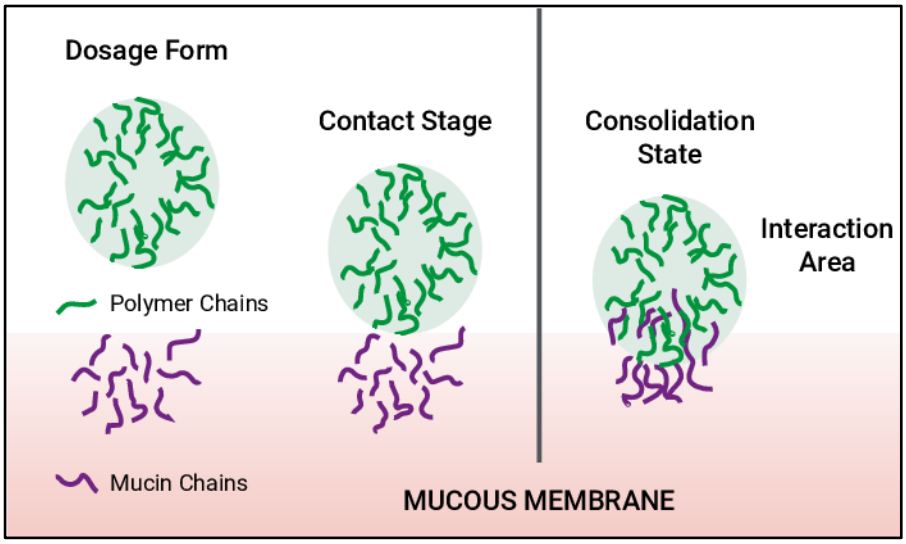

Figure PI 3.4 The different stages of mucoadhesion: contact stage first, followed by a consolidation step. From Medisca, A. (2020). Rheological and Clinical Evaluation of a Novel Concentrated Mucoadhesive Gel Base.

Polymers that can be exploited for mucoadhesion are frequently categorized based on the surface charge (non-ionic, anionic, cationic, amphoteric), the source of the polymer (natural, semi-synthetic, synthetic), or the kind of interaction that they can establish with the mucus layer (covalent bonding, electrostatic bonding, hydrogen bonding) [78]. Concerning the last

classification approach, it must be said that all traditionally employed mucoadhesive polymers, which are also named first-generation mucoadhesive polymers, are non-covalent binding macromolecules [78], while most of the adhesive agents capable of covalent bonding are polymeric thiomers [76]. The latter are synthetic macromolecules created by combining traditional mucoadhesive polymers with compounds containing thiol functional groups. Examples of polymeric thiomers include poly(acrylic acid)/cysteine, chitosan/N-acetylcysteine, alginate/cysteine, chitosan/thioglycolic acid, and chitosan/thioethylamidine. Because of their ability to create disulfide bridges with cysteine-rich areas of mucus glycoproteins, these substances are characterized by an improved mucoadhesive character [76].

The mucoadhesive potential of non-ionic polymers is independent of the pH and relies on their ability to establish hydrogen bonds with the mucosal surface or to interpenetrate at the interface between the polymer and mucus. However, compared to anionic and cationic polymers, non-ionic polymers generally possess lower adhesiveness [78]. Polymers that belong to this class can be of any source. Guar gum, for instance, is a non-ionic polysaccharide obtained from the ground endosperms of guar beans and is listed among the GRAS products. In comparison to frequently employed mucoadhesive polymers like cellulose derivatives and carbomers, guar gum demonstrates favorable performance when used in a dry form or gel state, yet it might not possess the strong mucoadhesive properties of chitosan. As a result, guar gum is frequently used in combination with other compounds or is subjected to chemical modifications aimed at improving the final mucoadhesive character of the product [79]. Another natural polysaccharide is cellulose. It is the most represented biopolymer in nature obtained from fibrous plants but is poorly soluble in water as well as in most organic solvents, and does not show intrinsic mucoadhesive properties [78,79]. Therefore, semi-synthetic ether and ester derivatives of cellulose were obtained addressing both issues (solubility and mucoadhesiveness) and some received GRAS recognition. The most frequently used ethers include methylcellulose, ethylcellulose, hydroxyethylcellulose, hydroxypropyl cellulose, hydroxypropyl methylcellulose, and carboxymethyl cellulose salts [79]. Examples of non-ionic synthetic mucoadhesive polymers are poly(ethylene glycol)/ poly(ethylene oxide) (PEG/PEO), poloxamers (see Section 3.5.1), and poly(vinyl pyrrolidone). The former is a highly biocompatible poly(ether) whose mucoadhesive properties seem to be due to the PEG chain’s ability to quickly interpenetrate the mucus layer. The latter, instead, is a chemically inert and non-toxic polymer whose

employment in mucoadhesive dosage forms is limited because of its mild adhesive character [79].

Anionic polymers feature negatively charged groups, typically denoted by -COOH that become ionized at physiological pH, and these groups are responsible for mucoadhesion. Indeed, the existence of negative charges leads to significant intramolecular repulsion, which causes the extension of polymer chains and facilitates the interpenetration between the polymer and mucus interfaces [78]. Most of the naturally occurring anionic mucoadhesive polymers are polysaccharides, which are also commonly utilized as pharmaceutical excipients due to their cost-effectiveness, wide availability, low toxicity, compatibility with biological systems, and degradable nature [78]. For example, alginates are unbranched polyanionic polysaccharides of both algal or bacterial origin that are known for their being mucoadhesive, biocompatible, and non-irritant. Xanthan gum also originates from bacteria, specifically from the bacterium *Xanthomonas campestris*, and as alginates, it received the GRAS status. However, despite the presence of carboxylic acid groups in its chemical structure, xanthan gum is referred to as a mild mucoadhesive polymer, probably due to its high molecular weight that hampers the interpenetration process. Consequently, it is not surprising to find it used together with other adhesive polymers or to come across chemically modified forms of xanthan gum [79]. Also pectin, which is mostly derived from citrus peel or apple pomace, is regarded as a mild mucoadhesive biopolymer with GRAS status, whose adhesive properties are often enhanced through deamidation and thiolation [79]. Lastly, the most relevant anionic and natural adhesive polymer is hyaluronic acid. This is a biocompatible and biodegradable glycosaminoglycan that plays a physiological role in the composition of the extracellular matrix and synovial fluids of mammals. Hyaluronic acid is currently obtained as a product of *Streptococcus* spp. fermentation, is included in many medicines and medical devices, and its mucoadhesive properties are likely to be due to its ability to form hydrogen bonds and electrostatic interactions, as well as to interpenetrate mucin chains [79]. If synthetic anionic mucoadhesive polymers are considered, polyacrylic acids (PAA), also named carbomers, are surely the most widely used [78]. PAA show good compatibility and their mucoadhesive potential is reported to be the result of hydrogen bonds between the carboxylic acid units of the polymer and the proton-accepting groups in mucins [79].

The last two categories of mucoadhesive polymers are cationic and amphoteric ones. Chitosan, trimethylated chitosan, and polylysine (discussed in Section 3.3.3) are examples of cationic polymers, and because of their positively charged surface can adhere to mucus

by electrostatic binding with the sialic acid within the mucus gel layer [78]. On the other hand, gelatin is the most common example of adhesive polymer bearing both cationic and anionic functional groups [76]. Amphoteric polymers exhibit a reduced mucoadhesive ability comparable to that of non-ionic polymers, therefore chemical modification has been adopted to improve their interaction with mucosal barriers [79].

3.5. *In situ* gelling polymers

Another commonly used method to improve the effectiveness of existing nasal formulations involves reducing mucociliary clearance by increasing the viscosity of the drug vehicle. This alteration can extend the time that drugs remain at the nasal administration site, aiding in the absorption of the therapeutic substances [80]. Nevertheless, the current market situation does not reflect the relevance of hydrophilic semisolid nasal formulations, named gels, in nasal delivery. Indeed, available nasal gels are just medical devices used for nasal mucosa hydration, while there is a lack of hydrogels intended for drug administration [81]. This seems to be due to the difficulties encountered while administering highly viscous solutions: the correct dosing and delivery of the formulation may be hampered by gel drying and, consequently, applicator blockage. As a result, the will to address traditional gels' constraints and the limited residence time of conventional nasal dosage forms prompted the research into *in situ* gel-forming systems [80,81]. These formulations owe their success to the ability of some polymers to undergo stimuli-triggered gelation, thus being liquid at room temperature (20 – 25 °C) and showing an increased viscosity just upon instillation in the nasal cavity because of environmental changes [82,83]. The free-flowing liquid state of *in situ* gelling vehicles before administration offers convenience in delivery and precise dosing, while the transition to a gel phase ensures prolonged contact time, enhancing bioavailability [80,82,83]. Additionally, the creation of a gel product guarantees the development of a sustained-release formulation, which can improve patient compliance by reducing the need for multiple daily administrations, minimizing fluctuations in drug levels, thereby reducing unwanted side effects and achieving improved therapeutic outcomes [80,83]. Because of the advantages they offer, *in situ* gelling formulations grabbed researchers' attention leading to the investigation of stimuli-sensitive polymers as new intranasal vehicles. By looking up in the scientific literature, it is observed that *in situ* gelation has been exploited for the local treatment of allergy through the delivery of APIs such as mometasone furoate [84], chlorpheniramine malate [85], and fexofenadine hydrochloride [86], but also for the administration of systemic-acting drugs like metoclopramide hydrochloride [87] used in the

management of nausea and vomiting. Besides, *in situ* gelation has been considered an attractive strategy for the nose-to-brain administration of different kinds of neurotherapeutics: ropinirole [88] and rasagiline mesylate [89] for Parkinson's disease, curcumin [90] and rivastigmine tartrate [91] for Alzheimer's disease, sumatriptan succinate [92] and almotriptan malate [93] for migraine treatment, doxepine [94] and tramadol [95] as anti-depressant drugs. Last but not least, even intranasal immunization might take advantage of these "smart" polymers. Indeed, Wu and co-workers demonstrated the feasibility of an *in situ* gelling system containing the split antigen H5N1 intended for immunization against the influenza virus [96].

Based on the stimulus that drives the sol-to-gel transition, *in situ* gelling formulations are classified into chemically cross-linked or physically cross-linked. The formers are not often used because they can potentially be harmful. For instance, photopolymerization, a widely employed technique to obtain chemically cross-linked hydrogels, may generate significant heat effects due to the exothermic reaction that occurs during polymerization. Alternatively, chemical compounds such as initiators, and co-cross-linkers, which all contain reactive groups, can be used, but they are to various extents toxic. Therefore, physical cross-linked hydrogels are usually preferred, because they require mild stimuli like temperature modulation, pH alteration, and changes in ions composition/abundance to gel [80].

3.5.1. Temperature-induced in situ gel systems

Among *in situ* gelling systems, temperature-induced ones are the most often used in drug delivery formulations. The ease of controlling temperature changes, applicability both *in vivo* and *in vitro*, and the fact that there is no need for external heat make them highly favorable [83]. In this case, gelling formulations contain polymers that undergo sol-to-gel transition once deposited on the mucosa because of an increase in temperature, which for the nasal cavity is considered between 35 and 37°C [81,82]. Polymers exhibiting this behavior may belong to different categories: synthetic examples include poloxamers; semi-synthetic varieties like methylcellulose and hydroxypropyl methylcellulose; and natural forms such as chitosan and xyloglucan [81].

Poloxamers (P) are amphiphilic surfactants made of a series of ABA tri-block copolymers containing hydrophilic-end groups of poly(ethylene oxide) (PEO) and hydrophobic core units of poly(propylene oxide) (PPO) [81,97]. These polymers, known under various trade names (Pluronics®, Lutrol®, Kolliphor®, Antarox®, and Synperonics®), have obtained approval from the FDA and are also listed in both the US and European Pharmacopoeia as safe, non-

toxic, and non-irritating excipients [97]. Poloxamers, when used at a concentration above their CMC, assemble to form micelles whose hydrophobic core can incorporate water-insoluble molecules facilitating their solubilization in aqueous media [80]. These micelles are also involved in the mechanism of gelation of the polymer: in a concentrated solution of poloxamers, micelles are formed; subsequently, the temperature rise determines the packing and entanglement of the micelles, as well as the dehydration of the PPO block and the removal of water from the micelle core, which ultimately result in the gelation of the system (**Figure PI 3.5**) [81]. Poloxamer 407 and poloxamer 188 are the most extensively utilized in pharmaceutical formulations, largely owing to their distinct attributes. These include their high solubilizing capacity, favorable drug-release qualities, and their compatibility with various biomolecules and chemical excipients [97]. Despite their advantageous features, there are some shortcomings linked to the use of poloxamers: they show low gelation temperatures, weak adhesion and mechanical strength, and rapid erosion. Consequently, these polymers are frequently blended with other macromolecules to tune their phase transition temperature, as well as gel strength and mucoadhesiveness [80,98].

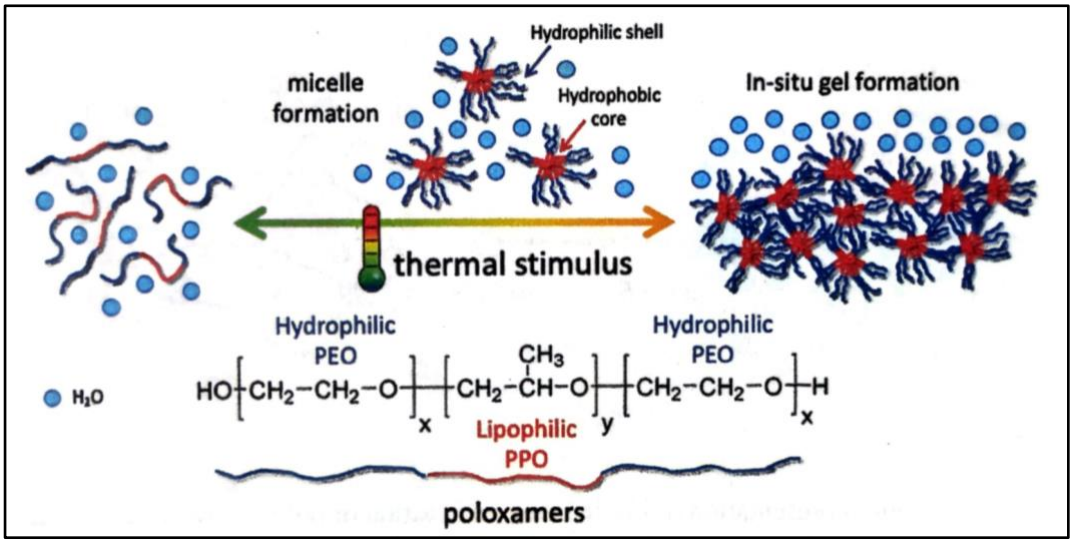

Figure PI 3.5 Molecular structure of poloxamers and their mechanism of gelation. From C. Pagano et al., 2023 [81].

Chitosan itself can be exploited as a thermosensitive polymer on the condition that polyol salts like β-glycerophosphate are used because they ensure the solubility of chitosan despite the increase in pH. The neutralizing effect of β-glycerophosphate makes the chitosan chain more flexible so that they can approach each other easily, thus increasing the strength of chitosan interchain hydrogen bonding. Afterward, upon exposure to higher temperatures, the internal energy of the system increases leading to the breakage of

hydrogen bonds between chitosan and water, thus hydrophobic side chains aggregate resulting in a gel form [80].

Along with chitosan, another naturally occurring gelling polymer that responds to temperature increase is xyloglucan, the main hemicellulose component of the cell wall of some dicotyledonous plants and most vascular plants. However, this polymer is rarely used for intranasal delivery because its low gelling temperatures (close to room temperature) hamper the correct administration of the product [80].

3.5.2. pH-induced in situ gel systems

Typically, polymers that undergo gelation in response to pH shifts are those containing acidic or basic groups, that either take or release protons depending on the environmental pH. An increase in external pH causes gelation in the case of anionic polymers, whereas with polycations the contrary is true [81,83]. Most of the polymers that are suitable for this approach are those containing anionic groups: polymethacrylic acid, carbomer and its derivatives, and polyethylene glycol to name a few [83]. The cross-linked poly acrylic acid Carbopol® is surely the most employed pH-responsive polymer; it is characterized by a high molecular weight and shows sol-to-gel transition at pH values above its pKa of 5.5. At a low pH of around 3.5, the carboxylic acid groups become protonated, causing the molecule to have no net charge. This situation restricts interactions between the polymer and the solvent, leading to a compacted polymer structure with a small hydrodynamic volume. When the pH increases, the carboxylic groups lose their protons, generating a negative charge along the polymer chain. These repelling forces cause the polymer to unwind, expanding into a highly swollen form, significantly increasing the viscosity of the solution. (**Figure PI 3.6**) [80,81]. Nevertheless, Carbopol® presents certain disadvantages: it necessitates a high concentration within a solution to create a rigid gel, and its acidic properties might provoke a stimulation of the nasal tissue. Consequently, to decrease the overall concentration of Carbopol® and improve the gel characteristics, it is advisable to blend it with another appropriate polymer [80].

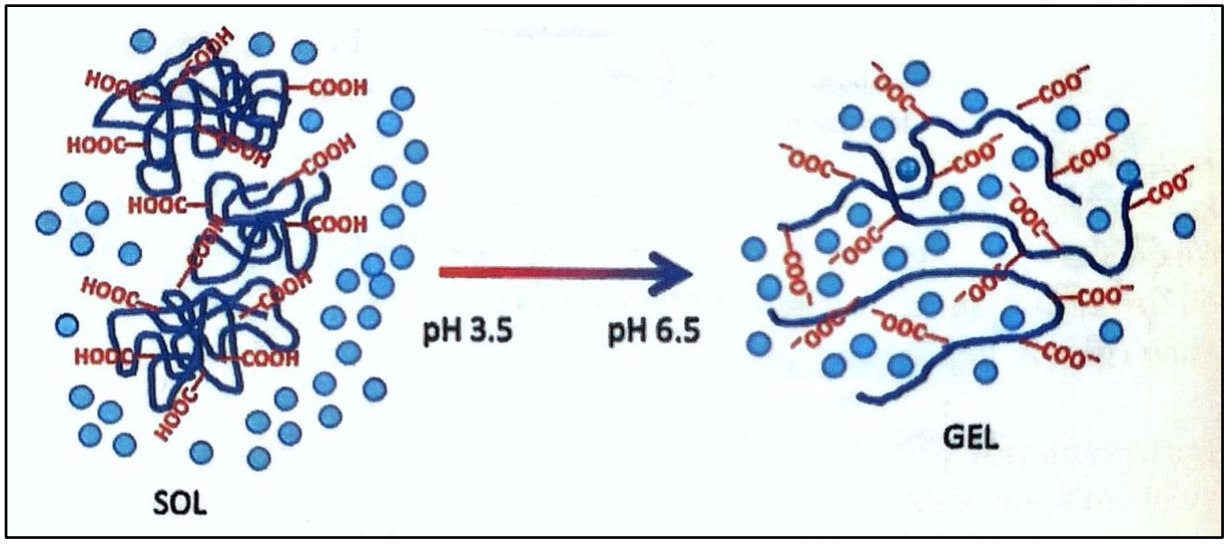

Figure PI 3.6 Mechanism of gelation of polyacrilic acid. From C. Pagano et al., 2023 [81].

3.5.3. Ion-induced in situ gel systems

The physiological composition of the nasal fluid offers another stimulus to trigger gelation in those polymers that are sensitive to the presence of various ions such as potassium, calcium, and sodium. This is the case of carrageenan, water-soluble biopolymers obtained from red algae. In particular, the κ-carrageenan creates firm and fragile gels in the presence of K^+ ions, while the ι-carrageenan forms flexible gels in the presence of Ca^{2+} ions [81]. Gellan gum is also subjected to ion-triggered sol-to-gel transition, which seems to be more efficient in the presence of divalent cations, like magnesium and calcium, rather than with monovalent ones. Moreover, its gelation mechanism is reported to be rapid because the concentration of cations in the nasal fluid is usually sufficient to drive the phase transition [80]. Further on, pectin exhibits ion-responsive gelation properties that vary depending on the degree of esterification of the galacturonic acid: when the content of esterified methoxy is below 50%, the hydrophilicity of the polymer increases and becomes sensitive to cations. Therefore, low methoxyl pectins are preferentially employed in nasal delivery, and their mechanism of gelation is well exemplified by the “egg box” model [80]. The latter, which applies to alginate as well, shows that upon increment of cations concentration, the polymer backbones align to favor the binding with ions. Thus cations are enclosed between two chains, enabling the formation of a three-dimensional network that leads to the gelation of the system (**Figure PI 3.7**) [80,81].

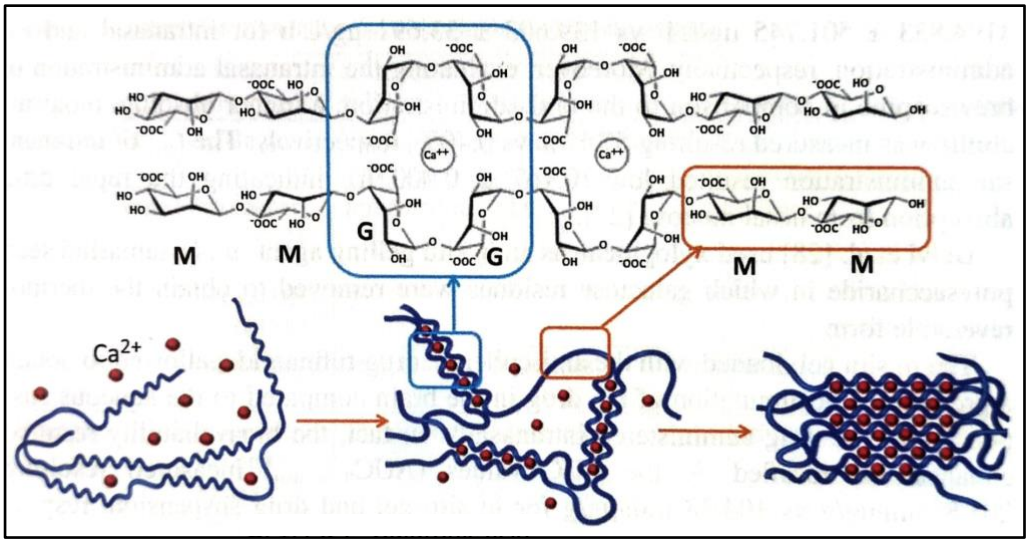

Figure PI 3.7 Mechanism of gelation of alginate in the presence of calcium ions. From C. Pagano et al., 2023 [81].

4. In vitro Permeation studies

The preclinical evaluation of novel drug candidates and formulations is a key point in the development of pharmaceuticals [99]. Numerous *in vitro* assays have been created and validated for initial-stage screening with the goal of eliminating molecules that do not demonstrate favorable characteristics in terms of delivery, toxicity, and efficacy [99,100]. In particular, the assessment of drug permeability, which involves evaluating the rate and extent of absorption across a specific biological barrier, is of paramount importance during research and development to identify drug candidates as well as the permeation enhancement ability of various compounds [101]. Granted that *in vivo* animal permeability studies better predict drug absorption in humans, tissue-based, cell-based, and cell-free models provide several advantages over the former. Indeed, the *in vitro* assay only requires a reduced amount of drug to be performed, implies minimal or no use of animals, enables the screening of a greater number of compounds, and the detection of analytes is simplified because of the absence of complex biological matrices [102]. In addition, *in vitro* models provide reproducibility, lower operational costs [102], standardization, because of the higher control of the experimental conditions, and simplicity, because they separate the permeation step across the epithelium from the subsequent absorption phase [103]. Numerous *in vitro* techniques aimed at predicting the extent as well as deepening the mechanism of *in vivo* drug permeation have been described, encompassing *ex vivo* tissue, *in vitro* primary or immortalized cell cultures, and cell-free permeation tools [104].

4.1. Tissue-based models

The most straightforward strategy to reproduce the complex composition of the nasal mucosa *in vitro* is to work with *ex vivo* models. These are obtained by extracting entire tissues, either from human donors who have undergone surgery in hospitals or, in situations where the availability of human nasal mucosa is limited, from animals. Thanks to some studies aimed at comparing the histology and morphology of both animal and human nasal mucosa, it was possible to identify animal species exploitable as tissue donors [105]. Among the most employed animals are rabbits, sheep, goats, calves, and pigs [101,105,106]. Furthermore, considering the animal source, the nasal epithelium is easily accessible from local slaughterhouses, implying that animals are not specifically sacrificed for tissue obtainment, and the explants are of high quality and safe to handle, as diseased animals are not processed for slaughter [101]. Properly named *ex vivo* models are those in which the collected tissues are used for permeation studies within 0.5 – 4 hours from harvesting (in the case of patients undergoing surgery) or animal sacrifice, in order to ensure cell viability [105]. If tissue viability is not maintained, for example because the post-mortem delay is longer than 4 hours or because excised tissues are not immediately used but stored at -20°C, then it is suggestable to refer to tissue-based models. These latter are characterized by membrane integrity, meaning that they can be still used for permeation tests, but cannot account for mechanisms that suppose living cells [105,107]. After retrieving the nasal tissue, the permeability assay is conducted by securing it onto a diffusion apparatus, often represented by either a Ussing chamber or a Franz vertical diffusion cell [105]. The Ussing chamber technique, which was first developed to study transepithelial ion transport and was only later adapted to evaluate the permeability of drugs, exploits a chamber divided into two halves by the mucosal tissue. Both halves of the chamber, named donor and acceptor compartments, are loaded with a physiological buffer, maintained at a specific temperature, and constantly supplied with 95% O_2 and 5% CO_2, which serves a pivotal role: the gas mixture ensures sufficient oxygenation of the tissue and induces fluid circulation in both compartments. This helps mitigate the impact of the unstirred water layer, which can compromise the permeability of poorly soluble drugs. The drug to be tested is added to the buffer in the donor chamber and sampled from the acceptor chamber at regular time intervals; moreover, the presence of two electrodes placed in both chambers allows the monitoring of parameters like barrier integrity and tissue viability (**Figure PI 4.1a**) [108]. The Franz diffusion cell system is known for being the officially recognized Pharmacopoeial method primarily designed for studying transdermal formulation diffusion. However, having

a look at the scientific literature, it also stands out as one of the most frequently employed methods for investigating intranasal dosage forms [109]. As the name suggests, the apparatus is arranged in a vertical orientation, comprising an upper donor chamber and a bottom acceptor chamber. The two are connected by a flat ground glass joint and physically separated by a membrane, in this case, the excised epithelial tissue. The sample to be tested is released directly on the nasal mucosa and allowed to permeate across the biological barrier reaching the acceptor chamber, which is filled with the diffusion medium. The acceptor chamber is enveloped by a water jacket, in which heated water circulates to keep the diffusion medium at the required body temperature, and is also supplied with both a sampling port for withdrawing medium aliquots, and a magnetic stirring bar to ensure a uniform distribution of the permeated API (**Figure PI 4.1b**) [104].

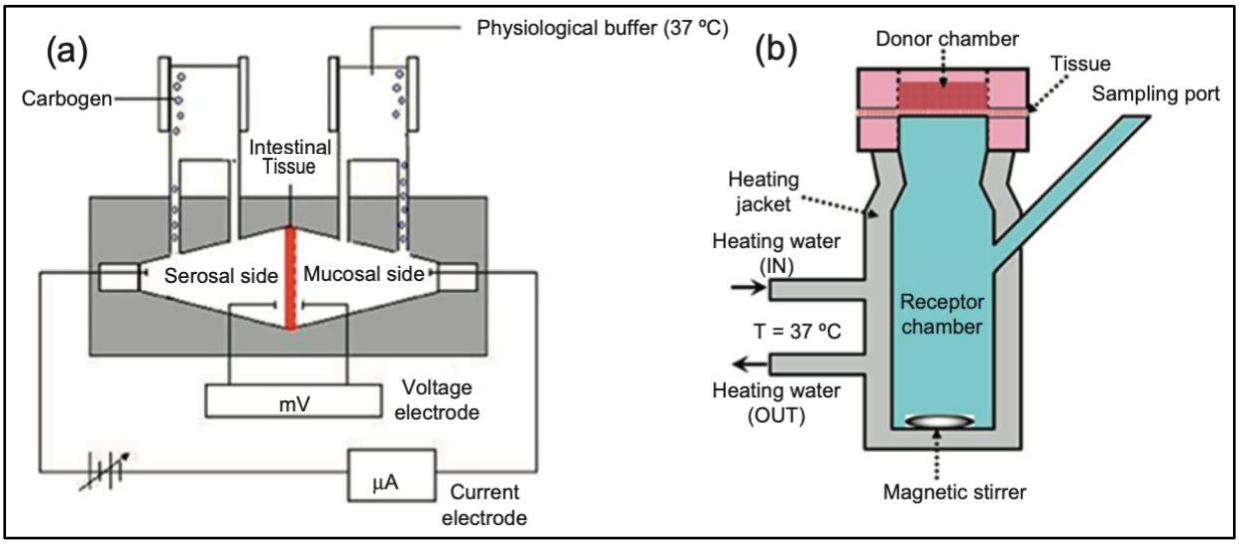

Figure PI 4.1 Typical set up for *in vitro* permeation studies using donor-acceptor diffusion apparatus. (a) Ussing chamber. (b) Franz diffusion cell. From R. Nunes *et al.*, 2016 [108].

Research involving excised tissues serves as a valuable tool for gathering insights into the impact of enhancers on flux and their concentration-dependent effects. These studies also investigate the reversibility and recovery time of enhancement, assess tissue damage through histological examination, and evaluate the effect on ciliary beat frequency. Nevertheless, tissue-based models are affected by some shortcomings. In particular, the short period of tissue viability, together with attributes like the thickness of nasal epithelial tissues, and the distribution and activity of metabolic enzymes which may significantly differ among species, but also across specimens obtained from the same source. Due to the inter and intraspecies variations, achieving a strong correlation between *in vitro* and *in vivo* nasal absorption studies is exceptionally challenging. Hence, the employment of excised tissue in

preclinical drug development studies is primarily recognized as a valuable method for comprehending solute transport across the nasal epithelium and exploring diverse strategies to enhance mucosal drug permeation [101].

4.2. Cell-based models

Even though the tissue-based model provides numerous advantages, such as the use of actual nasal tissue instead of a mimicked model, the limitations that present fostered the search for other *in vitro* alternatives [105]. In this context, cell culture models have gained a lot of attention, as they are easily standardized, are suitable for routine testing, and allow for high-throughput screening [104,105]. Cell-based permeability studies may be performed across either primary or immortalized cells and usually employ the transwell support system. In the assay, epithelial cells are grown to create a dense monolayer on a microporous semipermeable membrane filter, which provides mechanical support to the cell layer without hampering the solutes' diffusion. Subsequently, the cell-covered membrane is positioned in a multiwell plate between two fluid compartments, so that any solute flux from one compartment to the other can only occur by crossing the cell layer. The uppermost compartment, named apical, corresponds to the luminal side of the epithelium and is where the formulation/compound to be tested is placed; instead, the compartment underneath the support membrane is called basal, corresponds to the basolateral side of the epithelium, and is filled with a diffusion medium capable of maintaining cell viability and barrier integrity (**Figure PI 4.2**) [110].

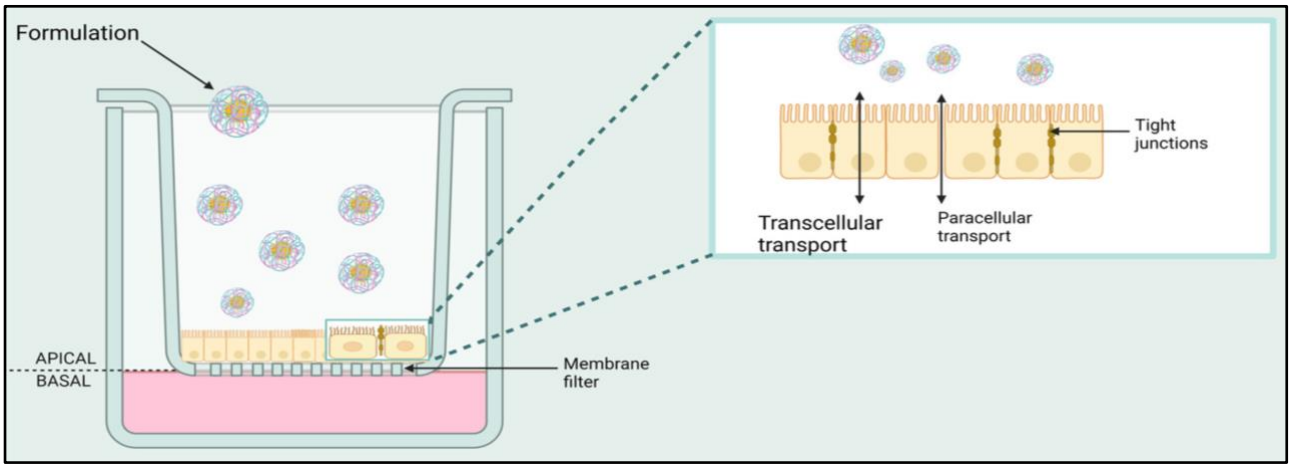

Figure PI 4.2 An overview of a transwell support setup. From R. Boyuklieva *et al.*, 2023 [112].

4.2.1. Primary cell models

Primary cells are isolated from living organisms and are then cultured using *in vitro* techniques to create a barrier system mimicking those physiological traits that can influence drug pharmacokinetic properties upon nasal administration [104]. Human nasal epithelial primary cells (HNEpC) are the most reliable for closely resembling the natural airway epithelium as they are sourced directly from patients subjected to endonasal surgery. Moreover, their significant differentiative capacity allows the formation of a cell monolayer that exhibits essential features such as mucin secretion, microvilli, cilia, aminopeptidases, and tight junctions [111]. However, the use of HNEpC may be constrained by ethical considerations associated with obtaining human tissues, as well as the reduced number of nasal cells derived from a single donor. This necessitates the collection of multiple samples from various individuals, resulting in heterogeneity among cell cultures due to donor-to-donor variability [104,111,112]. Just as with *ex vivo* models, issues such as the shortage of human tissues and ethical concerns can be tackled by using animal models as donors of primary cells, which can differentiate into a tissue with a histologically heterogeneous cell composition resembling that of the human nasal mucosa. To date, murine [113] and porcine [114] cells from different nasal regions have been isolated and successfully employed to develop *in vitro* models of the respiratory and olfactory mucosa [104,112]. The main challenges that are common to both human and animal primary cells include the need for substantial cell quantities, the limited lifespan of cultures, restricted possibilities for subculturing, the constant necessity to acquire fresh cell sources for each study, and variability between and within cultures [103]. Discrepancies observed in *in vitro* differentiation outcomes can be attributed to variations in the isolation process, the composition of the culture medium, the nature of the cell-support substrate, the cell seeding density, and the choice of cultivating primary cells in submerged conditions rather than at the air-liquid interface (ALI). Regarding the latter point, it is worth mentioning that when cell monolayers are cultivated in submerged conditions, it means that both the apical and basolateral side of the epithelium are in contact with the culture medium; differently, when the ALI condition is adopted, the culture medium is removed from the apical compartment. Opting for one method or the other has a significant impact on cell morphology: submerged conditions originate denuded and flattened ciliated cells with microvilli and incomplete cilia, while ALI cultures show cubical and cobblestone cells with a great number of long cilia [115]. Culturing conditions also affect the barrier function of the developed cell monolayer. As it was observed, the primary cell-based model tends to express an excessive number of tight

junctions compared to *ex vivo* tissues, which ultimately may lead to an underestimation of the permeability of molecules absorbed through the paracellular pathway; but, more notably, submerged cultured primary cells exhibit less tight junction that those maintained in ALI conditions, as demonstrated by significant differences in transepithelial electrical resistance (TEER) values [106]. An alternative solution to exploit the reliability of primary cell-based models while reaching a higher standardization level and saving the time required for cell differentiation is to use some precultured tissue models, like MucilAir™ and EpiAirway™, commercialized by Epithelix and MatTek Corporation, respectively [104]. These models are developed using freshly isolated HNEpC obtained from nasal biopsies (MucilAir™) or bronchial biopsies (EpiAirway™). They accurately replicate the physiology of human airway epithelia, encompassing a functional mucociliary system and the secretion of mucus in a homeostatic state [116].

4.2.2. Immortalized cell models

Immortalized cell lines were developed to overcome the disadvantages of primary cells. Indeed, they have a high proliferation capacity, are characterized by an extended or permanent lifespan, in terms of *in vitro* cultivation, are less expensive and effort-demanding, and offer better standardization because of their genetic stability [115]. The most used cell lines for nasal drug permeability studies are RPMI 2650, 16HBE14o, and Calu-3 [112].

So far, RPMI 2650 is the sole nasal immortalized cell line derived from humans [105]. Originating from an anaplastic squamous cell carcinoma of the nasal septum, this cell line has been frequently employed for investigating drug metabolism and toxicity, but it was initially found unsuitable for drug transport studies [111]. In fact, its metabolic activity resembles that of normal nasal tissue with reported aminopeptidase activity, but it tends to grow in multilayer aggregates rather than produce confluent monolayers. Moreover, neither goblet cells, nor ciliated cells are developed after RPMI 2650 *in vitro* cultivation, and instead of tight junctions, only perijunctional actin rings can be detected [117]. However, in recent years, efforts have been made to optimize this cell model. By utilizing specific cell supports, incorporating an extracellular matrix into the cell substrate, and employing either ALI or submerged culture conditions, it has become feasible to generate tight barrier properties and form confluent monolayers [111].

16HBE14o and Calu-3 are immortalized human cell lines as well, but they are not derived from the nasal cavity. The former is a bronchial epithelial cell line, derived from a 1-year-old male, and was immortalized using the SV40 plasmid with a defective origin of replication. It

has served as a valuable model for studying the airway epithelium, as it shows morphological characteristics, barrier properties, and expression of drug transporters similar to those observed *in vivo* [112]. Calu-3 cells, instead, are sourced from a lung submucosal adenocarcinoma. Despite their origin, these cells exhibit features close to serous nasal cells, making them valuable for studies focused on nasal permeability. These cells can form differentiated, tight, and polarized layers with a combined phenotype, encompassing both ciliated and secretory cells. They possess microvilli, express various cell junction proteins, and contain mucin granules [111].

Even though permanent cell lines are regarded as a valuable alternative to primary cells, the immortalization process might cause changes in the morphological features of the original cells. Consequently, immortalized cell models are not as close as primary cell-based membranes and *ex vivo* tissues to the human nasal mucosa. As a result, during the initial stages of drug development, especially when evaluating different APIs, excipients, and formulations, it can be useful to employ well-standardized models to minimize additional variabilities. It is only in the later stages, once the most promising compounds are identified, that research can be expanded by including information from more complex models [105].

4.3. Cell-free models

Although tissue and cell-based permeation models offer reasonable predictive accuracy, their drawback lies in the time-consuming and costly preparation process, which could be significantly reduced if cell-free tools are employed [118]. This is not the only advantage that these kinds of *in vitro* models can offer. Cell-free permeation assays, readily available in the commercial market, are appropriate for industrial applications. Their standardized production not only enhances result reproducibility but also offers versatility through different formats, such as multiwell diffusion cells suitable for high-throughput screening or vertical/horizontal diffusion systems [119]. As with any other *in vitro* model, cell-free tools also have their limit: they can only account for passive diffusion mechanisms. Anyway, it must be highlighted that while active transport of molecules takes place only in specific cases, passive diffusion occurs for all compounds, affecting every ADME (Absorption, Distribution, Metabolism, and Excretion) property of the tested drug [119,120]. Based on the composition of the barrier, cell-free models are commonly categorized into two classes: biomimetic barriers, containing phospholipids, and non-biomimetic barriers which rely on dialysis membranes [118].

4.3.1. Parallel Artificial Membrane Permeation Assay (PAMPA)

PAMPA, developed in the late 90s, has stood as the prevailing cell-free permeation assay over the years. Initially, it was designed for a 96-well plate configuration, with the hydrophobic support filter featuring pores ranging from 0.22 to 0.45 μm. This filter was saturated with a solution comprising 1–20% egg lecithin in an organic solvent to replicate the phospholipid composition of the mammalian cell membrane. Because of this configuration, the mechanism that controls drug permeability across the membrane is the partitioning/distribution coefficient and the diffusivity of the solute in the lipid barrier (**Figure PI 4.3**) [118,119].

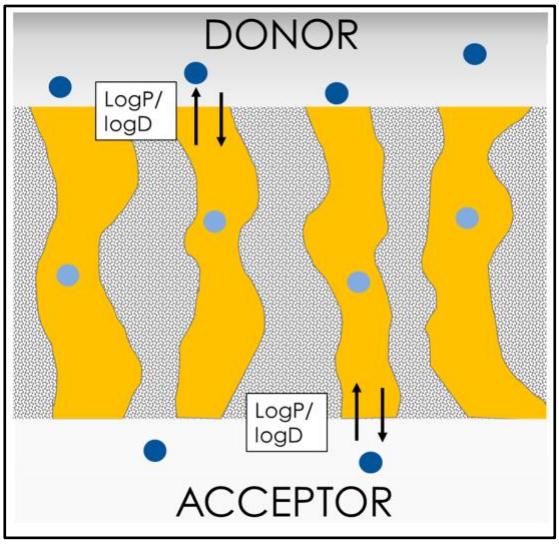

Figure PI 4.3 Architecture of the PAMPA biomimetic model. From A. Jacobsen *et al.*, 2023 [119].

In the following years, the PAMPA model has given rise to multiple iterations featuring different lipid compositions, which has paved the way for research in the creation of tissue-specific variants of the barrier [119,121]. Recently, P. Henriques and colleagues developed the first nasal-PAMPA model for the prediction of drug permeability across the nasal epithelium. The resultant biomimetic barrier comprises 2% phosphatidylcholine, the prevalent lipid component in biological membranes as well as the primary lipid in bovine, porcine, and rat nasal epithelium. Additionally, it incorporates 0.5% mucin, the principal constituent of the mucus layer, which plays a key role in hampering the transport of molecules across the mucosa. The authors illustrated that incorporating mucin into the PAMPA model enhanced its predictive accuracy and that the permeability values obtained exhibited an improved correlation with those derived from the RPMI 2650 cell-based model [122]. To date, the PAMPA model has been able to satisfy both the academic and the

industrial perspectives. The former takes particular advantage of the flexibility of the cell-free tool as it can be easily modified according to the aim of the research; at the same time, the availability of ready-to-use PAMPA barriers (i.e. precoated versions), better suits the need for pharmaceutical companies to minimize experiment variabilities as much as possible [119]. However, due to the absence of a physical separation between the donor media and the lipophilic barrier components, there is a potential for dissolution/emulsification phenomena to take place [118]. This is particularly true when testing enabling formulations, which might contain permeation or solubility enhancers. In fact, according to the specific composition of the barrier, some concentration-dependent incompatibilities have been observed: the use of Cremophor EL, Tween 80, Brij 35, Solutol HS 15, and Triton-X over a certain threshold can cause the solubilization of the lipids that fill the membrane pores. Furthermore, owing to its structural configuration, the PAMPA model appears to be incapable of accounting for paracellular diffusion, resulting in a limitation in predicting the permeability of hydrophilic compounds [119].

4.3.2. Phospholipids vesicles-based permeation assay (PVPA)

PVPA is a relatively novel *in vitro* method representative of the intestinal epithelium and thus intended for the estimation of passive permeation of orally administered drugs. This membrane comprises liposomes prepared through film hydration and filter extrusion methods, with the aim to produce vesicles with diverse size distributions and lamellarity, which are then deposited onto a porous filter. A portion of the liposome suspension is allowed to accumulate within the pores of the filter, while another portion forms a surface layer. Ultimately, the liposomes are fused through solvent evaporation and a freeze-thawing cycle. (**Figure PI 4.4**) [118,121].

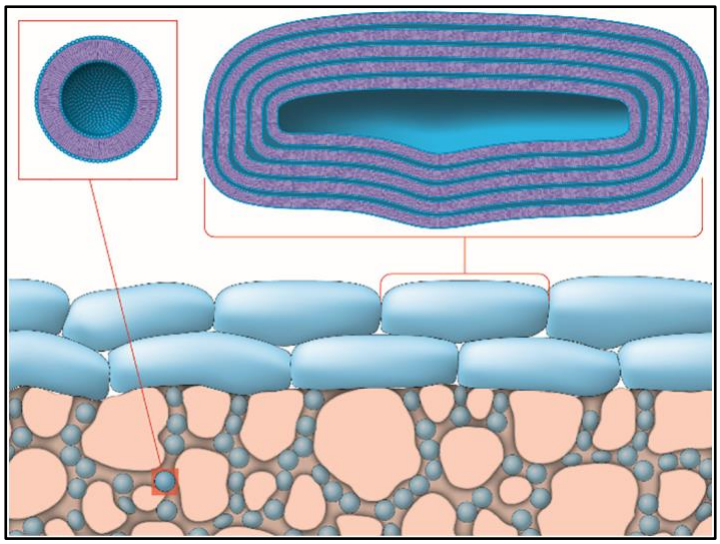

Figure PI 4.4 Architecture of the PVPA biomimetic model. From P. Berben *et al.*, 2018 [118].

In contrast to the PAMPA model, this biomimetic membrane does not incorporate any organic solvent, and studies conducted to evaluate barrier integrity have ensured that any observed effects are not due to changes in the barrier structure. Additionally, compatibility with various solubilizing excipients has been demonstrated. [121]. Much like the PAMPA model, this cell-free tool provides the flexibility to adjust the lipid composition based on the targeted site of absorption. However, due to its inherent components and structural design, the PVPA model has the potential to function as a general model, simulating various biological barriers, including the nasal mucosa [118]. This was demonstrated by G. Corace and co-workers who investigated the ability of some multifunctional liposomes, containing α-tocopherol and Omega3 fatty acids, to influence tacrine hydrochloride nose-to-brain permeability. Permeation assays were performed across both the original PVPA model and the *ex vivo* sheep nasal mucosa and, although the permeability absolute values were different for the two assays employed, the predicted trend was very similar [123].

4.3.3. Permeapad®

Since its main constituents are immobilized phospholipids, the Permeapad® barrier can be considered an evolution of the PVPA model [119]. Specifically, this commercially available biomimetic membrane is characterized by a dry film of soybean phosphatidylcholine S-100 which is sandwiched between two low-retention layers of regenerated cellulose, that serve as support sheets. When the barrier encounters water, the dry lipids undergo swelling, thus forming a dense layer of vesicles (**Figure PI 4.5**). Their distribution within the support sheets produces an alternate structure made of two layers, one consisting of phospholipids and the other of water, which is also typical of cell membranes. Moreover, the single vesicles remain

in close contact with each other, mimicking cell organization within a tissue [118]. Based on its architecture, the PermeaPad® model does not only allow for the evaluation of passive diffusion across the lipid bilayer, but it also accounts for paracellular diffusion. In fact, as previously said, the interspaces between the phospholipid vesicles are filled with water, thus being comparable to the intercellular spaces [119].

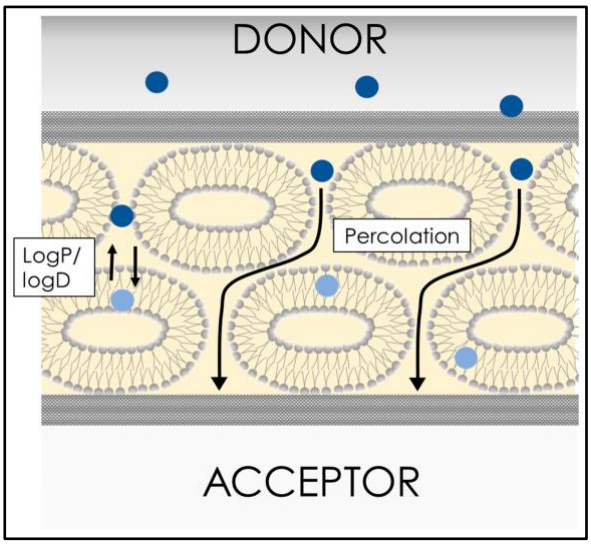

Figure PI 4.5 Architecture of the PermeaPad® barrier. From A. Jacobsen *et al.*, 2023 [119].

Blocking of the liposomal gel between the support layers gives the PermeaPad® a striking advantage over both the PAMPA and the PVPA models: since lipids do not come in direct contact with the solution contained in the donor compartment, are not subjected to solubilization or leakage [118]. In addition, this layered structure is also probably responsible for the barrier's improved stability over a wide range of pH [124], and in the presence of different surfactants and co-solvents [125]. Nevertheless, the same architecture that enhances stability can be viewed as a limitation in terms of the flexibility of lipid composition, because it cannot be as easily modified as in the case of the PAMPA and PVPA models [119]. Despite it was originally designed as a membrane capable of mimicking the mucosa of the gastrointestinal tract, the PermeaPad® barrier has also been used in the nasal drug delivery field. I.Y. Wu et al., for example, employed this cell-free model to dig into the drug release mechanisms from large unilamellar vesicles, obtaining some interesting results that might be of relevance for the development of similar formulations intended for nose-to-brain delivery [126].

4.3.4. Non-biomimetic barriers

Non-biomimetic *in vitro* models are commercially available membranes consisting of a thin sheet of fibrous material that does not comprise lipids. Regenerate cellulose is the most frequently employed material to obtain this cell-free models, which are distinguished not by the presence of micrometric pores of uniform size, but by a dense and non-uniform network of cellulose fibers. Hence, as the fiber density increases, the molecular weight cut-off size decreases. In this model, the examined molecule will diffuse through the hydrated pores with minimal partitioning; thus, drug permeability profiling will be significantly affected by the solute's diffusivity in water and by its hydrodynamic radius. Nevertheless, even though some may argue that non-biomimetic barriers should be mainly considered a size exclusion membrane, cell-free models based on regenerate cellulose have been extensively used for permeability measurements, in the context of nasal delivery as well [119]. Some nasal powders of quercetin-β-cyclodextrin derivatives complexes were subjected to diffusion studies across both a regenerated cellulose membrane cut-off 5000 Da and the *ex vivo* rabbit nasal mucosa. The study revealed that despite the different structures of the two barriers, the permeated amount achieved was almost the same and they predicted as most successful the same formulations [127].

5. References Part I

1. Keller, L.-A.; Merkel, O.; Popp, A. Intranasal Drug Delivery: Opportunities and Toxicologic Challenges during Drug Development. Drug Deliv. Transl. Res. 2021, doi:10.1007/s13346-020-00891-5.
2. Cingi, C.; Bayar Muluk, N.; Mitsias, D.I.; Papadopoulos, N.G.; Klimek, L.; Laulajainen-Hongisto, A.; Hytönen, M.; Toppila-Salmi, S.K.; Scadding, G.K. The Nose as a Route for Therapy: Part 1. Pharmacotherapy. Front. Allergy 2021, 2, 638136, doi:10.3389/falgy.2021.638136.
3. Lobaina Mato, Y. Nasal Route for Vaccine and Drug Delivery: Features and Current Opportunities. Int. J. Pharm. 2019, 572, 118813, doi:10.1016/j.ijpharm.2019.118813.
4. Pires, A.; Fortuna, A.; Alves, G.; Falcão, A. Intranasal Drug Delivery: How, Why and What For? J. Pharm. Pharm. Sci. 2009, 12, 288, doi:10.18433/J3NC79.
5. Kapoor, M.; Cloyd, J.C.; Siegel, R.A. A Review of Intranasal Formulations for the Treatment of Seizure Emergencies. J. Controlled Release 2016, 237, 147–159, doi:10.1016/j.jconrel.2016.07.001.

6. Harkema, J.R.; Carey, S.A.; Wagner, J.G. The Nose Revisited: A Brief Review of the Comparative Structure, Function, and Toxicologic Pathology of the Nasal Epithelium. Toxicol. Pathol. 2006, 34, 252–269, doi:10.1080/01926230600713475.
7. Martin, V.; Hoekman, J.; Aurora, S.K.; Shrewsbury, S.B. Nasal Delivery of Acute Medications for Migraine: The Upper Versus Lower Nasal Space. J. Clin. Med. 2021, 10, 2468, doi:10.3390/jcm10112468.
8. Gänger, S.; Schindowski, K. Tailoring Formulations for Intranasal Nose-to-Brain Delivery: A Review on Architecture, Physico-Chemical Characteristics and Mucociliary Clearance of the Nasal Olfactory Mucosa. Pharmaceutics 2018, 10, 116, doi:10.3390/pharmaceutics10030116.
9. Laffleur, F.; Bauer, B. Progress in Nasal Drug Delivery Systems. Int. J. Pharm. 2021, 607, 120994, doi:10.1016/j.ijpharm.2021.120994.
10. Illum, L. Nasal Drug Delivery—Possibilities, Problems and Solutions. J. Controlled Release 2003, 87, 187–198, doi:10.1016/S0168-3659(02)00363-2.
11. Aulton, M.E.; Taylor, K.M.G.; Caviglioli, G.; Campani, V. Aulton tecnologie farmaceutiche: progettazione e allestimento dei medicinali; Edra: Milano, 2015; ISBN 978-88-214-3870-7.
12. Chung, S.; Peters, J.M.; Detyniecki, K.; Tatum, W.; Rabinowicz, A.L.; Carrazana, E. The Nose Has It: Opportunities and Challenges for Intranasal Drug Administration for Neurologic Conditions Including Seizure Clusters. Epilepsy Behav. Rep. 2023, 21, 100581, doi:10.1016/j.ebr.2022.100581.
13. Behl, C.R.; Pimplaskar, H.K.; Sileno, A.P.; deMeireles, J.; Romeo, V.D. Effects of Physicochemical Properties and Other Factors on Systemic Nasal Drug Delivery. Adv. Drug Deliv. Rev. 1998, 29, 89–116, doi:10.1016/S0169-409X(97)00063-X.
14. Zhang, Y.-B.; Xu, D.; Bai, L.; Zhou, Y.-M.; Zhang, H.; Cui, Y.-L. A Review of Non-Invasive Drug Delivery through Respiratory Routes. Pharmaceutics 2022, 14, 1974, doi:10.3390/pharmaceutics14091974.
15. Costantino, H.R.; Illum, L.; Brandt, G.; Johnson, P.H.; Quay, S.C. Intranasal Delivery: Physicochemical and Therapeutic Aspects. Int. J. Pharm. 2007, 337, 1–24, doi:10.1016/j.ijpharm.2007.03.025.
16. Keller, L.-A.; Merkel, O.; Popp, A. Intranasal Drug Delivery: Opportunities and Toxicologic Challenges during Drug Development. Drug Deliv. Transl. Res. 2022, 12, 735–757, doi:10.1007/s13346-020-00891-5.

17. Hussain, A.A. Intranasal Drug Delivery. Adv. Drug Deliv. Rev. 1998, 29, 39–49, doi:10.1016/S0169-409X(97)00060-4.
18. Grassin-Delyle, S.; Buenestado, A.; Naline, E.; Faisy, C.; Blouquit-Laye, S.; Couderc, L.-J.; Le Guen, M.; Fischler, M.; Devillier, P. Intranasal Drug Delivery: An Efficient and Non-Invasive Route for Systemic Administration. Pharmacol. Ther. 2012, 134, 366–379, doi:10.1016/j.pharmthera.2012.03.003.
19. Fortuna, A.; Alves, G.; Serralheiro, A.; Sousa, J.; Falcão, A. Intranasal Delivery of Systemic-Acting Drugs: Small-Molecules and Biomacromolecules. Eur. J. Pharm. Biopharm. 2014, 88, 8–27, doi:10.1016/j.ejpb.2014.03.004.
20. Illum, L. Transport of Drugs from the Nasal Cavity to the Central Nervous System. Eur. J. Pharm. Sci. 2000, 11, 1–18, doi:10.1016/S0928-0987(00)00087-7.
21. Dhas, N.; Yadav, D.; Singh, A.; Garkal, A.; Kudarha, R.; Bangar, P.; Savjani, J.; Pardeshi, C.V.; Garg, N.; Mehta, T. Direct Transport Theory: From the Nose to the Brain. In Direct Nose-to-Brain Drug Delivery; Elsevier, 2021; pp. 15–37 ISBN 978-0-12-822522-6.
22. Jeong, S.-H.; Jang, J.-H.; Lee, Y.-B. Drug Delivery to the Brain via the Nasal Route of Administration: Exploration of Key Targets and Major Consideration Factors. J. Pharm. Investig. 2023, 53, 119–152, doi:10.1007/s40005-022-00589-5.
23. Sridhar, V.; Gaud, R.; Bajaj, A.; Wairkar, S. Pharmacokinetics and Pharmacodynamics of Intranasally Administered Selegiline Nanoparticles with Improved Brain Delivery in Parkinson's Disease. Nanomedicine Nanotechnol. Biol. Med. 2018, 14, 2609–2618, doi:10.1016/j.nano.2018.08.004.
24. Chang, Y.; Wang, L.-B.; Li, D.; Lei, K.; Liu, S.-Y. Efficacy of Rasagiline for the Treatment of Parkinson's Disease: An Updated Meta-Analysis. Ann. Med. 2017, 49, 421–434, doi:10.1080/07853890.2017.1293285.
25. Jogani, V.V.; Shah, P.J.; Mishra, P.; Mishra, A.K.; Misra, A.R. Intranasal Mucoadhesive Microemulsion of Tacrine to Improve Brain Targeting. Alzheimer Dis. Assoc. Disord. 2008, 22, 116–124, doi:10.1097/WAD.0b013e318157205b.
26. Van Woensel, M.; Wauthoz, N.; Rosière, R.; Mathieu, V.; Kiss, R.; Lefranc, F.; Steelant, B.; Dilissen, E.; Van Gool, S.W.; Mathivet, T.; et al. Development of siRNA-Loaded Chitosan Nanoparticles Targeting Galectin-1 for the Treatment of Glioblastoma Multiforme via Intranasal Administration. J. Controlled Release 2016, 227, 71–81, doi:10.1016/j.jconrel.2016.02.032.

27. Czerkinsky, C.; Holmgren, J. Topical Immunization Strategies. Mucosal Immunol. 2010, 3, 545–555, doi:10.1038/mi.2010.55.
28. Kraehenbuhl, J.-P.; Neutra, M. Mucosal Vaccines: Where Do We Stand? Curr. Top. Med. Chem. 2013, 13, 2609–2628, doi:10.2174/15680266113136660186.
29. Ghadiri, M.; Young, P.; Traini, D. Strategies to Enhance Drug Absorption via Nasal and Pulmonary Routes. Pharmaceutics 2019, 11, 113, doi:10.3390/pharmaceutics11030113.
30. Govender, M.; Indermun, S.; Kumar, P.; Choonara, Y.E. Potential Targeting Sites to the Brain Through Nasal Passage. In Nasal Drug Delivery; Pathak, Y.V., Yadav, H.K.S., Eds.; Springer International Publishing: Cham, 2023; pp. 83–99 ISBN 978-3-031-23111-7.
31. Arora, P.; Sharma, S.; Garg, S. Permeability Issues in Nasal Drug Delivery. Drug Discov. Today 2002, 7, 967–975, doi:10.1016/S1359-6446(02)02452-2.
32. Merkus, F.W.; Verhoef, J.C.; Schipper, N.G.; Marttin, E. Nasal Mucociliary Clearance as a Factor in Nasal Drug Delivery. Adv. Drug Deliv. Rev. 1998, 29, 13–38, doi:10.1016/s0169-409x(97)00059-8.
33. Sigurdsson, H.H.; Kirch, J.; Lehr, C.-M. Mucus as a Barrier to Lipophilic Drugs. Int. J. Pharm. 2013, 453, 56–64, doi:10.1016/j.ijpharm.2013.05.040.
34. Pandey, V.; Gadeval, A.; Asati, S.; Jain, P.; Jain, N.; Roy, R.K.; Tekade, M.; Soni, V.; Tekade, R.K. Formulation Strategies for Nose-to-Brain Delivery of Therapeutic Molecules. In Drug Delivery Systems; Elsevier, 2020; pp. 291–332 ISBN 978-0-12-814487-9.
35. Martins, P.P.; Smyth, H.D.C.; Cui, Z. Strategies to Facilitate or Block Nose-to-Brain Drug Delivery. Int. J. Pharm. 2019, 570, 118635, doi:10.1016/j.ijpharm.2019.118635.
36. Morimoto, K.; Yamaguchi, H.; Iwakura, Y.; Miyazaki, M.; Nakatani, E.; Iwamoto, T.; Ohashi, Y.; Nakai, Y. Effects of Proteolytic Enzyme Inhibitors on the Nasal Absorption of Vasopressin and an Analogue. Pharm. Res. 1991, 8, 1175–1179, doi:10.1023/a:1015862603939.
37. Bernkop-Schnürch, A. The Use of Inhibitory Agents to Overcome the Enzymatic Barrier to Perorally Administered Therapeutic Peptides and Proteins. J. Controlled Release 1998, 52, 1–16, doi:10.1016/S0168-3659(97)00204-6.
38. Dhamankar, V.; Donovan, M.D. Modulating Nasal Mucosal Permeation Using Metabolic Saturation and Enzyme Inhibition Techniques. J. Pharm. Pharmacol. 2017, 69, 1075–1083, doi:10.1111/jphp.12749.

39. Maher; Casettari; Illum Transmucosal Absorption Enhancers in the Drug Delivery Field. Pharmaceutics 2019, 11, 339, doi:10.3390/pharmaceutics11070339.
40. Deruyver, L.; Rigaut, C.; Lambert, P.; Haut, B.; Goole, J. The Importance of Pre-Formulation Studies and of 3D-Printed Nasal Casts in the Success of a Pharmaceutical Product Intended for Nose-to-Brain Delivery. Adv. Drug Deliv. Rev. 2021, 175, 113826, doi:10.1016/j.addr.2021.113826.
41. Velloso, M.I.; Landoni, F. Penetration Enhancers for the Development of Intranasal Formulations for Use in Equines. Int. J. Equine Sci. 2022, 1.
42. Kim, D.-H.; Lee, S.-E.; Pyo, Y.-C.; Tran, P.; Park, J.-S. Solubility Enhancement and Application of Cyclodextrins in Local Drug Delivery. J. Pharm. Investig. 2020, 50, 17–27, doi:10.1007/s40005-019-00434-2.
43. Yang, P.; Li, Y.; Li, W.; Zhang, H.; Gao, J.; Sun, J.; Yin, X.; Zheng, A. Preparation and Evaluation of Carfentanil Nasal Spray Employing Cyclodextrin Inclusion Technology. Drug Dev. Ind. Pharm. 2018, 44, 953–960, doi:10.1080/03639045.2018.1425426.
44. Marcello, E.; Chiono, V. Biomaterials-Enhanced Intranasal Delivery of Drugs as a Direct Route for Brain Targeting. Int. J. Mol. Sci. 2023, 24, 3390, doi:10.3390/ijms24043390.
45. Qin, L.; Cui, Z.; Wu, Y.; Wang, H.; Zhang, X.; Guan, J.; Mao, S. Challenges and Strategies to Enhance the Systemic Absorption of Inhaled Peptides and Proteins. Pharm. Res. 2023, 40, 1037–1055, doi:10.1007/s11095-022-03435-3.
46. Miyamoto, M.; Natsume, H.; Satoh, I.; Ohtake, K.; Yamaguchi, M.; Kobayashi, D.; Sugibayashi, K.; Morimoto, Y. Effect of Poly-l-Arginine on the Nasal Absorption of FITC-Dextran of Different Molecular Weights and Recombinant Human Granulocyte Colony-Stimulating Factor (rhG-CSF) in Rats. Int. J. Pharm. 2001, 226, 127–138, doi:10.1016/S0378-5173(01)00797-9.
47. Suhail, M.; Janakiraman, A.K.; Khan, A.; Naeem, A.; Badshah, S.F. Surfactants and Their Role in Pharmceutical Product Development: An Overview. J. Pharm. Pharm. 2019, 6, 72–82, doi:https://doi.org/10.15436/2377-1313.19.2601.
48. Maher, S.; Geoghegan, C.; Brayden, D.J. Safety of Surfactant Excipients in Oral Drug Formulations. Adv. Drug Deliv. Rev. 2023, 202, 115086, doi:10.1016/j.addr.2023.115086.
49. Rai, S.; Acharya-Siwakoti, E.; Kafle, A.; Devkota, H.P.; Bhattarai, A. Plant-Derived Saponins: A Review of Their Surfactant Properties and Applications. Sci 2021, 3, 44, doi:10.3390/sci3040044.

50. Ding, W.-X.; Qi, X.-R.; Fu, Q.; Piao, H.-S. Pharmacokinetics and Pharmacodynamics of Sterylglucoside-Modified Liposomes for Levonorgestrel Delivery via Nasal Route. Drug Deliv. 2007, 14, 101–104, doi:10.1080/10717540600740102.
51. Moghimipour, E.; Ameri, A.; Handali, S. Absorption-Enhancing Effects of Bile Salts. Molecules 2015, 20, 14451–14473, doi:10.3390/molecules200814451.
52. Katdare, A.; Thakkar, S.; Dhepale, S.; Khunt, D.; Misra, M. Fatty Acids as Essential Adjuvants to Treat Various Ailments and Their Role in Drug Delivery: A Review. Nutrition 2019, 65, 138–157, doi:10.1016/j.nut.2019.03.008.
53. Ghadiri, M.; Canney, F.; Pacciana, C.; Colombo, G.; Young, P.M.; Traini, D. The Use of Fatty Acids as Absorption Enhancer for Pulmonary Drug Delivery. Int. J. Pharm. 2018, 541, 93–100, doi:10.1016/j.ijpharm.2018.02.027.
54. Li, Y.; Li, J.; Zhang, X.; Ding, J.; Mao, S. Non-Ionic Surfactants as Novel Intranasal Absorption Enhancers: In Vitro and in Vivo Characterization. Drug Deliv. 2016, 23, 2272–2279, doi:10.3109/10717544.2014.971196.
55. Ujhelyi, Z.; Fenyvesi, F.; Váradi, J.; Fehér, P.; Kiss, T.; Veszelka, S.; Deli, M.; Vecsernyés, M.; Bácskay, I. Evaluation of Cytotoxicity of Surfactants Used in Self-Micro Emulsifying Drug Delivery Systems and Their Effects on Paracellular Transport in Caco-2 Cell Monolayer. Eur. J. Pharm. Sci. 2012, 47, 564–573, doi:10.1016/j.ejps.2012.07.005.
56. Banat, I.M.; Makkar, R.S.; Cameotra, S.S. Potential Commercial Applications of Microbial Surfactants. Appl. Microbiol. Biotechnol. 2000, 53, 495–508, doi:10.1007/s002530051648.
57. Akbari, S.; Abdurahman, N.H.; Yunus, R.M.; Fayaz, F.; Alara, O.R. Biosurfactants—a New Frontier for Social and Environmental Safety: A Mini Review. Biotechnol. Res. Innov. 2018, 2, 81–90, doi:10.1016/j.biori.2018.09.001.
58. Karnwal, A.; Shrivastava, S.; Al-Tawaha, A.R.M.S.; Kumar, G.; Singh, R.; Kumar, A.; Mohan, A.; Yogita; Malik, T. Microbial Biosurfactant as an Alternate to Chemical Surfactants for Application in Cosmetics Industries in Personal and Skin Care Products: A Critical Review. BioMed Res. Int. 2023, 2023, 1–21, doi:10.1155/2023/2375223.
59. Ismail, R.; Baaity, Z.; Csóka, I. Regulatory Status Quo and Prospects for Biosurfactants in Pharmaceutical Applications. Drug Discov. Today 2021, 26, 1929–1935, doi:10.1016/j.drudis.2021.03.029.
60. Liang, B.; Xing, D. The Current and Future Perspectives of Postbiotics. Probiotics Antimicrob. Proteins 2023, doi:10.1007/s12602-023-10045-x.

61. Salminen, S.; Collado, M.C.; Endo, A.; Hill, C.; Lebeer, S.; Quigley, E.M.M.; Sanders, M.E.; Shamir, R.; Swann, J.R.; Szajewska, H.; et al. The International Scientific Association of Probiotics and Prebiotics (ISAPP) Consensus Statement on the Definition and Scope of Postbiotics. Nat. Rev. Gastroenterol. Hepatol. 2021, 18, 649–667, doi:10.1038/s41575-021-00440-6.
62. Liu, C.; Ma, N.; Feng, Y.; Zhou, M.; Li, H.; Zhang, X.; Ma, X. From Probiotics to Postbiotics: Concepts and Applications. Anim. Res. One Health 2023, 1, 92–114, doi:10.1002/aro2.7.
63. Moradi, M.; Molaei, R.; Guimarães, J.T. A Review on Preparation and Chemical Analysis of Postbiotics from Lactic Acid Bacteria. Enzyme Microb. Technol. 2021, 143, 109722, doi:10.1016/j.enzmictec.2020.109722.
64. Thorakkattu, P.; Khanashyam, A.C.; Shah, K.; Babu, K.S.; Mundanat, A.S.; Deliephan, A.; Deokar, G.S.; Santivarangkna, C.; Nirmal, N.P. Postbiotics: Current Trends in Food and Pharmaceutical Industry. Foods 2022, 11, 3094, doi:10.3390/foods11193094.
65. Hajfarajollah, H.; Eslami, P.; Mokhtarani, B.; Akbari Noghabi, K. Biosurfactants from Probiotic Bacteria: A Review. Biotechnol. Appl. Biochem. 2018, 65, 768–783, doi:10.1002/bab.1686.
66. Jahan, R.; Bodratti, A.M.; Tsianou, M.; Alexandridis, P. Biosurfactants, Natural Alternatives to Synthetic Surfactants: Physicochemical Properties and Applications. Adv. Colloid Interface Sci. 2020, 275, 102061, doi:10.1016/j.cis.2019.102061.
67. Paraszkiewicz, K.; Moryl, M.; Płaza, G.; Bhagat, D.; K. Satpute, S.; Bernat, P. Surfactants of Microbial Origin as Antibiofilm Agents. Int. J. Environ. Health Res. 2021, 31, 401–420, doi:10.1080/09603123.2019.1664729.
68. Perinelli, D.R.; Vllasaliu, D.; Bonacucina, G.; Come, B.; Pucciarelli, S.; Ricciutelli, M.; Cespi, M.; Itri, R.; Spinozzi, F.; Palmieri, G.F.; et al. Rhamnolipids as Epithelial Permeability Enhancers for Macromolecular Therapeutics. Eur. J. Pharm. Biopharm. 2017, 119, 419–425, doi:10.1016/j.ejpb.2017.07.011.
69. Rodríguez-López, L.; Shokry, D.S.; Cruz, J.M.; Moldes, A.B.; Waters, L.J. The Effect of the Presence of Biosurfactant on the Permeation of Pharmaceutical Compounds through Silicone Membrane. Colloids Surf. B Biointerfaces 2019, 176, 456–461, doi:10.1016/j.colsurfb.2018.12.072.
70. Aguilar-Toalá, J.E.; Garcia-Varela, R.; Garcia, H.S.; Mata-Haro, V.; González-Córdova, A.F.; Vallejo-Cordoba, B.; Hernández-Mendoza, A. Postbiotics: An Evolving Term within

the Functional Foods Field. Trends Food Sci. Technol. 2018, 75, 105–114, doi:10.1016/j.tifs.2018.03.009.

71. Compare, D.; Rocco, A.; Coccoli, P.; Angrisani, D.; Sgamato, C.; Iovine, B.; Salvatore, U.; Nardone, G. Lactobacillus Casei DG and Its Postbiotic Reduce the Inflammatory Mucosal Response: An Ex-Vivo Organ Culture Model of Post-Infectious Irritable Bowel Syndrome. BMC Gastroenterol. 2017, 17, 53, doi:10.1186/s12876-017-0605-x.
72. Raknam, P.; Balekar, N.; Teanpaisan, R.; Amnuaikit, T. Thermoresponsive Sol–Gel Containing Probiotic's Cell Free Supernatant for Dental Caries Prophylaxis. J. Oral Microbiol. 2022, 14, 2012390, doi:10.1080/20002297.2021.2012390.
73. Canonici, A.; Siret, C.; Pellegrino, E.; Pontier-Bres, R.; Pouyet, L.; Montero, M.P.; Colin, C.; Czerucka, D.; Rigot, V.; André, F. Saccharomyces Boulardii Improves Intestinal Cell Restitution through Activation of the A2β1 Integrin Collagen Receptor. PLoS ONE 2011, 6, e18427, doi:10.1371/journal.pone.0018427.
74. Duarte, M.; Oliveira, A.L.; Oliveira, C.; Pintado, M.; Amaro, A.; Madureira, A.R. Current Postbiotics in the Cosmetic Market—an Update and Development Opportunities. Appl. Microbiol. Biotechnol. 2022, 106, 5879–5891, doi:10.1007/s00253-022-12116-5.
75. Javia, A.; Kore, G.; Misra, A. Polymers in Nasal Drug Delivery: An Overview. In Applications of Polymers in Drug Delivery; Elsevier, 2021; pp. 305–332 ISBN 978-0-12-819659-5.
76. Khutoryanskiy, V.V. Advances in Mucoadhesion and Mucoadhesive Polymers. Macromol. Biosci. 2011, 11, 748–764, doi:10.1002/mabi.201000388.
77. Bandi, S.P.; Bhatnagar, S.; Venuganti, V.V.K. Advanced Materials for Drug Delivery across Mucosal Barriers. Acta Biomater. 2021, 119, 13–29, doi:10.1016/j.actbio.2020.10.031.
78. Yaqoob, M.; Jalil, A.; Bernkop-Schnürch, A. Mucoadhesive Polymers: Gateway to Innovative Drug Delivery. In Modeling and Control of Drug Delivery Systems; Elsevier, 2021; pp. 351–383 ISBN 978-0-12-821185-4.
79. Sosnik, A.; Das Neves, J.; Sarmento, B. Mucoadhesive Polymers in the Design of Nano-Drug Delivery Systems for Administration by Non-Parenteral Routes: A Review. Prog. Polym. Sci. 2014, 39, 2030–2075, doi:10.1016/j.progpolymsci.2014.07.010.
80. Wang, X.; Liu, G.; Ma, J.; Guo, S.; Gao, L.; Jia, Y.; Li, X.; Zhang, Q. In Situ Gel-Forming System: An Attractive Alternative for Nasal Drug Delivery. Crit. Rev. Ther. Drug Carrier Syst. 2013, 30, 411–434, doi:10.1615/CritRevTherDrugCarrierSyst.2013007362.

81. Pagano, C.; Perioli, L.; Ricci, M. Novel Approaches in Nasal In Situ Gel Drug Delivery. In Nasal Drug Delivery; Pathak, Y.V., Yadav, H.K.S., Eds.; Springer International Publishing: Cham, 2023; pp. 235–252 ISBN 978-3-031-23111-7.
82. Karavasili, C.; Fatouros, D.G. Smart Materials: In Situ Gel-Forming Systems for Nasal Delivery. Drug Discov. Today 2016, 21, 157–166, doi:10.1016/j.drudis.2015.10.016.
83. Mahajan, H.S.; Patil, P.H. Gel-Based Delivery of Neurotherapeutics via Naso-Brain Pathways. In Direct Nose-to-Brain Drug Delivery; Elsevier, 2021; pp. 225–245 ISBN 978-0-12-822522-6.
84. Altuntaş, E.; Yener, G.; Doğan, R.; Aksoy, F.; Şerif Aydın, M.; Karataş, E. Effects of a Thermosensitive In Situ Gel Containing Mometasone Furoate on a Rat Allergic Rhinitis Model. Am. J. Rhinol. Allergy 2018, 32, 132–138, doi:10.1177/1945892418764951.
85. Kumar, M.; Upadhayay, P.; Shankar, R.; Joshi, M.; Bhatt, S.; Malik, A. Chlorpheniramine Maleate Containing Chitosan-Based Nanoparticle-Loaded Thermosensitive in Situ Gel for Management in Allergic Rhinitis. Drug Deliv. Transl. Res. 2019, 9, 1017–1026, doi:10.1007/s13346-019-00639-w.
86. Cho, H.-J.; Balakrishnan, P.; Park, E.-K.; Song, K.-W.; Hong, S.-S.; Jang, T.-Y.; Kim, K.-S.; Chung, S.-J.; Shim, C.-K.; Kim, D.-D. Poloxamer/Cyclodextrin/Chitosan-Based Thermoreversible Gel for Intranasal Delivery of Fexofenadine Hydrochloride. J. Pharm. Sci. 2011, 100, 681–691, doi:10.1002/jps.22314.
87. Zaki, N.M.; Awad, G.A.; Mortada, N.D.; Abd ElHady, S.S. Enhanced Bioavailability of Metoclopramide HCl by Intranasal Administration of a Mucoadhesive in Situ Gel with Modulated Rheological and Mucociliary Transport Properties. Eur. J. Pharm. Sci. 2007, 32, 296–307, doi:10.1016/j.ejps.2007.08.006.
88. Khan, S.; Patil, K.; Bobade, N.; Yeole, P.; Gaikwad, R. Formulation of Intranasal Mucoadhesive Temperature-Mediated in Situ Gel Containing Ropinirole and Evaluation of Brain Targeting Efficiency in Rats. J. Drug Target. 2010, 18, 223–234, doi:10.3109/10611860903386938.
89. Ravi, P.R.; Aditya, N.; Patil, S.; Cherian, L. Nasal in-Situ Gels for Delivery of Rasagiline Mesylate: Improvement in Bioavailability and Brain Localization. Drug Deliv. 2015, 22, 903–910, doi:10.3109/10717544.2013.860501.
90. Chen, X.; Zhi, F.; Jia, X.; Zhang, X.; Ambardekar, R.; Meng, Z.; Paradkar, A.R.; Hu, Y.; Yang, Y. Enhanced Brain Targeting of Curcumin by Intranasal Administration of a Thermosensitive Poloxamer Hydrogel. J. Pharm. Pharmacol. 2013, 65, 807–816, doi:10.1111/jphp.12043.

91. Abouhussein, D.M.N.; Khattab, A.; Bayoumi, N.A.; Mahmoud, A.F.; Sakr, T.M. Brain Targeted Rivastigmine Mucoadhesive Thermosensitive In Situ Gel: Optimization, in Vitro Evaluation, Radiolabeling, in Vivo Pharmacokinetics and Biodistribution. J. Drug Deliv. Sci. Technol. 2018, 43, 129–140, doi:10.1016/j.jddst.2017.09.021.
92. Galgatte, U.C.; Kumbhar, A.B.; Chaudhari, P.D. Development of in Situ Gel for Nasal Delivery: Design, Optimization, in Vitro and in Vivo Evaluation. Drug Deliv. 2014, 21, 62–73, doi:10.3109/10717544.2013.849778.
93. Verekar, R.R.; Gurav, S.S.; Bolmal, U. Thermosensitive Mucoadhesive in Situ Gel for Intranasal Delivery of Almotriptan Malate: Formulation, Characterization, and Evaluation. J. Drug Deliv. Sci. Technol. 2020, 58, 101778, doi:10.1016/j.jddst.2020.101778.
94. Naik, A.; Nair, H. Formulation and Evaluation of Thermosensitive Biogels for Nose to Brain Delivery of Doxepin. BioMed Res. Int. 2014, 2014, 1–10, doi:10.1155/2014/847547.
95. Kaur, P.; Garg, T.; Vaidya, B.; Prakash, A.; Rath, G.; Goyal, A.K. Brain Delivery of Intranasal in Situ Gel of Nanoparticulated Polymeric Carriers Containing Antidepressant Drug: Behavioral and Biochemical Assessment. J. Drug Target. 2015, 23, 275–286, doi:10.3109/1061186X.2014.994097.
96. Wu, J.; Wu, Y.-B.; Hao, D.-X.; Zhou, M.; Fan, Q.-Z.; Wang, Y.-Q.; Ma, G.-H. Research Spotlight: Thermal-Sensitive Hydrogels as Nasal Vaccine Delivery Systems. Ther. Deliv. 2012, 3, 1151–1153, doi:10.4155/tde.12.95.
97. Mfoafo, K.; Kwon, Y.; Omidi, Y.; Omidian, H. Contemporary Applications of Thermogelling PEO-PPO-PEO Triblock Copolymers. J. Drug Deliv. Sci. Technol. 2022, 70, 103182, doi:10.1016/j.jddst.2022.103182.
98. Mfoafo, K.; Omidi, Y.; Omidian, H. Thermoresponsive Mucoadhesive Hybrid Gels in Advanced Drug Delivery Systems. Int. J. Pharm. 2023, 636, 122799, doi:10.1016/j.ijpharm.2023.122799.
99. Goh, J.-Y.; Weaver, R.J.; Dixon, L.; Platt, N.J.; Roberts, R.A. Development and Use of in Vitro Alternatives to Animal Testing by the Pharmaceutical Industry 1980–2013. Toxicol. Res. 2015, 4, 1297–1307, doi:10.1039/C5TX00123D.
100. Schweinlin, M.; Rossi, A.; Lodes, N.; Lotz, C.; Hackenberg, S.; Steinke, M.; Walles, H.; Groeber, F. Human Barrier Models for the in Vitro Assessment of Drug Delivery. Drug Deliv. Transl. Res. 2017, 7, 217–227, doi:10.1007/s13346-016-0316-9.

101. Agu, R.U.; Ugwoke, M.I. In Situ and Ex Vivo Nasal Models for Preclinical Drug Development Studies. In Drug Absorption Studies; Ehrhardt, C., Kim, K.-J., Eds.; Biotechnology: Pharmaceutical Aspects; Springer US: Boston, MA, 2008; Vol. VII, pp. 112–134 ISBN 978-0-387-74900-6.
102. Cabrera-Pérez, M.Á.; Sanz, M.B.; Sanjuan, V.M.; González-Álvarez, M.; Álvarez, I.G. Importance and Applications of Cell- and Tissue-Based in Vitro Models for Drug Permeability Screening in Early Stages of Drug Development. In Concepts and Models for Drug Permeability Studies; Elsevier, 2016; pp. 3–29 ISBN 978-0-08-100094-6.
103. Schmidt, M.C.; Peter, H.; Lang, S.R.; Ditzinger, G.; Merkle, H.P. In Vitro Cell Models to Study Nasal Mucosal Permeability and Metabolism. Adv. Drug Deliv. Rev. 1998, 29, 51–79, doi:10.1016/S0169-409X(97)00061-6.
104. Haasbroek-Pheiffer, A.; Van Niekerk, S.; Van Der Kooy, F.; Cloete, T.; Steenekamp, J.; Hamman, J. In Vitro and Ex Vivo Experimental Models for Evaluation of Intranasal Systemic Drug Delivery as Well as Direct Nose-to-brain Drug Delivery. Biopharm. Drug Dispos. 2023, 44, 94–112, doi:10.1002/bdd.2348.
105. Salade, L.; Wauthoz, N.; Goole, J.; Amighi, K. How to Characterize a Nasal Product. The State of the Art of in Vitro and Ex Vivo Specific Methods. Int. J. Pharm. 2019, 561, 47–65, doi:10.1016/j.ijpharm.2019.02.026.
106. Sosnik, A. Tissue-Based in Vitro and Ex Vivo Models for Nasal Permeability Studies. In Concepts and Models for Drug Permeability Studies; Elsevier, 2016; pp. 237–254 ISBN 978-0-08-100094-6.
107. Nicolazzo, J.A.; Reed, B.L.; Finnin, B.C. The Effect of Various In Vitro Conditions on the Permeability Characteristics of the Buccal Mucosa. J. Pharm. Sci. 2003, 92, 2399–2410, doi:10.1002/jps.10505.
108. Nunes, R.; Silva, C.; Chaves, L. Tissue-Based in Vitro and Ex Vivo Models for Intestinal Permeability Studies. In Concepts and Models for Drug Permeability Studies; Elsevier, 2016; pp. 203–236 ISBN 978-0-08-100094-6.
109. Bartos, C.; Szabó-Révész, P.; Horváth, T.; Varga, P.; Ambrus, R. Comparison of Modern In Vitro Permeability Methods with the Aim of Investigation Nasal Dosage Forms. Pharmaceutics 2021, 13, 846, doi:10.3390/pharmaceutics13060846.
110. Bednarek, R. In Vitro Methods for Measuring the Permeability of Cell Monolayers. Methods Protoc. 2022, 5, 17, doi:10.3390/mps5010017.
111. Costa, C.P.; Barreiro, S.; Moreira, J.N.; Silva, R.; Almeida, H.; Sousa Lobo, J.M.; Silva, A.C. In Vitro Studies on Nasal Formulations of Nanostructured Lipid Carriers (NLC) and

Solid Lipid Nanoparticles (SLN). Pharmaceuticals 2021, 14, 711, doi:10.3390/ph14080711.

112. Boyuklieva, R.; Zagorchev, P.; Pilicheva, B. Computational, In Vitro, and In Vivo Models for Nose-to-Brain Drug Delivery Studies. Biomedicines 2023, 11, 2198, doi:10.3390/biomedicines11082198.
113. Gartziandia, O.; Egusquiaguirre, S.P.; Bianco, J.; Pedraz, J.L.; Igartua, M.; Hernandez, R.M.; Préat, V.; Beloqui, A. Nanoparticle Transport across in Vitro Olfactory Cell Monolayers. Int. J. Pharm. 2016, 499, 81–89, doi:10.1016/j.ijpharm.2015.12.046.
114. Ladel, S.; Schlossbauer, P.; Flamm, J.; Luksch, H.; Mizaikoff, B.; Schindowski, K. Improved In Vitro Model for Intranasal Mucosal Drug Delivery: Primary Olfactory and Respiratory Epithelial Cells Compared with the Permanent Nasal Cell Line RPMI 2650. Pharmaceutics 2019, 11, 367, doi:10.3390/pharmaceutics11080367.
115. Sousa, F.; Castro, P. Cell-Based in Vitro Models for Nasal Permeability Studies. In Concepts and Models for Drug Permeability Studies; Elsevier, 2016; pp. 83–100 ISBN 978-0-08-100094-6.
116. Mercier, C.; Jacqueroux, E.; He, Z.; Hodin, S.; Constant, S.; Perek, N.; Boudard, D.; Delavenne, X. Pharmacological Characterization of the 3D MucilAirTM Nasal Model. Eur. J. Pharm. Biopharm. 2019, 139, 186–196, doi:10.1016/j.ejpb.2019.04.002.
117. Werner, U.; Kissel, T. In-vitro Cell Culture Models of the Nasal Epithelium: A Comparative Histochemical Investigation of Their Suitability for Drug Transport Studies. Pharm. Res. 1996, 13, 978–988, doi:10.1023/A:1016038119909.
118. Berben, P.; Bauer-Brandl, A.; Brandl, M.; Faller, B.; Flaten, G.E.; Jacobsen, A.-C.; Brouwers, J.; Augustijns, P. Drug Permeability Profiling Using Cell-Free Permeation Tools: Overview and Applications. Eur. J. Pharm. Sci. 2018, 119, 219–233, doi:10.1016/j.ejps.2018.04.016.
119. Jacobsen, A.-C.; Visentin, S.; Butnarasu, C.; Stein, P.C.; Di Cagno, M.P. Commercially Available Cell-Free Permeability Tests for Industrial Drug Development: Increased Sustainability through Reduction of In Vivo Studies. Pharmaceutics 2023, 15, 592, doi:10.3390/pharmaceutics15020592.
120. Di, L.; Artursson, P.; Avdeef, A.; Benet, L.Z.; Houston, J.B.; Kansy, M.; Kerns, E.H.; Lennernäs, H.; Smith, D.A.; Sugano, K. The Critical Role of Passive Permeability in Designing Successful Drugs. ChemMedChem 2020, 15, 1862–1874, doi:10.1002/cmdc.202000419.

121. Buckley, S.T.; Fischer, S.M.; Fricker, G.; Brandl, M. In Vitro Models to Evaluate the Permeability of Poorly Soluble Drug Entities: Challenges and Perspectives. Eur. J. Pharm. Sci. 2012, 45, 235–250, doi:10.1016/j.ejps.2011.12.007.
122. Henriques, P.; Bicker, J.; Silva, S.; Doktorovová, S.; Fortuna, A. Nasal-PAMPA: A Novel Non-Cell-Based High Throughput Screening Assay for Prediction of Nasal Drug Permeability. Int. J. Pharm. 2023, 643, 123252, doi:10.1016/j.ijpharm.2023.123252.
123. Corace, G.; Angeloni, C.; Malaguti, M.; Hrelia, S.; Stein, P.C.; Brandl, M.; Gotti, R.; Luppi, B. Multifunctional Liposomes for Nasal Delivery of the Anti-Alzheimer Drug Tacrine Hydrochloride. J. Liposome Res. 2014, 24, 323–335, doi:10.3109/08982104.2014.899369.
124. di Cagno, M.; Bibi, H.A.; Bauer-Brandl, A. New Biomimetic Barrier PermeapadTM for Efficient Investigation of Passive Permeability of Drugs. Eur. J. Pharm. Sci. 2015, 73, 29–34, doi:10.1016/j.ejps.2015.03.019.
125. Bibi, H.A.; di Cagno, M.; Holm, R.; Bauer-Brandl, A. PermeapadTM for Investigation of Passive Drug Permeability: The Effect of Surfactants, Co-Solvents and Simulated Intestinal Fluids (FaSSIF and FeSSIF). Int. J. Pharm. 2015, 493, 192–197, doi:10.1016/j.ijpharm.2015.07.028.
126. Wu, I.Y.; Bala, S.; Škalko-Basnet, N.; di Cagno, M.P. Interpreting Non-Linear Drug Diffusion Data: Utilizing Korsmeyer-Peppas Model to Study Drug Release from Liposomes. Eur. J. Pharm. Sci. 2019, 138, 105026, doi:10.1016/j.ejps.2019.105026.
127. Papakyriakopoulou, P.; Manta, K.; Kostantini, C.; Kikionis, S.; Banella, S.; Ioannou, E.; Christodoulou, E.; Rekkas, D.M.; Dallas, P.; Vertzoni, M.; et al. Nasal Powders of Quercetin-β-Cyclodextrin Derivatives Complexes with Mannitol/Lecithin Microparticles for Nose-to-Brain Delivery: In Vitro and Ex Vivo Evaluation. Int. J. Pharm. 2021, 607, 121016, doi:10.1016/j.ijpharm.2021.121016.

PART II: OUTLINE OF THE PROJECT

1. Aim of the thesis

Possibility for self-medication, avoidance of needles, fast onset of action, minor presystemic metabolism, and direct accessibility to the central nervous system (CNS), are some of the features that make the nasal route an attractive strategy for drug administration. Even though it shows undeniable advantages over other conventional delivery approaches, the feasibility of local, systemic as well as CNS treatment through the nose is hampered by some shortcomings. Among these, the restricted nasal tissue surface area, which limits the applicable volume of formulations, the barrier effect posed by the mucus gel layer covering the mucosa and the underlying epithelium, together with the mucociliary clearance are not negligible. As a result, my commitment to the present Ph.D. project was to investigate possible strategies capable of overcoming the downsides associated with nasal drug delivery and therefore improving therapeutics' permeation across the nasal mucosa. A clear-cut method is the addition of permeation enhancers in the nasal dosage form, such as surfactants. These bear the ability to interact with lipids and perturb lipid bilayers to various extents, thus favoring drug absorption; moreover, since they can spontaneously assemble in micelles, are extremely useful at increasing the solubility of lipophilic compounds. Alongside increasing membrane permeability, the bioavailability of drugs can be improved by extending their residence time at the absorption site by counteracting the mucociliary clearance. This can be achieved by formulating the active ingredient together with mucoadhesive agents and/or "smart" polymers, like those that increase the viscosity of the vehicle because of a gelation process triggered by a physiological stimulus. Furthermore, because pharmaceuticals appeared to be an emerging class of pollutants, the thesis also aimed to prove the applicability of some postbiotics as innovative excipients in the nasal drug delivery field. Indeed, as naturally occurring materials, they are regarded to be more biocompatible and eco-compatible compared to synthetic substances, and because obtainable through green procedures, they suit the current demand for sustainable products. Lastly, a great part of the project concerned *in vitro* tools for the early investigation of the permeability features of enabling formulations intended for nasal delivery. Particular attention was paid to the recently developed PermeaPad® biomimetic membrane, its suitability as a model of the nasal mucosa also in comparison to other tissue-based and cell-based models, as well as its possible optimization.

2. List of the papers

The scientific achievements of the present Ph.D. thesis are described in the following publications, which are reprinted with the Editors' permission:

1) Corazza, E.; Abruzzo, A.; Giordani, B.; Cerchiara, T.; Bigucci, F.; Vitali, B.; di Cagno, M.P.; Luppi, B. Human *Lactobacillus* Biosurfactants as Natural Excipients for Nasal Drug Delivery of Hydrocortisone. Pharmaceutics 2022, *14*, 524, doi:10.3390/pharmaceutics14030524.
2) Corazza, E.; di Cagno, M.P.; Bauer-Brandl, A.; Abruzzo, A.; Cerchiara, T.; Bigucci, F.; Luppi, B. Drug Delivery to the Brain: In Situ Gelling Formulation Enhances Carbamazepine Diffusion through Nasal Mucosa Models with Mucin. Eur. J. Pharm. Sci. 2022, 106294, doi:10.1016/j.ejps.2022.106294.
3) Corazza, E.; Martin, J.; Schindowski, K.; Giordani, B.; Vitali B.; Rossi, M.; Abruzzo, A.; Bigucci, F.; Cerchiara, T.; di Cagno, M. P.; Luppi, B. Lactobacilli cell-free supernatants: potential green and natural enhancers for nose-to-brain delivery of small hydrophilic molecules. Submitted to the Journal of Drug Delivery Science and Technology.

I performed all the experiments that are described in the different works of research with the only exception of the immunostaining assay reported in the third scientific publication. In this latter case, I took part in the design of the experiment, but it was carried out by the Ph.D. candidate Janik Martin from the Institute of Applied Biotechnology, University of Applied Science Biberach, in Germany.

Alongside, I had the opportunity to contribute to other research articles that do not directly pertain to the present Ph.D. project:

1) Abruzzo, A.; Croatti, V.; Zuccheri, G.; Pasquale Nicoletta, F.; Sallustio, V.; Corazza, E.; Vitali, B.; Cerchiara, T.; Luppi, B.; Bigucci, F. Drug-in-Cyclodextrin-in-Polymeric Nanoparticles: A Promising Strategy for Rifampicin Administration. Eur. J. Pharm. Biopharm. 2022, 180, 190–200, doi:10.1016/j.ejpb.2022.10.001.
2) Abruzzo, A.; Parolin, C.; Corazza, E.; Giordani, B.; di Cagno, M.P.; Cerchiara, T.; Bigucci, F.; Vitali, B.; Luppi, B. Influence of *Lactobacillus* Biosurfactants on Skin Permeation of Hydrocortisone. Pharmaceutics 2021, 13, 820, doi:10.3390/pharmaceutics13060820.

PART III: EXPERIMENTAL SECTION

1. Human *Lactobacillus* biosurfactants as natural excipients for nasal drug delivery of hydrocortisone

Elisa Corazza [1], Angela Abruzzo [1, *], Barbara Giordani [1], Teresa Cerchiara [1], Federica Bigucci [1], Beatrice Vitali [1], Massimiliano Pio di Cagno [2] and Barbara Luppi [1]

[1] Department of Pharmacy and Biotechnology, Alma Mater Studiorum, University of Bologna, Via San Donato 19/2, 40127 Bologna, Italy

[2] Department of Pharmacy, Faculty of Mathematics and Natural Sciences, University of Oslo, Sem Sælands vei 3, 0371 Oslo, Norway

[*] Corresponding author

Published on Pharmaceutics (doi: 10.3390/pharmaceutics14030524)

Abstract: The inclusion of a chemical permeation enhancer in a dosage form is considered an effective approach to improve absorption across the nasal mucosa. Herein we evaluated the possibility of exploiting biosurfactants (BS) produced by *Lactobacillus gasseri* BC9 as innovative natural excipients to improve nasal delivery of hydrocortisone (HC). BC9-BS ability to improve HC solubility and the BS mucoadhesive potential were investigated using the surfactant at a concentration below and above the critical micelle concentration (CMC). *In vitro* diffusion studies through the biomimetic membrane PermeaPad® and the same synthetic barrier functionalized with a mucin layer were assessed to determine BC9-BS absorption-enhancing properties in the absence and presence of the mucus layer. Lastly, the diffusion study was performed across the sheep nasal mucosa using BC9-BS at a concentration below the CMC. Results showed that BC9-BS was able to interact with the main component of the nasal mucosa, and that it allowed for a greater solubilization and also permeation of the drug when it was employed at a low concentration. Overall, it seems that BC9-BS could be a promising alternative to chemical surfactants in the nasal drug delivery field.

Keywords: biosurfactants; *Lactobacillus*; nasal delivery; drug solubility; mucoadhesion; drug permeation; mucin layer.

1.1. Introduction

The nasal route has been conventionally used for the delivery of drugs aimed to treat local diseases, but it was also demonstrated to be potentially exploited as an alternative way of systemic administration [1,2]. Underlying the growing consideration towards nasal delivery are the advantages that it offers over conventional systemic delivery strategies [3,4]. Among these, it is worth mentioning its non-invasive character, its easy accessibility for the administration of drugs and a comparatively high drug uptake in the systemic circulation thanks to the great vascularization of the respiratory nasal mucosa. Furthermore, intranasal administered systemically acting drugs are subjected to a minor presystemic metabolism with a consequent higher bioavailability, and for those drugs intended to target the brain, there is the possibility to directly access the cerebrospinal fluid by-passing the blood–brain barrier [3–5].

Despite the numerous advantages of nasal delivery, there are also shortcomings to be considered, such as the restricted nasal tissue surface area limiting the applicable volume of formulations, the rapid drug clearance because of the mucociliary system, which is responsible for the low drug retention time in the nasal cavity, and also the enzymatic degradation [3–5]. Moreover, drugs delivered nasally should first overcome the physical barriers represented by the mucus gel layer and the nasal epithelium before reaching their target, either if it is local or systemic [4–6]. The mucus is a hydrophilic layer in which mineral salts, proteins, glycoproteins, and lipids are found. Among glycoproteins, mucins prevail, thus contributing to the mucus layer viscosity, its negative charge, and its meshlike structure [7,8]. As a result, the mucus layer acts as a barrier towards the diffusion of foreign entities, drugs included. The absorption of active pharmaceutical ingredients is also limited by the nasal epithelium which, being composed of pseudostratified columnar cells interconnected via tight junctions, acts as a second barrier. Based on their chemical features, drugs can overcome the epithelium through different strategies, such as transcellular diffusion, or partitioning across the membrane via a concentration gradient, that is characteristic of small hydrophobic molecules, but also activating some sorts of active transport that are usually required for the absorption of hydrophilic drugs [6].

Because of the difficulties involved in nasal delivery, auxiliary agents are needed to overcome these limits [4]. Although many approaches have been investigated to improve permeation of drugs through the nasal mucosa, the most frequently employed is the inclusion of absorption enhancers in the formulation, such as surfactants [5,6]. The latter are amphiphilic molecules able to enhance drug absorption in different ways: perturbing the cell

membrane, transiently opening the tight junctions, or preventing the enzymatic degradation of drugs [6,9]. Among the different molecules that belong to the group of permeation enhancers classified as surfactants are biosurfactants (BS) [6]. BS are drawing interest because they better suit the current trend of the scientific community that is looking for more eco-friendly materials obtainable from natural resources [9–11]. In fact, microorganisms like yeasts, bacteria, and some filamentous fungi can produce different substances, BS included, just using a set of carbon sources and energy for growth [9]. Along with their being natural compounds, what makes BS very appealing from an industrial point of view, are some features that make them more advantageous compared to chemical and synthetic surfactants. Indeed, BS are biodegradable molecules with a good safety profile and great surface, interfacial and emulsifying activity. BS also show an excellent tolerance towards temperature, pH, and ionic strength; furthermore, they exert a broad spectrum of biological activities useful for biomedical and pharmaceutical applications [9–13].

Abruzzo et al. have recently isolated a novel biosurfactant from the human strain *Lactobacillus gasseri* BC9 [14], which is a probiotic bacterium with a positive influence on human health [15,16] and which does not require a biosafe environment for its handling. BC9-BS consists of a peptide-like molecule, whose hydrophobic moiety is made of hydrocarbon chains of different lengths, whereas the hydrophilic moiety comprises the aminoacidic residues His, Val, and Thr [14]. This lipopeptidic biosurfactant exhibits surface active properties with a critical micelle concentration (CMC) of around 2 mg/mL and good emulsification activity [14]. Moreover, BC9-BS *in vitro* cytotoxicity has also been studied on both human and murine fibroblasts demonstrating that it does not affect cell viability when used at concentrations up to five-fold its CMC [17]. Considering the interesting properties of this natural surfactant, some of its possible applications in the pharmaceutical field have already been investigated. BC9-BS was demonstrated to be potentially exploited as a therapeutic agent to counteract infections caused by methicillin-resistant *Staphylococcus aureus* biofilms [17], and it was also employed as a green excipient in drug formulations. In fact, BC9-BS was used on the one hand to develop mixed vesicles active against chronic vaginal infections [14] and, on the other hand, as a permeation enhancer in transdermal drug delivery [18].

Based on these assumptions, we purposed to evaluate BC9-BS as an innovative natural excipient to improve nasal administration of the Biopharmaceutical Classification System class II drug hydrocortisone (HC). *In vitro* diffusion studies through different membranes, the biomimetic membrane PermeaPad®, the same barrier functionalized with a mucin layer and

the sheep nasal mucosa, were performed in the presence of BC9-BS at concentrations below and above its CMC, and HC solubility was measured. Additionally, mucoadhesive studies were conducted to investigate BS interaction with mucin. The ability of BC9-BS to act as a solubilizing agent and permeation enhancer, together with its capacity to interact with the main component of the mucus layer, were then compared to those of two other surfactants: d-α-tocopheryl polyethylene glycol 1000 succinate (TPGS) as an example of the non-ionic surfactants, that together represent the most clinically advanced permeation enhancers in nasal delivery [19], and cocamidopropyl betaine (CAPB), a mild zwitterionic surfactant frequently used in cosmetic industries [20].

1.2. Materials and Methods

1.2.1. Materials

Cocamidopropyl betaine (CAPB) Amphotensid B4/C was provided from Farmalabor srl (Canosa di Puglia, Italy), whereas D-α-tocopheryl polyethylene glycol 1000 succinate (TPGS) was a kind gift from BASF SE (Ludwigshafen, Germany). Hydrocortisone, mucin type II from porcine stomach, all chemicals, and solvents were of analytical grade and purchased from Sigma-Aldrich (Milan, Italy), except for sodium chloride (NaCl) that was supplied by Carlo Erba (Milan, Italy). Phosphate buffer solution (PBS) at pH 7.4 was composed of 7.4 mM $Na_2HPO_4 \cdot 12H_2O$, 1.1 mM KH_2PO_4, and 136 mM NaCl. PBS at pH 5.5 was employed to simulate the pH of the nasal cavity and it was composed of 4.2 mM Na_2HPO_4*$12H_2O$, 100 mM KH_2PO_4, 45.5 mM NaCl. Man, Rogosa and Sharpe (MRS) culture media and GasPak EZ were supplied by Difco (Detroit, MI, USA) and Becton Dickinson & Co. (Sparks, MD, USA), respectively. L-cysteine hydrochloride monohydrate was purchased from Merck (Darmstadt, Germany).

1.2.2. L. gasseri BC9 cultivation and BC9 biosurfactant isolation

The biosurfactant (BS) produced by *Lactobacillus gasseri* BC9 was obtained following a well-established procedure designed to isolate the fraction of biosurfactant that is bound to the bacterial cell surface [17]. Briefly, 100 mL of an overnight lactobacilli culture was inoculated in 900 mL of MRS broth and allowed to grow inside an anaerobic jar in the presence of GasPak EZ for 24 h. Cells were separated from the culture medium by centrifugation at 3650 × *g* for 20 min (Centrisart® D-16C, Sartorius, Göttingen, Germany), then cell pellets were washed twice in sterile water and lastly re-suspended in 240 mL of PBS pH 7.4. The suspensions were left for 2 h at room temperature on an orbital shaker

(Certomat® Sartorius AG, Göttingen, Germany) at 100 rpm to enable the release of the cell-bound BS. The supernatant containing the BS was isolated by two sequential centrifugations at 2543 × g for 20 min (ALC 4222MKII centrifuge, ALC International s.r.l., Milan, Italy) and any remaining cellular components were removed by filtration through a 0.22 μm pore size filter (Cellulose acetate syringe filter, Sanford, FL, USA). Removal of PBS salts and impurities was obtained through dialysis against demineralized water in a standard RC tubing (molecular weight cut-off 6000–8000 Da; Spectra/Por 1 dialysis membrane Spectrum Laboratories Inc., Rancho Dominguez, CA, USA) for 24 h at room temperature, and lastly the dialyzed supernatant was freeze-dried at 0.01 atm and −45 °C (Christ Freeze Dryer ALPHA 1–2, Milan, Italy).

1.2.3. Surface activity and critical micelle concentration of surfactants

The surface-active properties of surfactants and their critical micelle concentration (CMC) were determined through the ring method using a tensiometer (K8600E Krüss GmbH, Hamburg, Germany). The surface tension (dyne/cm) was measured at room temperature as the force required to detach the platinum ring (1.9 cm diameter) from 2 mL of PBS pH 5.5 solution containing different concentrations of BC9-BS (0.0625–8.005 mg/mL), CAPB (0.005–5.275 mg/mL) and TPGS (0.02–2 mg/mL). The concentration at which surfactants change their organization from single molecules to micelles was determined by plotting the surface tension as function of the logarithm of surfactants concentration. Precisely, the CMC coincides with the intersection between the curve that describes the linear decrease in surface tension and the one that includes the points for which the increase in surfactants concentration corresponds to constant values of surface tension.

1.2.4. Chromatographic conditions

HPLC analytical assay was performed using a Shimadzu (Milan, Italy) LC-10ATVP chromatographic pump and a Shimadzu SPD-10AVP UV–vis detector set at 244 nm. Separation was obtained on a Phenomenex (Torrance, CA, USA) Sinergy™ 4 μm Hydro-RP 80Å LC column (150 × 4.60 mm) coupled to a Phenomenex Security Guard C18 guard cartridge (4 × 3.0 mm i.d., 5 μm). The mobile phase consisted of a mixture of acetonitrile/PBS pH 7.4 40:60 (v/v) and it was flushed at a rate of 0.5 mL/min. Manual injections were made using a Rheodyne 7125 injector with a 20 μL sample loop and data analysis was carried out through the CromatoPlus software (Shimadzu Italia, Milan, Italy). Because of the different purposes of this work, more than one calibration curve was

obtained. The calibration curve of HC in ethanol/PBS pH 5.5 (1:1 v/v) was characterized by a drug concentration range of 2.625–105 µg/mL, a linearity coefficient (R^2) equal to 1, and it was employed to determine HC solubility. The calibration curve of HC in PBS pH 7.4/ ethanol (80:20 v/v), obtained with drug concentrations ranging from 0.10 µg/mL to 41.52 µg/mL, showed a good linearity (R^2 = 1) and it was used to evaluate the drug permeated during the *in vitro* diffusion studies. Limits of detection (LOD) and quantification (LOQ) were 0.14 µg/mL and 0.41 µg/mL, respectively.

1.2.5. Surfactants solubilizing activity

To investigate surfactants ability to increase solubility of HC, an excess amount of drug was dispersed in PBS pH 5.5 in absence (CTRL sample) or in presence of BC9-BS, CAPB or TPGS at two different concentrations: below and above their CMC, which corresponded to half and five-fold the CMC, respectively. Dispersions were left under stirring for 48 h at room temperature (25 °C), and subsequently were subjected to centrifugation at 5890 × *g* for 15 min (Microspin 12, Biosan, Riga, Latvia) and filtration through syringe filters 0.22 µm cut-off to remove the fraction of undissolved drug. The samples obtained through this procedure were used as such for the *in vitro* permeation study (see Section 1.2.7), whereas, to assess the maximum solubility of HC in the presence of surfactants, specimens were diluted 1:1 (v/v) in ethanol prior to HPLC analytical assay.

1.2.6. Surfactants interaction with mucin

The ability of surfactants to interact with the main component of the mucus gel layer was investigated through turbidimetric measurement of a suspension containing mucin and surfactants at concentrations below and above the CMC, as reported by Abruzzo et al., 2018 [14] with some modifications. Mucin previously dialyzed and lyophilized, as reported in Section 1.2.7, was used to prepare a mucin dispersion (0.08 % w/v) in PBS pH 5.5. After stirring for 6 h, mucin dispersion was centrifuged (3310 × *g*, 20 min) to remove the excess amount of mucin. The mucin obtained was thus mixed at a 1:4 volume ratio with the suspension containing surfactants in PBS pH 5.5, and then vortexed for 1 min. The turbidity of the samples was measured at 650 nm through a UV–visible spectrophotometer (UV-1601 Shimadzu, Milan, Italy). The absorbance (ABS) of mucin dispersion itself and surfactants suspensions without mucin were measured as references. In fact, data were reported as the percentage increase in sample absorbance in the presence of mucin with respect to the same sample without mucin, according to the following equation:

$$\%ABS = \frac{ABS\ sample\ with\ mucin - ABS\ mucin}{ABS\ sample\ without\ mucin} * 100$$

1.2.7. Surfactants permeation enhancing properties

To evaluate surfactants ability to act as permeation enhancers, diffusion studies of HC in the presence of BC9-BS, CAPB or TPGS at concentrations below and above the respective CMC (half and five-fold the CMC, respectively) were performed using Franz-type static glass vertical diffusion cells (15 mm jacketed cell with a flat-ground joint and clear glass with a 12 mL receptor volume; diffusion surface area = 1.77 cm^2) equipped with a V6A Stirrer (PermeGearInc., Hellertown, PA, USA). Diffusion studies were conducted across different *in vitro* barriers:

1. PermeaPad® barrier (InnoMe GmbH, Espelkamp, Germany), which had already been used to predict the nasal absorption of drugs [21], and thus was here employed to simulate the nasal epithelium;
2. PermeaPad® barrier functionalized with the addition of an artificial mucus layer on its surface, that enabled us to better mimic the *in vivo* conditions of the nasal cavity;
3. Sheep nasal mucosa, that was exploited due to its similarity to the human one in terms of morphology [22] and because it was found adequate in previous studies [23,24].

The different membranes, PermeaPad® barrier, PermeaPad® barrier functionalized with a mucin layer and sheep nasal mucosa, were clamped between the receptor and donor compartments. The receptor medium was composed of 12 mL of the mixture PBS pH 7.4/ethanol (80:20 v/v), previously sonicated to avoid air bubble formation beneath the membranes, thermostated at 35 ± 1 °C thanks to a surrounding jacket and maintained under constant stirring to ensure a uniform distribution of the diffused drug. The temperature was chosen in accordance with previous *in vitro* diffusion studies aimed at investigating nasal drug delivery [21]. Then, 300 µL of the control sample and the samples containing surfactants at the two different concentrations tested, which were obtained as described in Section 1.2.5, were added to the donor compartment.

Diffusion studies were performed over 5 h, during which samplings were made pipetting 200 µL of the acceptor phase (replaced with fresh acceptor medium) every 15 min for the first 2 h and every 30 min for the subsequent 3 h. The permeability coefficient (Kp) was calculated according to the following equation [7]:

$$Kp = \frac{dM}{dt} * \frac{1}{S * C0}$$

where dM/dt (µg/s) is the slope at the steady state period, S (cm^2) is the diffusion surface area and C0 (µg/mL) is the initial drug concentration within different samples. To better explain the influence of the different surfactants on HC permeability across the *in vitro* models, the enhancement ratio (ER) was calculated based on the following equation [25]:

$$ER = \frac{Kp\ with\ surfactant}{Kp\ control\ sample}$$

For the preparation of the functionalized PermeaPad® barrier, mucin was dispersed in ultrapure water at the concentration of 50 mg/mL and subjected to dialysis overnight using standard RC tubing (molecular weight cut-off 6000–8000 Da), to remove those mucus glycoproteins characterized by a low molecular weight. These, in fact, could potentially diffuse across the PermeaPad® barrier, hindering the possibility of producing a stable mucus gel layer over the time. The purified mucin dispersion was freeze-dried and the powder obtained was stored at +2–8 °C until use. When diffusion studies were performed, 200 µL of purified mucin dispersion in PBS pH 5.5 (50 mg/mL) were placed on the top of the PermeaPad® barrier and left to equilibrate for 5 min prior to sample addition in the donor compartment.

The nasal mucosa was obtained from a local slaughterhouse and the tissue used for the permeation studies was precisely the one excised from the nasal turbinates. First, nasal turbinates were separated from the septum using forceps and a scalpel, then the mucosa was carefully detached from the adhering cartilaginous tissue and abundantly washed with NaCl 0.9% (w/v). The excised tissue was placed on a nitrate cellulose filter characterized by 0.45 µm pore size (Sartorius, Göttingen, Germany), with the epithelium side in direct contact with the filter itself and the mucosal side facing upwards, and finally stored in aluminum foils at −20 °C until use.

1.2.8. Statistical analysis

All results are shown as mean ± standard deviation (SD) and SD was calculated from the values of three independent experiments. Data from all experiments were analyzed using a t-test, and differences were deemed significant for $p < 0.05$.

1.3. Results and Discussion

1.3.1. BC9-BS as surface-active agent and critical micelle concentration

Beyond being natural compounds, biosurfactants (BS) are amphiphilic molecules, thus their potential applications rely on the ability to reduce surface and interfacial tension [10,12,25]. In the present study, surface activity of BC9-BS, CAPB, and TPGS was evaluated at room temperature (25 ◦C) and at pH 5.5 by means of a phosphate buffer used to mimic the nasal pH, which ranges from 5.5 to 6.5 in adults and from 5.0 to 6.7 in children [26]. **Figure PIII 1.1**, which shows the surface tension plotted as a function of surfactant concentration, confirmed that all tested compounds exhibit surface-active properties. Moreover, for each of them it was possible to calculate the CMC, known as the concentration that enables the lowest stable surface tension to be reached, and after which surfactants self-assemble in micelles [9,10].

When BC9-BS was solubilized at concentrations from 0.0625 mg/mL to 8.005 mg/mL, a decrease in surface tension from 66 ± 0.5 to 43 ± 1 dyne/cm was observed and the CMC was found to be around 2 mg/mL. Data obtained are in agreement with our previously published results: the presence of electrolytes allows for a greater reduction in surface tension with respect to water, without affecting the CMC value [18]. Regarding CAPB, it was demonstrated to reduce surface tension from 67.8 ± 0.3 to 34 ± 0 dyne/cm in the concentration range of 0.005–5.275 mg/mL and it exhibited a CMC value of 1.01 mg/mL, which is in line with what has been already reported in literature [27]. Lastly, the synthetic surfactant TPGS allowed for a decrease in surface tension from 64 ± 1.4 to 51.25 ± 0.3 dyne/cm when solubilized at concentrations from 0.02 mg/mL to 2 mg/mL and it was characterized by a CMC value of 0.54 mg/mL. The latter value was found to be higher than that obtained in previous studies (0.2 mg/mL [28]), probably because of the low pH at which the measurement was conducted. In fact, it has been demonstrated that the pH can affect the micelle properties of a non-ionic surfactant, the CMC included; at a constant temperature, an increase in the CMC can be observed while decreasing the pH [29].

Based on the calculated CMC values, surfactants activities as solubilizing and permeation enhancing agents were evaluated at concentrations of half and five-fold the respective CMC. The selected concentrations were thought to be suitable to investigate the different behavior of surface-active molecules as a function of their different organization in the buffer medium: single molecules or micelles. In fact, it is known from the literature that, differently from when employed at concentrations below the CMC, surfactants used at concentrations higher than the CMC are mainly responsible for drug solubility increase rather than for drug permeability

improvement [24,30]. Regarding the issue of toxicity, it is worth noting that none of the investigated surfactants was previously reported to be toxic at concentrations equal to those tested in the present study. As a matter of fact, cell viability assays using BC9-BS up to 10 mg/mL on human and murine fibroblasts indicated that BS is not cytotoxic [17]; similarly, CAPB exerted no toxic effect to NIH 3T3 cells when employed at concentrations up to 35.8 mg/mL [31] and its extensive use in detergent and cosmetic industries is well established because of its low irritative potential on the skin and mucous membranes [20]. Lastly, TPGS was exploited to develop curcumin loaded polymeric micelles intended for nose-to-brain delivery and, after treatment, neither epithelial changes nor sign of remarkable destructive effect were observed on the nasal mucosa [32].

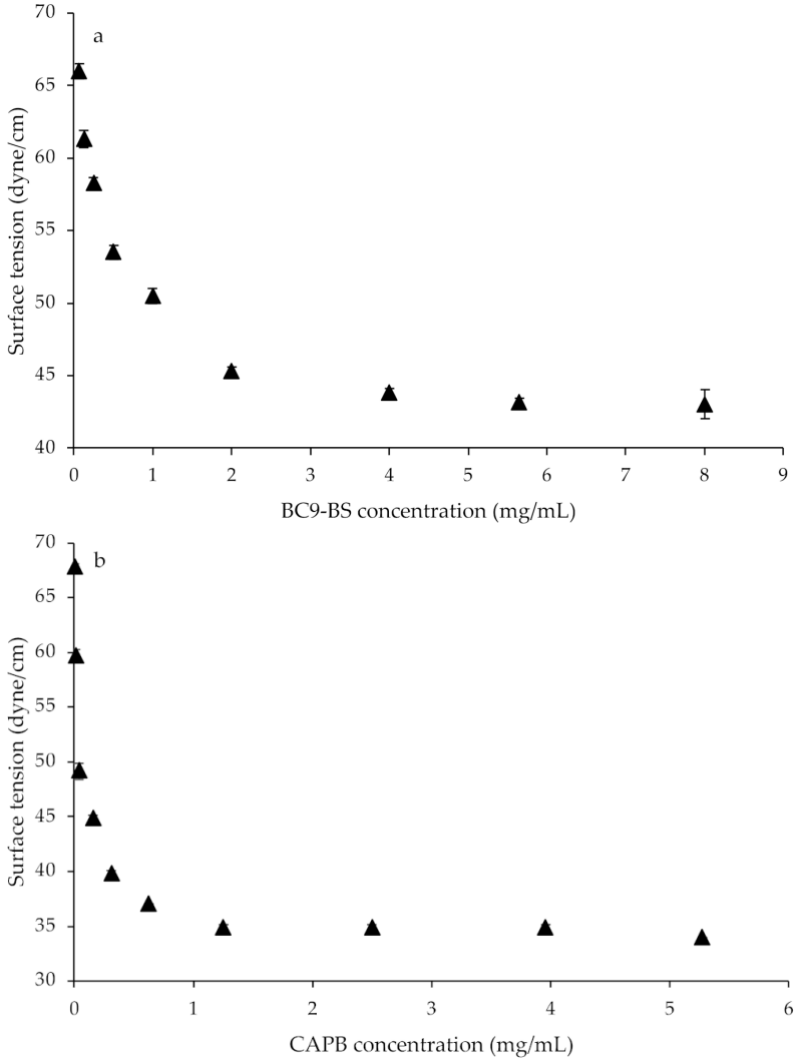

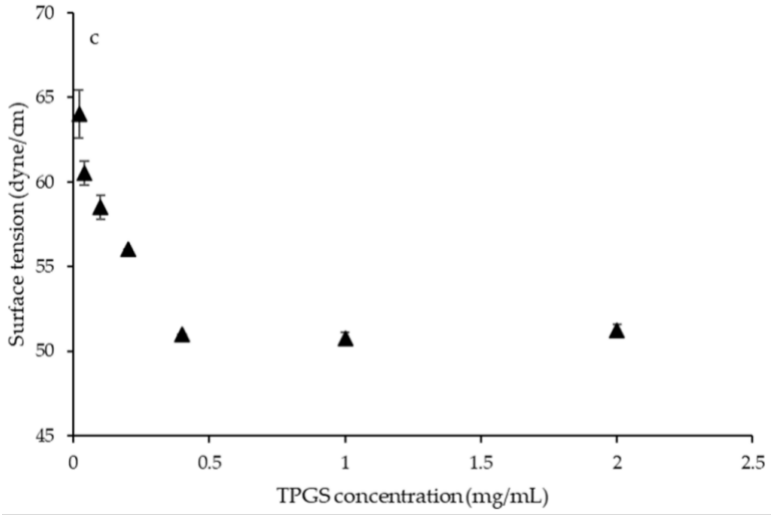

Figure PIII 1.1 Surface tension values as function of (a) biosurfactant from *L. gasseri* BC9 (BC9-BS), (b) Cocamidopropyl betaine (CAPB) and (c) D-α-tocopheryl polyethylene glycol 1000 succinate (TPGS) concentrations (mg/mL). Data are plotted as mean values of surface tension (dyne/cm) ± SD (n = 3).

1.3.2. BC9-BS as solubilizing agent

Drug solubility represents a key factor in pharmaceutical research and development, and it is even more relevant when it regards nasal drug delivery. In fact, due to the small volume of formulation that can be delivered to the nasal cavity, the administration of low water-soluble active ingredients in quantities that are sufficient to exert a therapeutic effect can be difficult [5,33]. As a result, in the present study, solubility experiments were performed to investigate whether BC9-BS and the two other surfactants used as models, CAPB and TPGS, could be employed as excipients to improve HC solubility and thus facing the limit posed by the volume restriction. Moreover, since according to the Fick's first law the diffusion of active molecules is directly proportional to the solubility of the drug, solubility measurements were strictly necessary to evaluate HC permeation during *in vitro* studies [24].

Figure PIII 1.2 displays results obtained by solubilizing HC at room temperature in PBS pH 5.5 in the absence and presence of surfactants at concentrations half-fold (<CMC) and five-fold (>CMC) the respective CMC.

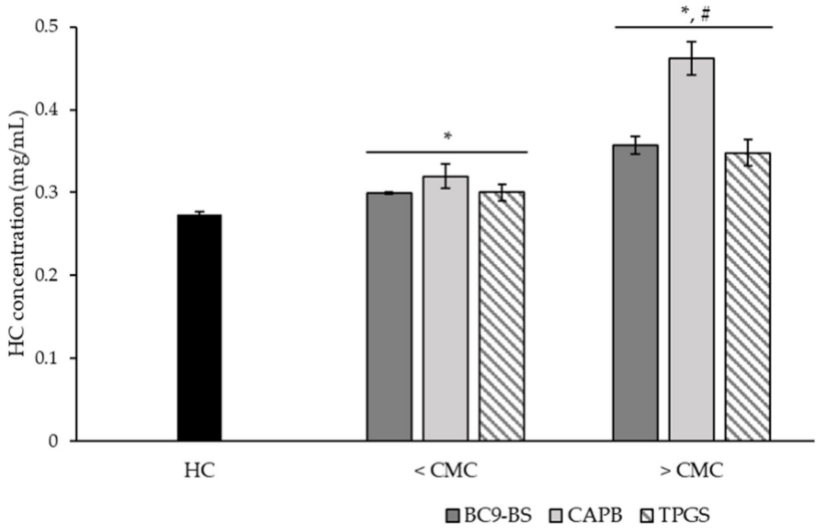

Figure PIII 1.2 Surfactants influence on hydrocortisone (HC) solubility at room temperature (25 °C) when used at concentrations below (<) and above (>) the respective critical micelle concentration (CMC). Data are expressed as means ± SD, n = 3. Significance indicated by * = $p < 0.05$ with respect to HC solubility without surfactants (black bar), by # = $p < 0.05$ compared to HC solubility in the presence of the same surfactant at a concentration < CMC.

The maximum solubility reached by HC in the buffer solution without the addition of any of the surfactants was 0.274 ± 0.004 mg/mL, which was lower than that observed in water (0.295 ± 0.003 mg/mL [30]). This result is reasonable if taking into consideration the "salting-out" effect, which consists of the ability of inorganic salts, such as NaCl, to decrease the solubility of nonelectrolytes by increasing the polarity of water [34].

Results clearly demonstrated that all tested surfactants, when added at a concentration below their CMC, already determined a significant increase in drug solubility ($p < 0.05$) with respect to the sole HC. Such an increment was even more noticeable when surfactants were used at a concentration five-fold the CMC, reasonably because of amphiphilic molecules tendency to self-assemble in micelles, which are characterized by a hydrophobic region available for the solubilization of HC. BC9-BS, in particular, led to an increase in HC solubility up to 0.300 ± 0.001 mg/mL and 0.357 ± 0.011 mg/mL below and above its CMC respectively, confirming our previous findings: biosurfactants act as solubilizing agents and are able to interact with the drug both as single molecules (i.e., true supersaturation) and micelles [18,24].

1.3.3. BC9-BS interaction with mucin

Another limiting factor in nasal delivery is the mucus turnover due to the mucociliary clearance in the upper respiratory tract, that negatively influences the efficacy of liquid nasal formulations. Therefore, a main goal would be to develop innovative formulations able to increase drug residence time and adhesion to the site of administration [35]. Because of

this, surfactant capability to interact with the main component of the mucus layer was investigated solubilizing the surface-active agents in PBS pH 5.5 at concentrations below and above their respective CMC, both in the presence and absence of mucin. Results reported in **Figure PIII 1.3** demonstrated that, below the CMC, only BC9-BS and CAPB were able to interact with mucin.

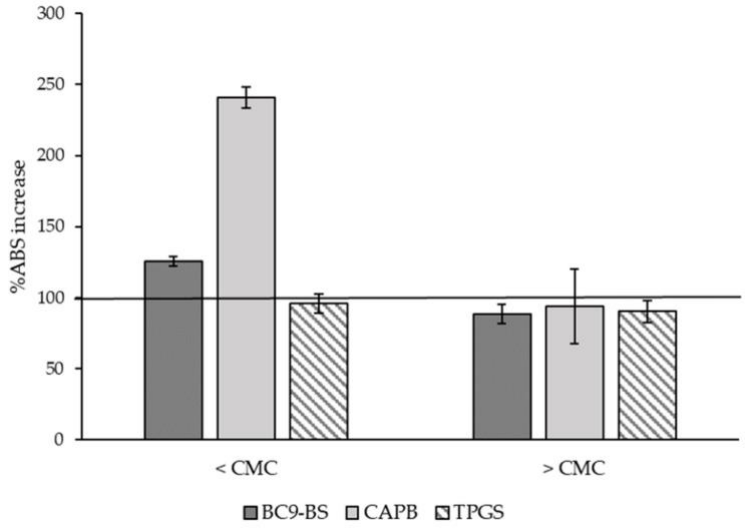

Figure PIII 1.3 Surfactants interaction with mucin as function of their concentration. Data are reported as percentage increase of the sample absorbance (ABS) in the presence of mucin with respect to the same sample without mucin, and are expressed as means ± SD, n = 3.

The percentage ABS (%ABS) increase might be due to the electrostatic interactions between mucin glycoproteins, in particular the sialic acid residues which are deprotonated at pH values above 2.6 [35], and the positive charges contained in the investigated molecules. Neither BC9-BS nor CAPB are cationic surfactants; nevertheless, the peptidic portion of the BS contains some residues of His [14], a basic amino acid, and the betaine is characterized by a balance between positive and negative charges, because at pH 5.5 it is present in its zwitterionic form [36]. This hypothesis is in agreement with what was obtained in the case of TPGS: because of its non-ionic nature, it did not allow for a %ABS increase. Interestingly, when surfactants were used at a concentration five-fold their CMC, none of them were able to interact with mucin. This was not surprising for TPGS, but the fact that BC9-BS and CAPB exhibited a mucoadhesive potential exclusively as single molecules suggested that the micellar organization could hide some functional groups that were previously available for mucin interaction.

1.3.4. BC9-BS as nasal permeation enhancer

Given the multiple barriers that active ingredients must overcome before reaching their target, drug absorption represents a great issue for nasal delivery. Therefore, formulation scientists frequently exploit permeation enhancers, which can increase drug absorption through the mucosal tissue by temporarily altering the nasal membrane [37]. The possibility to employ BC9-BS as an innovative absorption enhancer in the field of nasal drug delivery was investigated performing diffusion studies across different *in vitro* models, such as the innovative PermeaPad® barrier. The latter belongs to the cell-free permeation tools class and, since it is made of phospholipids sandwiched between two support sheets, mimics the cell membrane and thus it is referred as a biomimetic membrane [38]. PermeaPad® is considered a new cost-effective, easy to use and reliable system for drug permeability screening characterized by a good shelf-life and resistance to pH variations [39]. Moreover, its ability to predict passive drug permeability in the presence of surfactants, co-solvents and simulated fluids makes it suitable to study enabling formulations [40]. Initially, the PermeaPad® barrier was developed to investigate the permeability of drugs intended for oral delivery; then, it was further evaluated for its ability to foresee buccal [41] and nasal permeability [21].

Figure PIII 1.4 shows HC apparent permeability coefficient (Kp) across the PermeaPad® barrier in the absence and presence of surfactants used at concentrations below and above their CMC, half-fold and five-fold respectively. When used at a concentration below the CMC, all tested surfactants were able to significantly ($p < 0.05$) increase drug permeability with respect to the control. In particular, BC9-BS improved HC permeability from 7.300 ± 0.480 10^{-6} cm/s in the control sample to 9.000 ± 0.257 10^{-6} cm/s, thus demonstrating the biosurfactant ability to act as a permeation enhancer. Considering the samples containing surfactants at a concentration five-fold their CMC, the absorption-enhancing effect was still detectable only for BC9-BS and TPGS. Conversely, HC permeability in the presence of betaine was found to be significantly lower with respect to that of both the BS and the non-ionic surfactant, and it was also comparable to that of the control ($p > 0.05$). A decrease in drug permeability in the presence of a surfactant used at a concentration above the CMC with respect to that obtained with the same surface-active molecule but at a concentration below the CMC is not something new. Indeed, Abruzzo et al. [30] had already observed this phenomenon while studying the ability of some surfactants produced from itaconic acid to improve HC permeation across the skin. In the case of the present study, the different CAPB behavior compared to the other two surfactants might be the result of a higher HC

entrapment into micelles. Probably, since micelles act as a drug reservoir, they tend to gradually release HC in the buffer medium, thus slowing down its diffusion across the membrane.

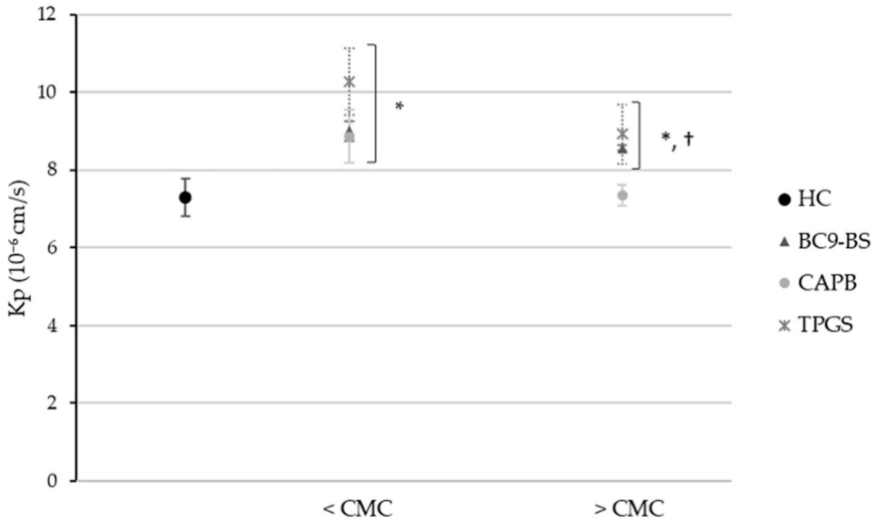

Figure PIII 1.4 HC permeability across the PermeaPad® barrier in the absence and presence of surfactants at concentrations below (<) and above (>) their CMC. Data are expressed as means ± SD, n = 3. Significance indicated by * = $p < 0.05$ with respect to Kp of HC without surfactants, and by † = $p < 0.05$ compared to Kp of HC in presence of CAPB > CMC.

The PermeaPad® barrier only reproduces the epithelium of the mucosal tissue, thus it does not take into account the mucus gel layer that covers the nasal cavity. To deepen the ability of BC9-BS to improve nasal absorption of HC, the PermeaPad® model was enriched with an artificial mucin layer. The latter was obtained through mucin dialysis and subsequent freeze-drying to remove from the initial mixture of glycoproteins, those low molecular weight molecules able to diffuse across the PermeaPad®, thus preventing the possibility of maintaining a stable mucus layer over the time. The results collected from the *in vitro* permeation study across the PermeaPad® and mucin system highlighted the impact of the mucus layer on the diffusion of the model drug (**Figure PIII 1.5**). As a matter of fact, HC permeability decreased from 7.300 ± 0.480 10^{-6} cm/s in the absence of mucin, to 3.275 ± 0.153 10^{-6} cm/s in the presence of the mucus layer, consequently underlining the negative influence of mucus on drug absorption. This phenomenon had already been observed by Falavigna et al. [7], who developed a mucus-covered artificial permeation membrane by pipetting a mucin dispersion on the top of a PVPA (phospholipid vesicles-based permeation assay) barrier, clarifying the impact of the mucus layer on the absorption of hydrophilic and lipophilic drugs. Moreover, our result was in line with previously reported data, which elucidated the tendency of lipophilic molecules to nonspecifically bind to hydrophobic

regions in mucin glycoproteins, resulting in drug diffusion hindrance through the mucus layer [35]. Despite the additional obstacle towards HC permeation, BC9-BS significantly ($p < 0.05$) increased drug permeability with respect to the control at both the concentrations tested, reaching values of 4.550 ± 0.159 10^{-6} cm/s and 4.383 ± 0.047 10^{-6} cm/s at half and five-fold its CMC, respectively. Moreover, the biosurfactant was demonstrated to be as effective as CAPB and TPGS in improving drug absorption. Surprisingly, CAPB, which did not appear as a permeation-enhancing molecule on the PermeaPad®, in the presence of the mucin layer allowed for a greater increase in HC permeability with respect to the control.

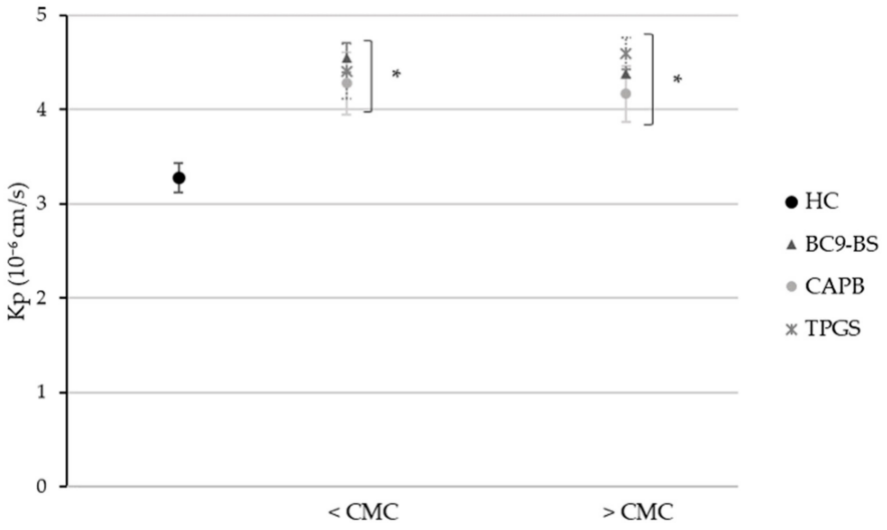

Figure PIII 1.5 HC permeability across the PermeaPad® barrier functionalized with a mucin layer in the absence and presence of surfactants at concentrations below (<) and above (>) their CMC. Data are expressed as means ± SD, n = 3. Significance indicated by * = $p < 0.05$ with respect to Kp of HC without surfactants.

For a better understanding of the permeation-enhancing properties of the tested surfactants when the mucus layer was included in the barrier system, the enhancement ratio (ER) was evaluated. Since on both PermeaPad®-based models the greater absorption enhancing effect was observed when surfactants were used at the lowest concentration tested, the ER value was calculated for each compound only when used at a concentration below the CMC. **Table PIII 1.1** shows that only BC9-BS and CAPB exhibited a higher ER value across the PermeaPad® barrier functionalized with mucin compared to the simple PermeaPad®. It is known that the mucus layer acts as a barrier towards the diffusion of foreign entities, such as drugs and particles, exploiting two main mechanisms: interaction and size filtering [8]. The first includes those weak interactions that occur between the mucus and the investigated molecule, whereas size filtering depends on the mucus mesh cut-off, which can avoid the diffusion of large entities [7]. Thus, probably, BC9-BS and CAPB, in virtue of their

interaction with mucin (see Section 1.3.3), can perturb the mucus layer, favoring HC diffusion toward the PermeaPad® membrane.

Table PIII 1.1 Enhancement ratio (ER) of surfactants employed at a concentration below the CMC using the PermeaPad® or PermeaPad® functionalized with a mucin layer.

Sample	PermeaPad®	PermeaPad® and Mucin
BC9-BS	1.23	1.39
CAPB	1.21	1.31
TPGS	1.41	1.35

Since BC9-BS was the surfactant characterized by the higher ER value on the PermeaPad® and mucin model, its absorption-enhancing properties were also investigated performing diffusion studies across the sheep nasal mucosa. Furthermore, since no significant differences ($p > 0.05$) in drug permeability were observed using the biosurfactant at a concentration below or above its CMC, neither with the PermeaPad® model nor with the PermeaPad® and mucin one, the experiment was conducted using BC9-BS only at a concentration of half its CMC. **Figure PIII 1.6** shows that BC9-BS was able to improve HC permeability across the sheep nasal mucosa too, as it was predicted by previous *in vitro* models. Despite the high standard deviations, that are a consequence of the inter-animal and inter-membrane differences, the Kp coefficient of HC in the presence of the biosurfactant was confirmed to be significantly improved with respect to the control ($p < 0.05$).

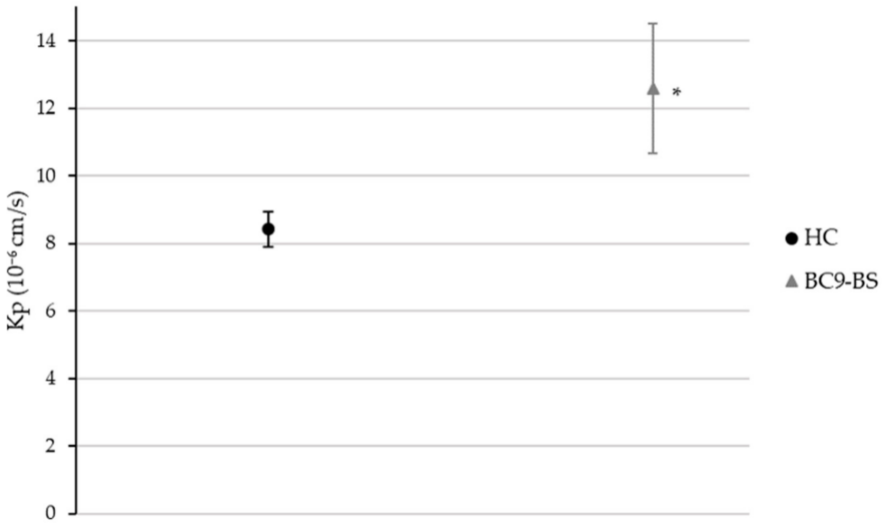

Figure PIII 1.6 HC permeability across the sheep nasal mucosa in the absence and presence of BC9-BS at a concentration below the CMC. Data are expressed as means ± SD, n = 3. Significance indicated by * = $p < 0.05$ with respect to the control.

1.4. Conclusions

The use of biosurfactants (BS) for drug delivery purposes has been attracting great interest in recent years and, as a result, proofs of their applicability as enhancer molecules for nasal administration of drugs have already been published [42,43]. Nevertheless, it can be stated that this is the first study that evaluated the employment of biosurfactants isolated from a human *Lactobacillus* strain as a natural excipient and absorption enhancer for nasal drug delivery. BC9-BS was able to increase HC solubility, as well as drug permeability, across both PermeaPad®-based models and, at a concentration below its CMC, it allowed for a greater HC diffusion across the excised animal tissue too. Of note, BC9-BS activity as a solubilizing agent and absorption enhancer was already visible at the lowest concentration tested, the same at which the biosurfactant was also found to be able to interact with the main component of the nasal mucosa, i.e., mucin.

With respect to the surfactants used as reference, the BS shows some features that are common to both: the biosurfactant shows a mucoadhesive potential as the betaine does and it exhibits a solubilizing activity that is equal to that of the non-ionic surfactant. However, considering the permeation across the PermeaPad® barrier functionalized with a mucin layer, which is the *in vitro* model that better mimics the *in vivo* conditions of the nasal cavity, BC9-BS proves to be the surface-active molecule with the higher permeation enhancing effect. Along with its demonstrated effectiveness, BC9-BS is considered more advantageous than the synthetic equivalents in virtue of its natural origin, because it is produced from renewable sources and, since it is a biosurfactant, it is reported to be more easily biodegraded and less toxic than chemical surfactants.

For a better comprehension of biosurfactants role as innovative excipients, future studies should investigate whether BS are also effective at improving the delivery of drugs with different physico-chemical features. Moreover, it could be interesting to evaluate the effect of BS inclusion in different kind of formulations aimed to improve nasal administration of active ingredients.

1.5. References Paper I

1. Illum, L. Nasal Drug Delivery—Possibilities, Problems and Solutions. J. Controlled Release 2003, 87, 187–198, doi:10.1016/S0168-3659(02)00363-2.
2. Fortuna, A.; Alves, G.; Serralheiro, A.; Sousa, J.; Falcão, A. Intranasal Delivery of Systemic-Acting Drugs: Small-Molecules and Biomacromolecules. Eur. J. Pharm. Biopharm. 2014, 88, 8–27, doi:10.1016/j.ejpb.2014.03.004.

3. Keller, L.-A.; Merkel, O.; Popp, A. Intranasal Drug Delivery: Opportunities and Toxicologic Challenges during Drug Development. Drug Deliv. Transl. Res. 2021, doi:10.1007/s13346-020-00891-5.
4. Rohrer, J.; Lupo, N.; Bernkop-Schnürch, A. Advanced Formulations for Intranasal Delivery of Biologics. Int. J. Pharm. 2018, 553, 8–20, doi:10.1016/j.ijpharm.2018.10.029.
5. Ozsoy, Y.; Güngör, S. Nasal Route: An Alternative Approach for Antiemetic Drug Delivery. Expert Opin. Drug Deliv. 2011, 8, 1439–1453, doi:10.1517/17425247.2011.607437.
6. Ghadiri, M.; Young, P.; Traini, D. Strategies to Enhance Drug Absorption via Nasal and Pulmonary Routes. Pharmaceutics 2019, 11, 113, doi:10.3390/pharmaceutics11030113.
7. Falavigna, M.; Stein, P.; Flaten, G.; di Cagno, M. Impact of Mucin on Drug Diffusion: Development of a Straightforward In Vitro Method for the Determination of Drug Diffusivity in the Presence of Mucin. Pharmaceutics 2020, 12, 168, doi:10.3390/pharmaceutics12020168.
8. Murgia, X.; Loretz, B.; Hartwig, O.; Hittinger, M.; Lehr, C.-M. The Role of Mucus on Drug Transport and Its Potential to Affect Therapeutic Outcomes. Adv. Drug Deliv. Rev. 2018, 124, 82–97, doi:10.1016/j.addr.2017.10.009.
9. Santos, D.; Rufino, R.; Luna, J.; Santos, V.; Sarubbo, L. Biosurfactants: Multifunctional Biomolecules of the 21st Century. Int. J. Mol. Sci. 2016, 17, 401, doi:10.3390/ijms17030401.
10. Bjerk, T.R.; Severino, P.; Jain, S.; Marques, C.; Silva, A.M.; Pashirova, T.; Souto, E.B. Biosurfactants: Properties and Applications in Drug Delivery, Biotechnology and Ecotoxicology. Bioengineering 2021, 8, 115, doi:10.3390/bioengineering8080115.
11. Naughton, P.J.; Marchant, R.; Naughton, V.; Banat, I.M. Microbial Biosurfactants: Current Trends and Applications in Agricultural and Biomedical Industries. J. Appl. Microbiol. 2019, 127, 12–28, doi:10.1111/jam.14243.
12. Kumar, A.; Singh, S.K.; Kant, C.; Verma, H.; Kumar, D.; Singh, P.P.; Modi, A.; Droby, S.; Kesawat, M.S.; Alavilli, H.; et al. Microbial Biosurfactant: A New Frontier for Sustainable Agriculture and Pharmaceutical Industries. Antioxidants 2021, 10, 1472, doi:10.3390/antiox10091472.
13. Ceresa, C.; Fracchia, L.; Fedeli, E.; Porta, C.; Banat, I.M. Recent Advances in Biomedical, Therapeutic and Pharmaceutical Applications of Microbial Surfactants. Pharmaceutics 2021, 13, 466, doi:10.3390/pharmaceutics13040466.
14. Abruzzo, A.; Giordani, B.; Parolin, C.; Vitali, B.; Protti, M.; Mercolini, L.; Cappelletti, M.; Fedi, S.; Bigucci, F.; Cerchiara, T.; et al. Novel Mixed Vesicles Containing Lactobacilli

Biosurfactant for Vaginal Delivery of an Anti- Candida Agent. Eur. J. Pharm. Sci. 2018, 112, 95–101, doi:10.1016/j.ejps.2017.11.012.

15. Abruzzo, A.; Giordani, B.; Parolin, C.; De Gregorio, P.R.; Foschi, C.; Cerchiara, T.; Bigucci, F.; Vitali, B.; Luppi, B. Lactobacillus Crispatus BC1 Biosurfactant Delivered by Hyalurosomes: An Advanced Strategy to Counteract Candida Biofilm. Antibiotics 2021, 10, 33, doi:10.3390/antibiotics10010033.
16. Satpute, S.K.; Kulkarni, G.R.; Banpurkar, A.G.; Banat, I.M.; Mone, N.S.; Patil, R.H.; Cameotra, S.S. Biosurfactant/s from Lactobacilli Species: Properties, Challenges and Potential Biomedical Applications: Biosurfactant/s from Lactobacilli Species. J. Basic Microbiol. 2016, 56, 1140–1158, doi:10.1002/jobm.201600143.
17. Giordani, B.; Costantini, P.E.; Fedi, S.; Cappelletti, M.; Abruzzo, A.; Parolin, C.; Foschi, C.; Frisco, G.; Calonghi, N.; Cerchiara, T.; et al. Liposomes Containing Biosurfactants Isolated from Lactobacillus Gasseri Exert Antibiofilm Activity against Methicillin Resistant Staphylococcus Aureus Strains. Eur. J. Pharm. Biopharm. 2019, 139, 246–252, doi:10.1016/j.ejpb.2019.04.011.
18. Abruzzo, A.; Parolin, C.; Corazza, E.; Giordani, B.; di Cagno, M.P.; Cerchiara, T.; Bigucci, F.; Vitali, B.; Luppi, B. Influence of Lactobacillus Biosurfactants on Skin Permeation of Hydrocortisone. Pharmaceutics 2021, 13, 820, doi:10.3390/pharmaceutics13060820.
19. Maher; Casettari; Illum Transmucosal Absorption Enhancers in the Drug Delivery Field. Pharmaceutics 2019, 11, 339, doi:10.3390/pharmaceutics11070339.
20. Gholami, A.; Golestaneh, M.; Andalib, Z. A New Method for Determination of Cocamidopropyl Betaine Synthesized from Coconut Oil through Spectral Shift of Eriochrome Black T. Spectrochim. Acta. A. Mol. Biomol. Spectrosc. 2018, 192, 122–127, doi:10.1016/j.saa.2017.11.007.
21. Wu, I.Y.; Bala, S.; Škalko-Basnet, N.; di Cagno, M.P. Interpreting Non-Linear Drug Diffusion Data: Utilizing Korsmeyer-Peppas Model to Study Drug Release from Liposomes. Eur. J. Pharm. Sci. 2019, 138, 105026, doi:10.1016/j.ejps.2019.105026.
22. Illum, L. Nasal Delivery. The Use of Animal Models to Predict Performance in Man. J. Drug Target. 1996, 3, 427–442, doi:10.3109/10611869609015963.
23. Abruzzo, A.; Cerchiara, T.; Bigucci, F.; Zuccheri, G.; Cavallari, C.; Saladini, B.; Luppi, B. Cromolyn-Crosslinked Chitosan Nanoparticles for the Treatment of Allergic Rhinitis. Eur. J. Pharm. Sci. 2019, 131, 136–145, doi:10.1016/j.ejps.2019.02.015.

24. di Cagno, M.; Luppi, B. Drug “Supersaturation” States Induced by Polymeric Micelles and Liposomes: A Mechanistic Investigation into Permeability Enhancements. Eur. J. Pharm. Sci. 2013, 48, 775–780, doi:10.1016/j.ejps.2013.01.006.
25. Jahan, R.; Bodratti, A.M.; Tsianou, M.; Alexandridis, P. Biosurfactants, Natural Alternatives to Synthetic Surfactants: Physicochemical Properties and Applications. Adv. Colloid Interface Sci. 2020, 275, 102061, doi:10.1016/j.cis.2019.102061.
26. Misra, A.; Jogani, V.; Jinturkar, K.; Vyas, T. Recent Patents Review on Intranasal Administration for CNS Drug Delivery. Recent Pat. Drug Deliv. Formul. 2008, 2, 25–40, doi:10.2174/187221108783331429.
27. Dai, C.; Zhao, J.; Yan, L.; Zhao, M. Adsorption Behavior of Cocamidopropyl Betaine under Conditions of High Temperature and High Salinity. J. Appl. Polym. Sci. 2014, 131, n/a-n/a, doi:10.1002/app.40424.
28. Sadoqi, M.; Lau-Cam, C.A.; Wu, S.H. Investigation of the Micellar Properties of the Tocopheryl Polyethylene Glycol Succinate Surfactants TPGS 400 and TPGS 1000 by Steady State Fluorometry. J. Colloid Interface Sci. 2009, 333, 585–589, doi:10.1016/j.jcis.2009.01.048.
29. Bloor, J.R.; Morrison, J.C.; Rhodes, C.T. Effect of pH on the Micellar Properties of a Nonionic Surfactant. J. Pharm. Sci. 1970, 59, 387–391, doi:10.1002/jps.2600590325.
30. Abruzzo, A.; Armenise, N.; Bigucci, F.; Cerchiara, T.; Gösser, M.B.; Samorì, C.; Galletti, P.; Tagliavini, E.; Brown, D.M.; Johnston, H.J.; et al. Surfactants from Itaconic Acid: Toxicity to HaCaT Keratinocytes in Vitro, Micellar Solubilization, and Skin Permeation Enhancement of Hydrocortisone. Int. J. Pharm. 2017, 524, 9–15, doi:10.1016/j.ijpharm.2017.03.056.
31. Chen, A.; An, Y.; Huang, W.; Xuan, T.; Zhang, Q.; Ye, M.; Luo, S.; Xuan, X.; He, H.; Zheng, J.; et al. Highly Water-Preserving Zwitterionic Betaine-Incorporated Collagen Sponges With Anti-Oxidation and Anti-Inflammation for Wound Regeneration. Front. Cell Dev. Biol. 2020, 8, 491, doi:10.3389/fcell.2020.00491.
32. Keshari, P.; Sonar, Y.; Mahajan, H. Curcumin Loaded TPGS Micelles for Nose to Brain Drug Delivery: In Vitro and in Vivo Studies. Mater. Technol. 2019, 34, 423–432, doi:10.1080/10667857.2019.1575535.
33. Warnken, Z.; Smyth, H.D.C.; Williams, R.O. Route-Specific Challenges in the Delivery of Poorly Water-Soluble Drugs. In Formulating Poorly Water Soluble Drugs; Williams III, R.O., Watts, A.B., Miller, D.A., Eds.; AAPS Advances in the Pharmaceutical Sciences

Series; Springer International Publishing: Cham, 2016; Vol. 22, pp. 1–39 ISBN 978-3-319-42607-5.

34. Nina, N.; El-Sayed, M.M.; Sanghvi, T.; Yalkowsky, S.H. Estimation of the Effect of NaCl on the Solubility of Organic Compounds in Aqueous Solutions. J. Pharm. Sci. 2000, 89, 1620–1625, doi:10.1002/1520-6017(200012)89:12<1620::AID-JPS13>3.0.CO;2-N.
35. Sigurdsson, H.H.; Kirch, J.; Lehr, C.-M. Mucus as a Barrier to Lipophilic Drugs. Int. J. Pharm. 2013, 453, 56–64, doi:10.1016/j.ijpharm.2013.05.040.
36. Danov, K.D.; Kralchevska, S.D.; Kralchevsky, P.A.; Ananthapadmanabhan, K.P.; Lips, A. Mixed Solutions of Anionic and Zwitterionic Surfactant (Betaine): Surface-Tension Isotherms, Adsorption, and Relaxation Kinetics. Langmuir 2004, 20, 5445–5453, doi:10.1021/la049576i.
37. Laffleur, F.; Bauer, B. Progress in Nasal Drug Delivery Systems. Int. J. Pharm. 2021, 607, 120994, doi:10.1016/j.ijpharm.2021.120994.
38. Berben, P.; Bauer-Brandl, A.; Brandl, M.; Faller, B.; Flaten, G.E.; Jacobsen, A.-C.; Brouwers, J.; Augustijns, P. Drug Permeability Profiling Using Cell-Free Permeation Tools: Overview and Applications. Eur. J. Pharm. Sci. 2018, 119, 219–233, doi:10.1016/j.ejps.2018.04.016.
39. di Cagno, M.; Bibi, H.A.; Bauer-Brandl, A. New Biomimetic Barrier PermeapadTM for Efficient Investigation of Passive Permeability of Drugs. Eur. J. Pharm. Sci. 2015, 73, 29–34, doi:10.1016/j.ejps.2015.03.019.
40. Bibi, H.A.; di Cagno, M.; Holm, R.; Bauer-Brandl, A. PermeapadTM for Investigation of Passive Drug Permeability: The Effect of Surfactants, Co-Solvents and Simulated Intestinal Fluids (FaSSIF and FeSSIF). Int. J. Pharm. 2015, 493, 192–197, doi:10.1016/j.ijpharm.2015.07.028.
41. Bibi, H.A.; Holm, R.; Bauer-Brandl, A. Use of Permeapad® for Prediction of Buccal Absorption: A Comparison to in Vitro, Ex Vivo and in Vivo Method. Eur. J. Pharm. Sci. 2016, 93, 399–404, doi:10.1016/j.ejps.2016.08.041.
42. Perinelli, D.R.; Vllasaliu, D.; Bonacucina, G.; Come, B.; Pucciarelli, S.; Ricciutelli, M.; Cespi, M.; Itri, R.; Spinozzi, F.; Palmieri, G.F.; et al. Rhamnolipids as Epithelial Permeability Enhancers for Macromolecular Therapeutics. Eur. J. Pharm. Biopharm. 2017, 119, 419–425, doi:10.1016/j.ejpb.2017.07.011.
43. Yu, Q.; Dong, S.; Yang, D.; Xing, X.; Zhao, X.; Qi, G. Bacillus-Produced Surfactin for Intranasal Delivery of Insulin in Diabetic Mice. Int. J. Diabetes Dev. Ctries. 2018, 38, 321–329, doi:10.1007/s13410-017-0564-3.

2. Drug delivery to the brain: In situ gelling formulation enhances carbamazepine diffusion through nasal mucosa models with mucin

Elisa Corazza[1], Massimiliano Pio di Cagno[2, *], Annette Bauer-Brandl[3], Angela Abruzzo[1], Teresa Cerchiara[1], Federica Bigucci[1], Barbara Luppi[1]

[1] Department of Pharmacy and Biotechnology, Alma Mater Studiorum, University of Bologna, Via San Donato 19/2, Bologna 40127, Italy

[2] Department of Pharmacy, Faculty of Mathematics and Natural Sciences, University of Oslo, Sem Sælands vei 3, Oslo 0371, Norway

[3] Department of Physics, Chemistry and Pharmacy, University of Southern Denmark, Campusvej 55, Odense 5230, Denmark

[*] Corresponding author

Published on European Journal of Pharmaceutical Sciences (doi: 10.1016/j.ejps.2022.106294)

Abstract: The objective of this work was to optimize a thermosensitive *in situ* gelling formulation to improve intranasal and nose-to-brain delivery of the antiepileptic drug carbamazepine (CBZ). A preliminary procedure of vehicles obtained just mixing different fractions of poloxamer 407 (P407) and poloxamer 188 (P188) revealed preparations with phase transition temperatures, times to gelation and pH values suitable for nasal delivery. Subsequently, the mucoadhesive properties of the most promising formulations were tuned by adding hydroxypropylmethylcellulose (HPMC) types of different viscosity grades, and the effect of the adhesive polymers was evaluated by testing *in vitro* time and strength of mucoadhesion on specimens of sheep nasal mucosa. The formulation that showed the greatest mucoadhesive potential *in vitro*, with a time and force of mucoadhesion equal to 1746.75 s and 3.66 $\times 10^{-4}$ N, respectively, was that composed of 22% P407, 5% P188 and 0.8% HPMC low-viscous and it was further investigated for its ability to increase drug solubility and to control the release of the drug. Lastly, the capability of the candidate vehicle to ensure drug permeation across the biomimetic membrane Permeapad®, an artificial phospholipid-based barrier with a stratified architecture, and the same barrier enriched with

a mucin layer was verified. The final formulation was characterized by a pH value of 6.0, underwent gelation at 32.33 °C in 37.85 s, thus showing all the features required by *in situ* gelling thermosensitive preparations designed for nasal delivery and, more notably, it conserved the ability to favor drug permeation in the presence of mucin. These findings suggest that the optimized gelling system could be a promising and easy to realize strategy to improve CBZ delivery to the brain exploiting both a direct and indirect pathway.

Keywords: Carbamazepine; Nasal delivery; Thermosensitive polymers; *In situ* gelling; Mucoadhesion; Drug permeation.

2.1. Introduction

The World Health Organization reported that about 50 million people worldwide are affected by a chronic and progressive brain disorder, named epilepsy [1–4]. Patients suffering from this neurological disease show recurrent and unpredictable seizures along with brain alterations, which both arise from an abnormal neuronal activity [2,3]. Currently available treatments mainly rely on the administration of antiepileptic drugs that only affect the symptoms [3].

Since it was first marketed in the 1960s, carbamazepine (CBZ) has been the most frequently prescribed drug for epileptic seizures management in patients of different ages, including pediatrics [1–6]. This dibenzoazepine derivative is commonly administered orally and is available in multiple dosage forms, such as tablets, chewable tablets, and oral suspensions [1], despite some limitations related to the pharmacokinetic properties of the drug and the route of administration. In fact, belonging to the class II of the Biopharmaceutics Classification System (BCS), CBZ shows a good permeability but a low water solubility, which makes the design of the formulation more complex and causes a slow and variable absorption of the active molecule [2,5]. CBZ is also subjected to considerable hepatic metabolism, which results in extensive inter-individual variability of bioavailability and in the production of metabolites with relevant clinical toxicity [1,5,7]. Moreover, the therapeutic effectiveness of CBZ is also limited by the need to cross the blood-brain barrier (BBB), which is characterized by a reduced permeability towards both large and small molecules due to the protective function exerted by tight junctions and efflux transporters [2,3]. CBZ is still representing the standard of care for epilepsy treatment and, even though a new generation of antiepileptic drugs with improved tolerability is available [1], new formulative strategies are needed to face the shortcomings associated with oral delivery. In fact, efforts have been

made to rethink CBZ delivery through the oral route, and some examples can be found in the literature [2,5,8]. In an attempt of achieving a more effective strategy for the treatment of epilepsy, drug development for psychiatric disorders is moving towards nasal delivery as a potential alternative to the oral route [3,9,10].

Intranasal administration is an established strategy to deliver active pharmaceutical ingredients with either local or systemic effect, and it is raising great consideration because of its unique anatomical connection with the brain [10–13]. Indeed, the olfactory and trigeminal nerves, located in the olfactory and respiratory region respectively, allow for the nose-to-brain absorption of drugs aimed to act at the central nervous system (CNS) level [9,10,12–14]. Hence, the availability of a direct access to the brain makes it possible for drugs to both escape the firs-pass effect and avoid crossing the BBB, resulting in an improved bioavailability, increased accumulation in the CNS, and faster onset of action, which is a key point in the management of acute seizure episodes [9–13]. Anyway, thanks to the high vascularization of the nasal mucosa, an indirect pathway towards the brain through the systemic absorption is available. Moreover, the intranasal route is considered a valid alternative for patients for whom the oral administration is not suitable and, because it is easily accessible and painless, it is supposed to improve both the compliance and the adherence to the treatment [11–13]. However, also nasal delivery presents some drawbacks. In fact, for drugs requiring high doses and characterized by low solubility, the first limit encountered is the small size of nostrils that reduces the applicable volume of formulations [10,13]. Secondly, the nasal cavity is covered by a relatively thick mucus layer, which is subjected to a high rate of turnover due to regular cilia beating that causes mucous to move, a mechanism known as mucociliary clearance (MCC). To address the downsides related to nasal delivery, multiple strategies have been proposed, including the employment of “smart” polymers.

In situ gelling formulations are initially present in a liquid state, but undergo sol-gel transition once administered in the nasal cavity due to hydrophobic interactions within the gel components, which are triggered by various physical (temperature, pH, and charge of the mucosal environment) or chemical factors (for instance, oxidative cross-linking) [11,12,14,15]. In virtue of their behavior, they exhibit many advantages over other delivery vehicles for nasal application: uniformly conform to the mucosal tissue, increase drug retention and bioavailability by reducing post-nasal drip and MCC, possibly provide sustained drug release, hence improving patient adherence, and reducing both dosing frequency and systemic side effects [9,15,16]. Hydrogels responsive to temperature

variation are one of the most broadly investigated environment-sensitive drug delivery systems [16–18] and particular, those based on poloxamers have been extensively studied to obtain *in situ* forming nasal gels [15]. Poloxamers are water-soluble tri-block non-ionic copolymers with amphiphilic and surface active properties, consisting of a central hydrophobic block of poly (propylene oxide) (PPO) and two hydrophilic terminal blocks of poly (ethylene oxide) (POE) [15,19]. The presence of both polar and non-polar monomers enables the formation of ordered structures in solution, named micelles, which allow for the encapsulation of hydrophobic drugs [17]. Further, heating the aqueous solution to the critical micelle temperature induces PPO chains to become less soluble resulting in micelle packing and entanglement followed by gelation [20]. Lastly, poloxamers are FDA-approved and listed in the United States and European Pharmacopoeia as they are neither toxic nor irritant, and have been widely exploited as potential excipients in pharmaceuticals with various applications, including targeting of the CNS and drug delivery [15–17,19].

Some preliminary studies have already proved the feasibility of the nasal delivery for examples of drugs targeting the brain, such as antidepressants [21,22] and antiepileptic drugs [2,3]; moreover, clinical trials demonstrated that benzodiazepine nasal delivery is as effective in preventing seizures as the same active molecule delivered using conventional approaches [13]. Hence, to take advantage of the favorable features associated with intranasal administration, the purpose of the present work was to develop an *in situ* gelling thermosensitive formulation based on poloxamers for CBZ nasal delivery. Firstly, poloxamer 407 (P407) and poloxamer 188 (P188) were mixed at different fractions to obtain delivery vehicles with sol-gel transition temperature and time of gelation suitable for nasal administration. The attention was then shifted towards the mucoadhesive properties of the final product; thus high-viscous and low-viscous hydroxypropylmethylcellulose (HPMC) types were evaluated for their ability to improve the time and the strength of mucoadhesion of the gels. The ability of the poloxamers to enhance the solubility of CBZ was also investigated, as well as the influence of drug loading on formulation properties. The most suitable thermosensitive gels were further examined for CBZ release behavior together with the drug absorption profiles across *in vitro* models of the nasal mucosa, i.e. Permeapad® barrier an artificial phospholipid-based membrane with a stratified architecture, stressing the role of the gelling formulation in presence of a reconstituted mucin layer.

2.2. Materials and Methods

2.2.1. Materials

CBZ was provided from Sigma-Aldrich (Søborg, Denmark), whereas Lutrol® F68 (P188) and Lutrol® F127 (P407) were a kind gift from BASF SE (Ludwigshafen, Germany). HPMC high-viscous Benecel™ K100M Pharm (75000-140000 cps at 2% w/w) (K100M) and low-viscous Methocel™ E50LV Premium 5P (35-65 cps at 2% w/w) (E50LV) were supplied by Ashland Industries Europe GmbH (Schaffhausen, Switzerland) and Sigma-Aldrich (Milan, Italy), respectively. Green food coloring E-102 E-131 was provided from Candi Gestro srl (Siderno, Italy). Mucin type II from porcine stomach, all chemicals, and solvents were of analytical grade and purchased from Sigma-Aldrich (Milan, Italy), except for sodium chloride (NaCl) that was supplied by Carlo Erba (Milan, Italy). Phosphate buffer solution (PBS) at pH 7.4 was composed of 7.4 mM $Na_2HPO_4 \cdot 12H_2O$, 1.1 mM KH_2PO_4, and 136 mM NaCl. PBS at pH 5.5 was employed to simulate the pH of the nasal cavity and it was composed of 4.2 mM $Na_2HPO_4 \cdot 12H_2O$, 100 mM KH_2PO_4, 45.5 mM NaCl.

2.2.2. Preparation of thermosensitive in situ gelling formulations

Thermosensitive nasal gels were prepared following the cold method, that is the procedure to be selected when poloxamers (but also chitosan or carbopol) are used as gelling polymers [23]. Precisely, when formulations containing only the gelling polymers were prepared, different concentrations of P407 21-23% (w/v) and P188 3-5% (w/v) were solubilized in MilliQ ultrapure water (Millipore, Milford, MA, USA) at 4 °C under gently stirring (magnetic stirrer, Velp Scientifica, Usmate Velate, Italy), then samples were stored at +2–8 °C for 24h to obtain a clear and uniform solution. In contrast, when HPMC should be incorporated into the nasal gels, the mucoadhesive polymer was first dispersed in MilliQ ultrapure water at room temperature (RT equal to 25 ±1 °C) and the preparation was kept in the fridge overnight before adding poloxamers and stored for another night in the fridge. In the present work, two different types of HPMC were employed in various fractions: high-viscous K100M 0.1-0.3% (w/v) and low-viscous E50LV 0.4-0.8% (w/v).

2.2.3. Characterization of in situ nasal gels

Initially, in order to identify the most suitable concentration ratio between the two poloxamers, plain formulations (without the mucoadhesive polymer) were prepared, and screened for three parameters: pH, sol-gel transition temperature, and time to gelation. The

vehicles possessing the properties required from an *in situ* gelling nasal formulation, were then prepared with the addition of HPMC (mucoadhesive formulations), and the influence of the adhesive polymer on the performance of the gels was investigated by evaluating the same features.

2.2.3.1. pH

The pH of the developed formulations was determined by means of pH indicator strips 0-14 (Whatman® Panpeha™, Sigma-Aldrich, Milan, Italy). The strip was completely immersed into the liquid-state sample and the evolving color compared to those depicted on the packaging.

2.2.3.2. Sol-gel transition temperature

The temperature at which the sol-gel transition ($T_{sol-gel}$) occurred was determined in accordance with the "magnetic stirring method", observing the interruption of a magnetic bar rotation as a result of the transition to the semi-solid state of a gelling formulation, as reported by Mura et al., but with slight modifications [24]: 5 ml of each formulation was poured in a 15 mm jacketed cell with a flat-ground joint equipped with a V6A Stirrer (230V/50 Hz) (PermeGearInc., Hellertown, USA), containing a magnetic bar (5 ×12 mm). Cells were connected to a thermostated water pump (Julabo EH, JULABO Labortechnik GmbH, Seelbach, Germany) and they were gradually heated at a rate of 1 °C/min from 25 °C to 35 °C. Since the temperature within the nasal cavity is reported to be in the range of 32 to 35 °C [25] and in previously published studies a temperature of 35 °C was found adequate to reproduce the condition of the nasal cavity [26,27], this value was chosen as the upper limit of the temperature interval. The temperature, at which the bar stopped moving, was read on the digital thermostat and recorded as the gelation temperature.

2.2.3.3. Time to gelation

The time required for the formulation to undergo sol-gel transition ($t_{sol-gel}$) was measured similarly to the $T_{sol-gel}$ (see Section 2.2.3.2). However, in this case, the jacketed cells were thermostated at 35 °C, filled with 1 ml of each respective formulation and the time to gelation, that is the span required for the magnetic bar to stop rotating, was recorded using a stopwatch.

2.2.4. Mucoadhesive properties of in situ nasal gels

The mucoadhesive potential of the *in situ* gelling vehicles was investigated employing *ex vivo* sheep nasal mucosa excised from nasal turbinates, due to its morphological similarity to the human one [28]. The animal tissue was obtained from a local slaughterhouse (Sarsina, Italy) and handled as previously reported [26]. Briefly, the septum was removed, and the nasal turbinates were pulled out from the nasal cavity using forceps and scalpel. Finally, the mucosa was detached from the adhering cartilaginous tissue and washed with NaCl 0.9% (w/v). The biological specimens were stored in aluminum foils at -20 °C until use.

2.2.4.1. Time of mucoadhesion

An *in vitro* evaluation of the time of mucoadhesion was carried out similarly to a previously described procedure [24]. A section of sheep nasal mucosa (3 cm long and 1.5 cm wide) was positioned on a glass support and hydrated with a dispersion of dialyzed and lyophilized mucin (see Section 2.2.10) 0.05% (w/v) in PBS pH 5.5 for 2 min. 2 g of each formulation sample was stained with 1% (w/w) of a green food coloring and 200 µl of this solution was applied on nasal mucosa sections. The formulation was left to gel on the nasal mucosa at 35 °C and subsequently placed on a heat mat thermostat (AIICIOO) already heated at the same temperature and positioned with an angle of inclination of 40°. Moreover, by means of a peristaltic pump (Gilson Miniplus2, Biolabo Intruments srl, Milan, Italy), the mucosa was subjected to a continuous flow (1 ml/min) of PBS pH 5.5 heated at 35 °C, to mimic the physiological conditions of the nasal cavity. The time required for the complete removal of the gel from the mucosa, that is to say when the green color was no longer visible, was measured using a stopwatch.

2.2.4.2. Force of mucoadhesion

The mucoadhesive formulation exhibiting the longest time of adhesion and its respective plain counterpart (the vehicle obtained using the same fractions of P407 and P188, but without the mucoadhesive polymer) were characterized for their ability to interact with the mucosal tissue. For this purpose, the force of mucoadhesion was measured exploiting an adapted tensiometer (Krüss 132869; Hamburg, Germany) as reported by Abruzzo and co-workers, with some adjustments [29]. The nasal mucosa (0.1 g) was fixed to a circular support (diameter 0.90 cm, thickness 0.35 cm) with cyanoacrylate adhesive, hydrated with a dispersion of dialyzed and lyophilized mucin 0.05% (w/v) in PBS pH 5.5 for 5 min and suspended from the tensiometer spring. Further on, 3 ml of each sample were poured into

a small beaker (diameter 3 cm), left to gel at 35 °C and maintained at this temperature by means of a water bath. The mucosa was lowered until it reached the surface of the formulation and the two were kept in contact without applying any force for 2 min. Afterwards, the nasal mucosa was raised, and the force required for its detachment from the gel represented the adhesive bond strength between the mucosa and the nasal gel.

2.2.5. Viscosity measurement

The viscosity of the selected formulations was measured at three different temperatures: 20 °C, at RT and at 35 °C, that is the temperature of the nasal cavity. To determine viscosities of formulations prior to gelation (20 and 25 °C) the falling ball viscometer (HAAKE falling ball viscometer type C, Thermo Fisher Scientific, Milan, Italy) was employed. This tool enables the measurement of the sample viscosity by correlating it to the time required for a sphere to cover a distance of 100 mm through the examined fluid, that is placed inside a cylinder inclined of 10°, which can also be thermostated by means of an external jacket. A sample volume of approximately 40 ml was poured into the measuring tube together with a nickel iron alloy ball (ø =15.595 mm; m =16.1332 g; ρ =8.124 g/cm3; constant K =0.10963 mPa ×s ×cm^3/g ×s) suitable to measure viscosities comprised between 40 – 700 mPa × s. The viscometer was connected to a liquid circulator to control the temperature and the sample was subjected to a tempering time of 30 min prior to the analysis. The time required for the sphere to move from one side to the other of the testing tube was measured using a stopwatch and the evaluation was repeated three times for each formulation replicate. The sample viscosity (mPa ×s) was calculated according to the following equation:

$$\eta = t * (\rho 1 - \rho 2) * K$$

where K is the ball constant (mPa ×s ×cm^3/g ×s), t is the falling time of the ball (s), ρ1 and ρ2 are the density (g/cm^3) of the ball and of the nasal gel, respectively.

Because of the phase transition of the *in situ* gelling formulations when they have reached $T_{sol\text{-}gel}$ at 35 °C, a rotational viscometer (Visco Star-R, Fungilab S.A., Barcelona, Spain) was used. Approximately 20 ml of formulation was allowed to gel for 15 min inside the testing tube thermostated by a water jacket at 35 °C. The measurement was conducted using the spindle TR 11 at a speed of 200 rpm.

2.2.6. Chromatographic conditions

HPLC analytical assay was performed using a Shimadzu (Milan, Italy) LC-10ATVP chromatographic pump and a Shimadzu SPD-10AVP UV–vis detector set at 286 nm.

Separation was obtained on a Phenomenex (Torrance, CA, USA) SinergyTM 4 µm Hydro-RP 80Å LC column (150 ×4.60 mm) coupled to a Phenomenex Security Guard C18 guard cartridge (4 × 3.0 mm i.d., 5 µm). The mobile phase consisted of a mixture of MilliQ water/acetonitrile/methanol 50:25:25 (v/v) with the addition of 0.1% of trifluoroacetic acid and it was flushed at a rate of 0.4 ml/min. Manual injections were made using a Rheodyne 7125 injector with a 20 µL sample loop and data analysis was carried out through the CromatoPlus software (Shimadzu Italia, Milan, Italy). Since release and permeation studies were conducted in slightly different conditions, it was necessary to obtain more than one calibration curve. The first, in PBS pH 5.5/ethanol (80:20 v/v) was characterized by a drug concentration range of 0.1 – 80.24 µg/ml, and a linearity coefficient (R^2) equal to 1. This curve was employed for the release study and limits of detection (LOD) and quantification (LOQ) were 0.43 µg/ml and 1.32 µg/ ml, respectively. The calibration curve of CBZ in PBS pH 7.4/ ethanol (80:20 v/v), obtained with drug concentrations ranging from 0.05 µg/ml to 84 µg/ml, showed a good linearity (R^2 =1) and it was used to evaluate the drug permeated during the *in vitro* diffusion studies. LOD and LOQ were 0.4 µg/ml and 1.21 µg/ml, respectively.

2.2.7. Solubility study and drug loading

CBZ does not show a pKa value in the physiological range [30], thus its solubility was studied both in MilliQ water and in the selected formulations.

To assess drug solubility in water, an excess amount (10 mg in 10 ml) of CBZ was dispersed in ultrapure water and the dispersion was left under stirring for 72 h at RT. Further on, the sample was centrifuged at 5890 × *g* for 15 min (Microspin 12, Biosan, Riga, Latvia) and the supernatant filtered through syringe filters 0.22 µm cut-off (cellulose acetate syringe filter, Sanford, FL, USA) to remove the fraction of undissolved drug. The sample was appropriately diluted and subjected to HPLC analytical assay, to quantify the maximum solubility of CBZ in the aqueous medium.

To investigate the solubilizing power of the thermosensitive vehicles, two different spectrophotometric approaches were employed: the turbidimetric analysis and the absorbance (ABS) measurement at 286 nm. In both cases, CBZ was dispersed in the selected mucoadhesive gelling system and in its respective plain counterpart at concentrations ranging from 0.25 mg/ml to 2 mg/ml. In contrast to what has been reported in the literature [23], where methods suggest dissolving the drug in water and storing it at low temperature prior to polymer addition, CBZ was added directly to the final formulations

at RT, with the aim to exploit the solubilization power of P407 and to avoid drug precipitation due to both its low water solubility and the reduced storage temperature. Moreover, to ensure drug solubilization, samples were kept under stirring at RT for 24h prior to analysis. The turbidity of the samples was measured at 650 nm through an UV–vis spectrophotometer (UV-1601 Shimadzu, Milan, Italy) and the baseline correction was made using the corresponding unloaded formulation. For the second analysis, samples were firstly centrifuged at 5890 × *g* for 15 min, then appropriately diluted and finally their ABS at 286 nm was measured.

2.2.8. Drug influence on formulation performance

To investigate whether CBZ loading would affect nasal gels performance, the selected mucoadhesive vehicle and its respective plain formulation were loaded with the drug at the concentration of 1 mg/ml [25], following the procedure reported in Section 2.2.7. pH, $T_{sol\text{-}gel}$ and $t_{sol\text{-}gel}$ were thus evaluated (see Section 2.2.3) together with the force of mucoadhesion (see Section 2.2.4.2) and results obtained for the loaded formulations were compared to the unloaded ones.

2.2.9. In vitro release study

The release profiles of the selected mucoadhesive formulation and its respective plain nasal gel, prepared as reported in Section 2.2.7 (final drug concentration 1 mg/ml), were compared to that of a control sample, obtained dissolving CBZ in ultrapure water at a concentration equal to its maximum solubility in the aqueous medium. The study was conducted using Franz-type static glass vertical diffusion cells equipped with a V6A Stirrer (PermeGearInc., Hellertown, PA, USA), and a dialysis membrane cut-off 6000 – 8000 Da (Spectra/Por 1 dialysis membrane Spectrum Laboratories Inc., Rancho Dominguez, CA, USA), that was previously soaked in release medium for 30 min before being clamped between the donor and the receiving compartments. The release medium (12 ml) was composed of a mixture of PBS pH 5.5/ethanol 80:20 (v/v) thermostated at 35 ± 1 °C and maintained under constant stirring, whereas the donor compartment was filled with 300 µl of the tested formulations. At predetermined time points, every 30 min for the first hour and every 60 min for the following 4 h, 200 µl were withdrawn from the acceptor chamber, replaced with fresh PBS pH 5.5/ethanol mixture, and finally analyzed by HPLC assay. The cumulative released drug was plotted as function of time.

2.2.10. In vitro permeation study

The most suitable thermosensitive formulation containing the mucoadhesive polymer and its respective plain counterpart were further compared to a CBZ solution, for their ability to enable drug passive diffusion across two different *in vitro* models of the nasal mucosa. Specifically, were employed Permeapad® barrier (InnoMe GmbH, Espelkamp, Germany) and Permeapad® functionalized with a mucin layer, which had already been exploited to predict *in vitro* absorption of active ingredients through the nasal mucosa, thanks to their capacity to mimic the cell membrane and the airway epithelium together with the mucus coating, respectively [26,27].

Regarding the Permeapad® and mucin model, the reconstituted mucin layer was obtained as described by Corazza et al. (2022). Briefly, a mucin dispersion (50 mg/ml) in ultrapure water was dialyzed overnight using a standard RC tubing (molecular weight cut-off 6000–8000 Da), freeze dried and stored at +2–8 °C until use. When diffusion studies were performed, the powder was reconstituted with PBS pH 5.5 (50 mg/ml) and 200 µl of purified mucin dispersion were placed on the top of the Permeapad® barrier and left to equilibrate for 5 min prior to sample addition in the donor compartment.

The permeation study was set out exactly as the release one, except for the composition of the receiving phase, that consisted of a PBS pH 7.4/ethanol mixture, the barrier system, that corresponded to the two Permeapad®-based models, and the time intervals for the samplings: every 15 min for the first 2 h and every 30 min for the following 3 h. Cumulative amounts of drug permeated per unit area (diffusion surface area =1.77 cm^2) of the membrane (µg/cm^2) were plotted against time (minutes), and the flux (j) was calculated from the slope of the initial linear section of the curve.

2.2.11. Statistical analysis

All results are shown as mean ± standard deviation (SD) and SD was calculated from the values of three independent experiments. Data from all experiments were analyzed using a t-test, and differences were deemed significant for $p < 0.05$.

2.3. Results and Discussion

2.3.1. Preparation and evaluation of thermosensitive nasal gels

Thermoresponsive nasal gels were developed using poloxamer P407 as the gelling polymer due to its advantageous features. In fact, it is characterized by good tolerability, low toxicity and it is almost not-irritant towards the mucosa, which make it a useful and safe excipient in nasal formulations [24]. Moreover, P407 is compatible with numerous biomolecules and chemical excipients [15]. Interestingly, the gelling ability of this polymer is concentration-dependent: at low concentration, P407 solution loses its gelling capacity, whereas at high concentration, its gelation temperature is lower than room temperature [31]. Consequently, to tailor the temperature at which the sol-gel transition takes place, P407 is often mixed with other excipients, for instance P188, as in the present work. It is known that the gelation process is driven by the formation of spherical micelles, that result from the breakage of the hydrogen bonds between the aqueous solvent and the hydrophilic moieties of P407 at temperatures above the lower critical solution temperature of the polymer [15]. However, the gelation temperature of poloxamer-based vehicles can be increased by adding the more hydrophilic P188 polymer. In fact, P188 causes a higher order of water molecules around the hydrophobic PPO units, making a further increase in temperature necessary to promote the hydrophobic interactions between the formed micelles [32].

To obtain *in situ* thermo-sensitive formulations, which can be administered into the nasal cavity and respond with sol–gel transition at nasal temperature, firstly it was necessary to identify the most suitable concentration ratio between P407 and P188. Considering that a minimum concentration of 15–20% of gelling polymer is essential to present the phase transition and to form thermo-sensitive hydrogels with adequate viscosity and partial rigidity [18], P407 and P188 were mixed at concentrations within the ranges of 21-23% (w/v) and 3-5% (w/v), respectively. The formulations obtained just using poloxamers (plain formulations) were characterized in terms of pH as well as concerning temperature and time of gelation, and results are summarized in **Table PIII 2.1**.

Table PIII 2.1 Characterization of plain formulations. Data are expressed as means ± SD, n =3.

P188 % (w/v)	P407 % (w/v)	pH	$T_{sol-gel}$ (°C)	$t_{sol-gel}$ (s)
	21	5.5-6	> 35	No gel
3	22	6	32.28 ± 1.04	33.98 ± 9.15
	23	6	28.95 ± 0.07	7.5 ± 0.71
	21	5.5-6	> 35	No gel
4	22	6	34.00 ± 0.00	59.47 ± 4.69
	23	5.5-6	30.00 ± 0.25	50.40 ± 1.45
	21	5.5-6	> 35	No gel
5	22	6	34.42 ± 0.42	62.56 ± 6.09
	23	6	31.85 ± 0.21	32.00 ± 2.83

Regarding the pH, all the formulations prepared using the cold method showed pH values of approximately 6, which fits with the physiological pH of the nasal cavity that is reported between 5.5 and 6.5 [33]. This is of great relevance to avoid developing formulations that cause inflammation or toxicity of the nasal epithelium [10,13]. The thermoresponsive behavior of the poloxamer-based vehicles was investigated considering the $T_{sol-gel}$ and the $t_{sol-gel}$, which were measured through the magnetic stirring method. As it can be derived from the data reported, the formulations behaved as expected according to the mechanism formerly described and the gelation temperature trend was coherent with that reported by He and coworkers [34]. Indeed, nasal gel temperatures of gelation decreased as the concentration of P407 was increased, whereas $T_{sol-gel}$ tended to raise when the concentration of P188 was increased. Among the screened formulations, three of them exhibited a temperature of phase transition comprised between 32 and 35 °C, that is the physiological temperature within the nasal cavity [25]. This is a key point in the development of delivery strategies aimed to improve nasal administration of active ingredients. In fact, nasal *in situ* gelling formulations with a $T_{sol-gel}$ lower than 32 °C would undergo sol-gel transition before being instilled in the nostril, thus hampering drug administration. Conversely, vehicles with a temperature of phase transition higher than 35 °C would rapidly leak from the nasal cavity reducing drug absorption. To improve drug residence time on the airway epithelium and prevent its fast clearance, gelation should occur within 60 s [33]. Except for the preparations characterized by $T_{sol-gel}$ above 35 °C, all tested plain formulations satisfied this last requirement. Overall, among the developed preparations, only nasal gels containing 22% (w/v) of P407 and from 3 to 5% (w/v) of P188 were found suitable for nasal delivery.

Despite their gelling properties, poloxamers also present some potential hurdles, including poor mucoadhesion. For this reason, they are frequently combined with mucoadhesive polymers in order to improve the bioadhesive properties of the nasal gel [20]. Here, HPMC of different viscosities were employed in different amounts: high-viscous K100M at 0.1-0.3% (w/v), and low-viscous E50LV at 0.4-0.8% (w/v). In particular, they were added to the plain formulations that were selected during the previous screening procedure. Initially, the impact of HPMC addition on the gel basic properties like pH, $T_{sol\text{-}gel}$ and the $t_{sol\text{-}gel}$ was considered, and results referring to the mucoadhesive formulations (nasal gels containing the adhesive polymer) are reported in **Table PIII 2.2**.

Table PIII 2.2 Characterization of mucoadhesive formulations. Data are expressed as means ± SD, n =3.

P188 % (w/v)	P407 % (w/v)	K100 % (w/v)	E50LV % (w/v)	pH	$T_{sol\text{-}gel}$ (°C)	$t_{sol\text{-}gel}$ (s)
3	22	0.1		6	30.30 ± 0.99	32.30 ± 1.25
		0.2		6	30.00 ± 0.20	35.60 ± 4,87
		0.3		6	29.00 ± 0.20	27.30 ± 6.11
4	22	0.1		6	32.60 ± 0.57	35.60 ± 6.02
		0.2		6	32.20 ± 0.20	42.85 ± 8.15
5	22	0.1		6	34.75 ± 0.35	91.30 ± 3.90
		0.2		6	32.50 ± 0.14	50.40 ± 1.25
			0.4	6	33.60 ± 0.57	60.20 ± 2.33
			0.8	6	32.33 ± 0.42	37.85 ± 6.52

K100M was firstly added to the formulation containing 22% (w/v) of P407 and 3% (w/v) of P188 at the three concentrations tested, observing a notable decrease in the temperature of gelation, that was far below the lower limit of the suitable range of temperatures. This was probably due to the thermal responsive gelation properties of HPMC itself [35]. Interestingly, the effect of K100M at 0.3% (w/v) on gel properties was already clear during the preparation steps, when an increase in sample viscosity was noted. These observations together with the higher poloxamer content of the following plain formulations, made it unnecessary to test the influence of K100M at the highest concentration considered. As expected, at both concentrations tested (0.1% and 0.2% w/v), HPMC high-viscous lowered the $T_{sol\text{-}gel}$ of the plain formulations containing 22% (w/v) of P407 and 4% or 5% (w/v) of P188, but in both cases the parameter was still between 32 and 35 °C.

The increase in the $T_{sol\text{-}gel}$ in presence of growing concentrations of P407 and HPMC K100M was probably due to the gelling properties of both polymers, but it might also be the result of polymeric chains tendency to overlap because of their being in a greater quantity in the same dispersion volume, as pointed out by J.B. da Silva and coworkers [36]. Because of these observations, we considered HPMC low-viscous as a potential alternative to K100M. In fact, we expected that the presence of shorter polymer chains would reduce overlapping regions, thus allowing E50LV to be used at higher concentration than K100M without strongly altering the features of the vehicle.

E50LV was added exclusively to the plain formulation characterized by 22% (w/v) of P407 and 5% (w/v) of P188, because it was initially described by a higher temperature of gelation. In agreement with the former evidences, also low-viscous HPMC decreased the sol-gel transition temperature. Nevertheless, the resulting mucoadhesive formulation maintained the desired properties for a nasal *in situ* gelling vehicle.

Finally, as it can be observed, the inclusion of neither K100M nor E50LV affected the pH of the mucoadhesive gels, that remained unchanged compared to the respective plain formulations. Moreover, the inclusion of both HPMC types contributed to the decrease of the $t_{sol\text{-}gel}$, that was around or below 60 s.

2.3.2. Mucoadhesive properties of nasal gels

A major drawback of nasal delivery is the defense mechanism represented by the MCC: the mucous coating together with its high rate of turnover, due to cilia beating, creates an obstacle towards xenobiotic entrance in the respiratory system. Unfortunately, intranasally administered formulations are subjected to the same clearance process, which strongly limits their retention time in the nasal cavity, thus reducing drug absorption. Nevertheless, drug residence time can be improved by including mucoadhesive agents, such as chitosan, cellulose derivatives, and polyacrylates in the delivery vehicles, exploiting their ability to both interact with the mucus layer and limit the MCC [9,14]. Based on these assumptions, the mucoadhesive formulations selected through the initial screening procedure were compared with the respective plain formulations for their ability to increase drug contact with the nasal mucosa.

Firstly, the influence of high and low-viscous HPMC on the time of mucoadhesion was investigated. Specifically, the *in vitro* evaluation was performed by recording the time required for the gelled system to be completely removed from a specimen of nasal mucosa, because of the continuous flush of buffer, that simulated the MCC phenomenon. As can be

observed in **Figure PIII 2.1**, the plain formulation containing 4% (w/v) of P188 was retained on the mucosa for a significantly ($p < 0.05$) longer time (990.40 ± 41.86 s) compared to the one with 5% (w/v) of P188 (715.00 ± 7.07 s). This result was probably a consequence of the increased hydrophilicity of the second formulation, due to the higher concentration of P188. When K100M at the two concentrations tested, 0.1% and 0.2% (w/v), was added to the plain nasal gel P407 22%-P188 4%, no improvement in the time of mucoadhesion was detected. In contrast, when HPMC high-viscous was included in the plain formulation P407 22%-P188 5%, the *in vitro* retention time improved as the concentration of K100M increased. Regarding the impact of E50LV on the time of mucoadhesion of the plain formulation containing 5% (w/v) of P188, it was not significant ($p > 0.05$) when employed at the lower concentration (487.00 ± 105.43 s). Differently, the use of HPMC low-viscous at 0.8% (w/v) allowed for a notable increase in the retention time reaching 1746.75 ± 274.00 s, which was significantly higher ($p < 0.05$) compared to both the plain formulation and the one containing 0.2% (w/v) of K100M. Considering the results obtained so far, the nasal gel P407 22%-P188 5%-E50LV 0.8% was selected as the candidate delivery system that underwent further characterization steps.

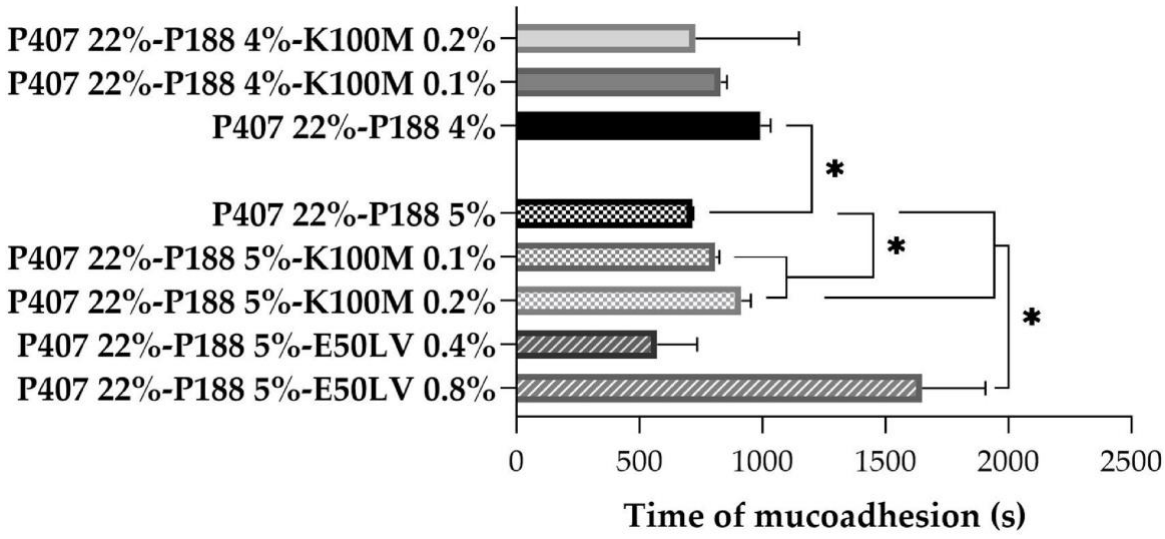

Figure PIII 2.1 Time of mucoadhesion measured for the selected mucoadhesive nasal formulations and the respective plain counterparts. Data are expressed as means ± SD, n =3. Significance indicated by * =$p < 0.05$ between samples indicated by the brackets.

The residence time of *in situ* gelling nasal formulations is also affected by the mucoadhesion strength. In fact, the stronger is the interaction between the vehicle and the mucosa, the higher is the probability that the system is longer retained at the absorption site [24]. For this reason, the force required to detach the nasal mucosa from the gelling system with E50LV 0.8% (w/v) was measured and it was compared to that of the respective plain formulation.

The graph in **Figure PIII 2.4c** (unloaded - CBZ) shows that the force necessary to separate the tissue from the gel notably increased from 2.51 ± 0.09 $\times 10^{-4}$ N in the absence of the mucoadhesive polymer to 3.66 ± 0.32 $\times 10^{-4}$ N in the presence of HPMC low-viscous. This last result demonstrated the role of the mucoadhesive polymer in strengthening the interaction between the formulation and the target tissue once more.

2.3.3. Sol-gel transition influence on nasal gel viscosity

In situ gelling thermoresponsive formulations are so called in virtue of their ability to change from a liquid to a semisolid state, with the latter being the form that comprise most of the interesting properties of such delivery system. However, these can be exploited provided that the formulation is properly instilled in the nostril. In this regard, if the formulation is to be administered by means of a nasal spray, the formulation must be characterized by a viscosity lower than 500 mPa × s at RT, otherwise the preparation would be difficult to handle, and the correct dosing would be prevented [37]. Herein viscosity was measured at three different temperatures (**Table PIII 2.3**) observing that both the selected mucoadhesive formulation and the respective plain one already showed a slight increase, around 35%, in viscosity when the temperature was raised from 20 to 25 °C. Anyway, gel viscosities always were lower than the limit, suggesting that the candidate vehicle could be easily administered either if it is stored at RT or once outside the fridge. When samples were heated up to 35 °C, the viscosity increase was even more noticeable, and it was the demonstration that the phase transition had occurred. Comprehensibly, the viscosities measured for the selected mucoadhesive formulation were higher compared to those of the
respective plain gel.

Table PIII 2.3 Viscosities of the selected mucoadhesive *in situ* nasal gel and the corresponding plain formulation at different temperatures. Data are expressed as means ± SD, n =3.

			Viscosity mPa × s		
P188 %(w/v)	P407 %(w/v)	E50LV %(w/v)	20°C	25°C	35°C
5	22		77.75 ± 1.96	105.89 ± 2.28	4150 ± 200
5	22	0.8	118.85 ± 0.64	160.70 ± 1.00	4650 ± 200

2.3.4. Nasal gels solubilizing properties

Belonging to the BCS class II group of active ingredients, CBZ is featured by a low aqueous solubility, that can make its delivery through the nasal route rather challenging, since just a limited volume of formulation can be administered to the nasal cavity. Nevertheless, P407 is well known not only for its gelling behavior, but also for its ability to remarkably improve the apparent solubility of hydrophobic molecules, thanks to its surface-active properties [15]. For example, Ban and co-workers observed that emodin solubility improved as the concentrations of both P407 and P188 increased, demonstrating that poloxamers were effective in enhancing the drug solubility [38]. As a result, in the present study the possibility to exploit poloxamers as solubilizing agents was evaluated.

The analysis performed demonstrated that, in ultrapure water, CBZ reached a maximum solubility equal to 0.118 ± 0.69 mg/ml. This value is in good agreement with previously reported results, that indicated 0.113 mg/ml [2] and 0.126 mg/ml [39] as the highest concentrations of CBZ that could be achieved in aqueous media.

To perform the solubility study of CBZ in the gelling system, the drug was loaded at increasing concentrations from 0.25 to 2 mg/ml in the selected mucoadhesive formulation and in the corresponding plain formulation. Samples were then subjected to a turbidimetric analysis and results are reported in **Figure PIII 2.2**. For both the preparations, no turbidity raise was observed for CBZ concentrations up to 1 mg/ml. Differently, the addition of CBZ at higher concentrations led to a notable increment in the turbidity of the specimen, suggesting that part of the drug remained undissolved. Besides, the mucoadhesive gel seemed to have an increased solubilization power compared to its respective plain formulation. In fact, when CBZ was included at 1.5 and 2 mg/ml in the gelling vehicles, the ABS measured at 650 nm was significantly higher ($p < 0.05$) for the plain formulation than for the one containing the mucoadhesive polymer. The latter result was consistent with data reported in a published research work, where HPMC low viscosity grade was successfully employed to increase the solubility of simvastatin, a poorly water soluble drug [40].

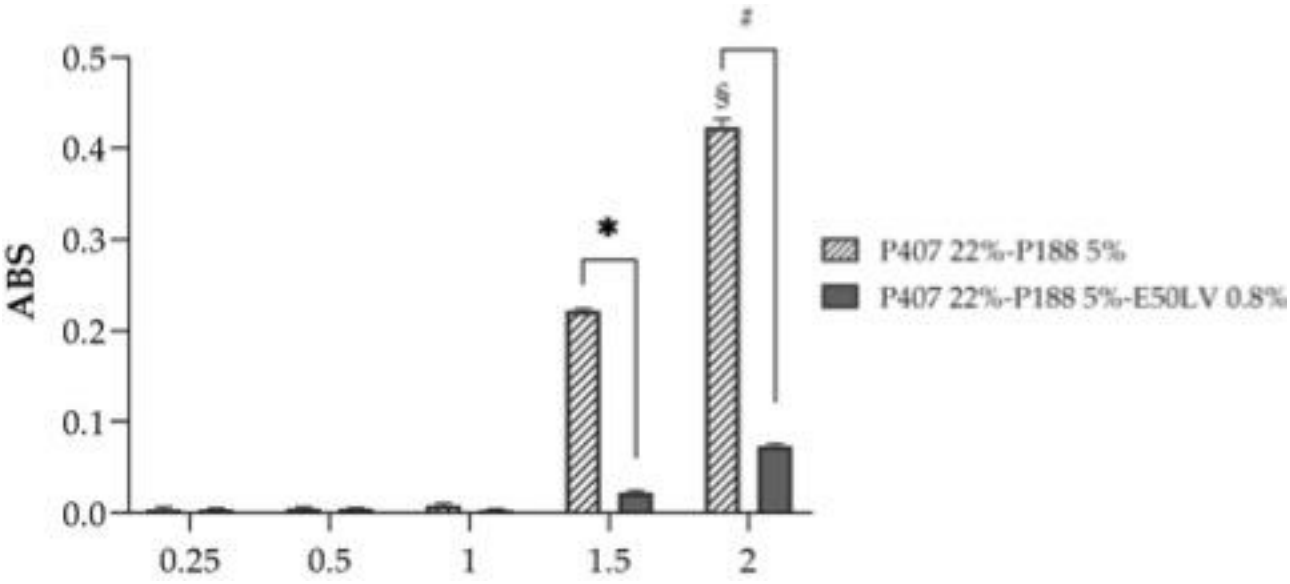

Figure PIII 2.2 Solubility study of CBZ in the selected mucoadhesive formulation and its respective plain counterpart using the turbidimetric method. Plotted absorbance at 650 nm for the formulations. Data are expressed as means ±SD, n =3. Significance indicated by * = $p < 0.05$ between samples indicated by the brackets and the respective samples containing a lower concentration of CBZ; # =$p < 0.05$ between samples indicated by the brackets and the respective samples containing 1.5 mg/ml CBZ; by §=$p < 0.05$ compared to the mucoadhesive formulation containing 2 mg/ml of CBZ.

To further confirm the findings of the turbidimetric analysis, samples were centrifuged to remove the fraction of undissolved drug and were evaluated for their ABS at 286 nm, that is the absorption peak of CBZ. This second evaluation clearly supported the previously reached conclusion (**Figure PIII 2.3**). For the plain formulation, the absorbance gradually increased in samples containing from 0.25 to 1 mg/ml of CBZ, then it remained constant, meaning that no more drug molecules could be solubilized. Differently, when CBZ was dispersed in the mucoadhesive formulation, a continuously growing trend was observed, which supported the hypothesis of the superior solubilizing properties of the gel containing the adhesive polymer. Overall, it can be stated that the poloxamer-based vehicles allowed for a significant ($p < 0.05$) increase in the drug solubility compared to CBZ solution and that CBZ at the concentration of 1 mg/ml was completely solubilized in both the tested formulations. On the basis of these results, and considering that previously reported *in vivo* preclinical studies were conducted by loading CBZ at the final concentration of 1 mg/ml in a thermoreversible nasal gel intended for intranasal administration of the antiepileptic drug [25], 1 mg/ml was chosen as the drug loading concentration during the following experiments.

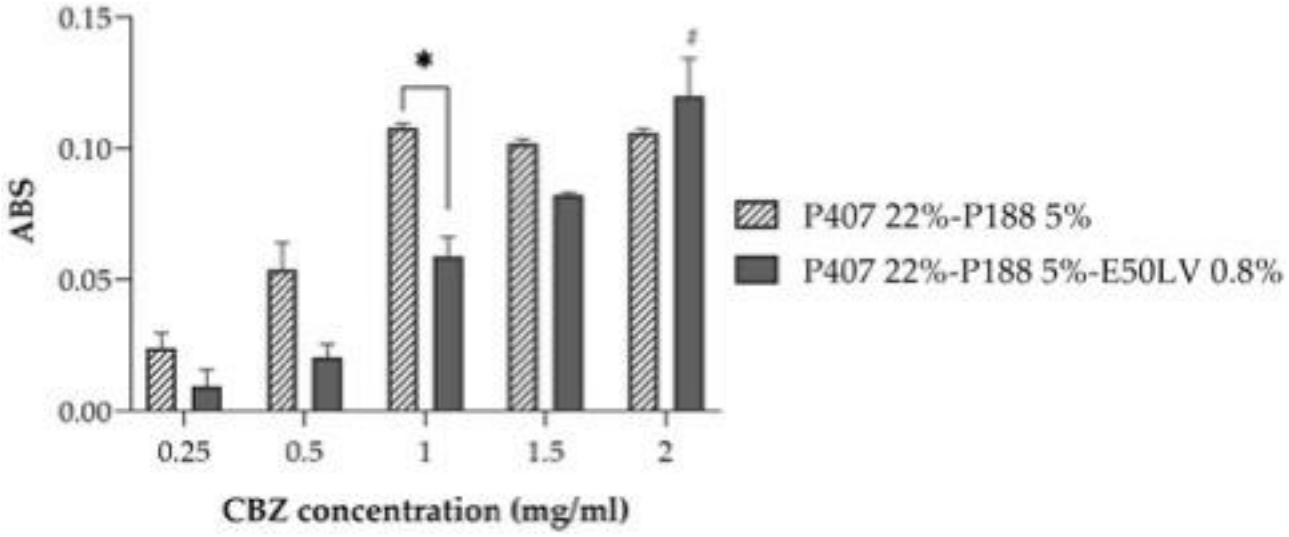

Figure PIII 2.3 Solubility study of CBZ in the selected mucoadhesive formulation and its respective plain counterpart by detection of absorbance at 286 nm. Data are expressed as means ±SD, n =3. Significance indicated by * =p <0.05 between samples indicated by the brackets and the respective samples containing a lower concentration of CBZ; # =p < 0.05 compared to the respective samples containing lower concentrations of CBZ.

2.3.5. Evaluation of drug loaded thermoresponsive nasal gels

Before going ahead with the *in vitro* release and permeation studies, the influence of the drug loading on the performance of the nasal gel was investigated. The formulation P407 22%-P188 5%-E50LV 0.8% and the same without the mucoadhesive polymer were loaded with 1 mg/ml of CBZ and four parameters, pH, temperature and time of gelation together with the detachment force, were measured. The obtained results are graphically represented in **Figure PIII 2.4 a-c**, which also shows the comparison with the data collected in the case of unloaded gels. Overall, none of the considered parameters, including pH (data not shown), was altered by the addition of CBZ and this was verified for both the formulation tested. This meant that, despite the presence of the drug, the candidate formulation maintained the desired features to be considered a suitable *in situ* thermosensitive vehicle for nasal and nose-to-brain delivery.

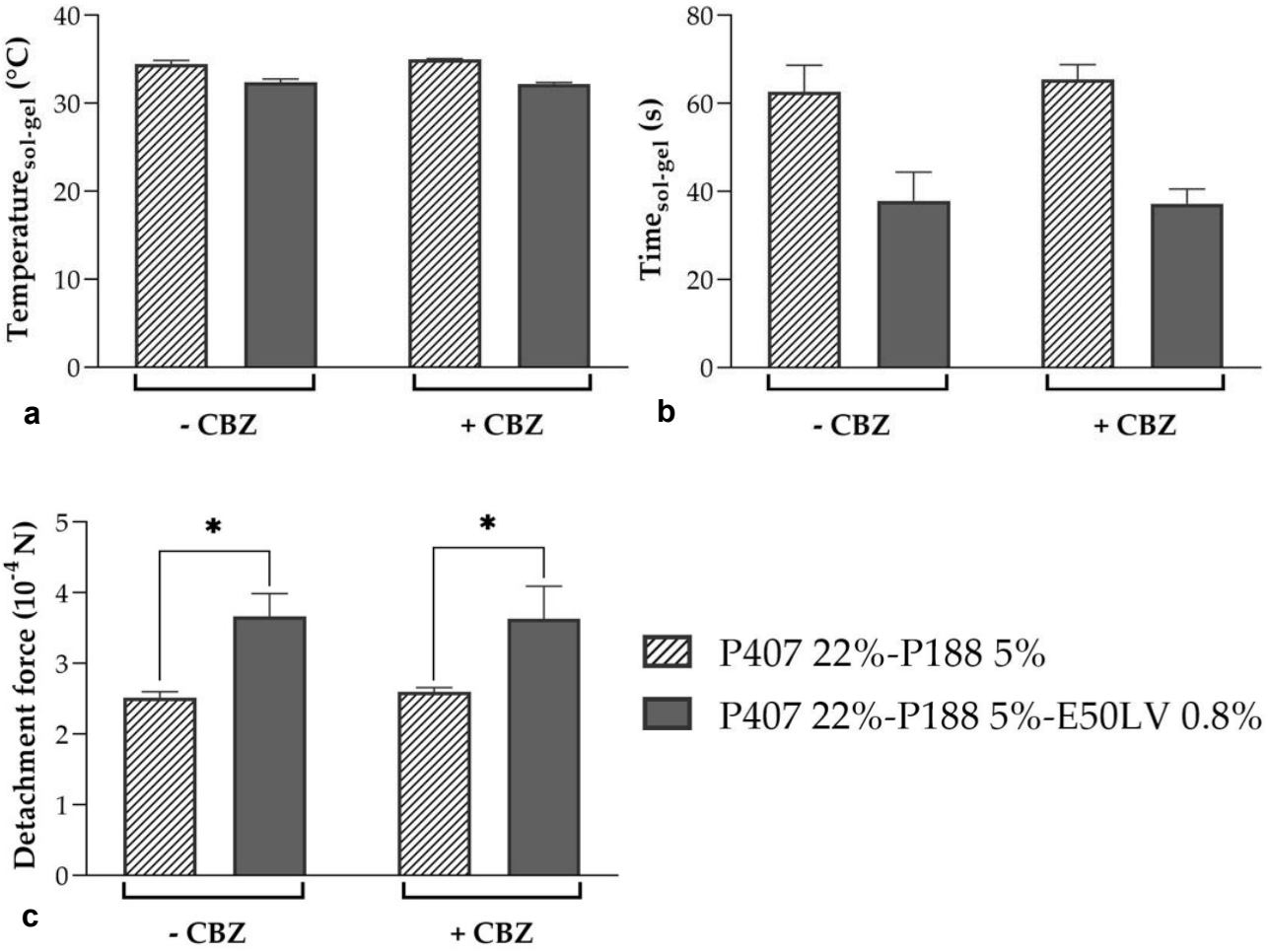

Figure PIII 2.4 Drug loading (1mg/mL) influence on a) Tsol-gel; b) tsol-gel and c) detachment force. For each considered parameter, the selected mucoadhesive formulation and the respective plain one were compared both in absence (- CBZ) and presence (+CBZ) of 1 mg/ml of CBZ. Data are expressed as means ±SD, n =3. Significance indicated by * =$p < 0.05$ between samples indicated by the brackets.

2.3.6. CBZ in vitro release from thermosensitive nasal gels

Along with solubility issues, CBZ effectiveness is also limited by its narrow therapeutic window, thus reduced blood concentrations may result in therapeutic failure, while high blood concentrations can increase the probability of toxicity occurrence [8]. Consequently, the use of formulations with a modified-release is preferred in order to reduce peak fluctuations, improve efficacy and tolerability and thus patient adherence to the pharmacological treatment [1,7]. *In vitro* release studies were performed to evaluate the ability of the thermoresponsive nasal formulations to allow for a controlled release of the loaded drug and their behavior was compared to that of a CBZ solution (control).

The mean cumulative percentage of CBZ released from the tested formulations over the considered time period is shown in **Figure PIII 2.5**. Since the control sample was prepared by dissolving CBZ as a saturated solution in ultrapure water, the drug was immediately available. In fact, 99.70 ± 0.50% of the drug was found released within 180 min. Differently,

both the mucoadhesive formulation and the corresponding plain thermosensitive gel showed a slower and prolonged release: after 5 h, only approximately half of the drug was released (49.58 ± 1.79% and 52.00 ± 2.74%, respectively). The release profiles of the two thermosensitive nasal gels underlined their ability to provide a controlled and sustained released of the loaded drug. This behavior may be hypothesized to be connected to the viscous nature of the *in situ* gelling preparations, however, the curves were found to overlap, despite the different viscosities of the vehicles (see Section 2.3.3). Other mechanisms apart from diffusion of free molecules may be involved, such as drug partitioning into poloxamers micelles and polymers chains relaxation. This hypothesis is inspired by a research study, in which poloxamers and different mucoadhesive polymers (HPMC included) were employed to develop *in situ* gelling vehicles for intranasal delivery of rivastigmine (RV) [41]. The authors obtained non-fickian mechanism of drug release for most of their formulations, and they proposed that it might indicate that RV release was controlled by an erosion-diffusion mechanism, thus fickian diffusion occurred together with the relaxation of the polymer matrix.

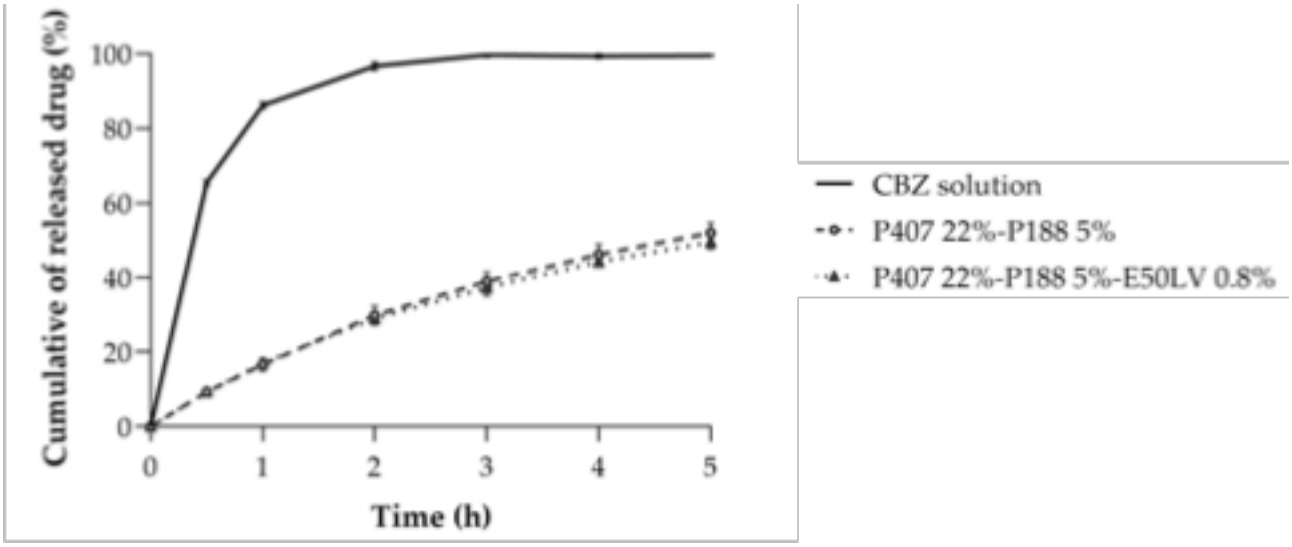

Figure PIII 2.5 Release profile of CBZ from the selected mucoadhesive formulation and its respective plain vehicle in comparison to a CBZ solution. Data are expressed as means ±SD, n =3.

CBZ in vitro permeation

The absorption of drugs, the targets of which are located in the brain, can occur through the intranasal route by means of three different pathways: trigeminal, olfactory and systemic. Despite the advantage of alternative ways of drug delivery to the CNS, the absorption is hampered by multiple barriers. In fact, the active molecule can reach the systemic circulation provided that it crosses both the pseudostratified columnar epithelium and the mucus layer

that lies on it. These obstacles partially remain also if the drug has to be absorbed by the neuronal pathway, because neither the trigeminal neuronal endings nor the olfactory neural cells are directly exposed to the nasal cavity [9]. As a result, to prove that the selected *in situ* gelling formulation containing poloxamers and low-viscous HPMC could be a promising vehicle for intranasal and nose-to-brain delivery of CBZ, permeation studies were assessed. The latter were performed across two different *in vitro* diffusion barriers, which had already been demonstrated to be promising models of the nasal mucosa [26].

The first was the recently developed Permeapad® barrier that, being composed of phospholipids (soybean phosphatidylcholine S-100) between two regenerated cellulose support sheets, it is known as a biomimetic and cell-free *in vitro* model useful for testing drug passive diffusion. In fact, it is assumed that the dry lipids, which correspond to the middle layer of the stratified architecture, spontaneously form a tightly packed vesicular structure upon contact with aqueous media, resembling the cell membrane. Moreover, in virtue of the barrier's structure, the formed phospholipid vesicles remain in close proximity between each other, thus mimicking the tissue morphology [42]. As a result of its mechanism of action, the PermeaPad® barrier was employed as a useful *in vitro* model to predict drug permeation across some biological barriers, such as the buccal [43], intestinal [44] and nasal mucosa [27]. **Figure PIII 2.6a** displays the cumulative amount of CBZ permeated through the barrier plotted against time, when the drug was dissolved in ultrapure water (control sample) or loaded in either the mucoadhesive formulation or in the respective plain gel. The permeation profile of the control sample shows a good linearity for up to 90 min, during which the rapid diffusion was triggered by the fact that the drug was already available for absorption (as demonstrated by the *in vitro* release study, see Section 2.3.6). Thereafter, the diffusion rate gradually decreased until it reached zero (after 300 min, more than 90% of the drug was found in the receptor phase). This behavior was due to the gradual loss of concentration gradient. Differently, when CBZ was loaded in the thermosensitive gels, the drug permeation profile maintained its linearity for almost 240 min, as a result of the controlled release mechanism of CBZ from the gelling formulations. In fact, the graph indicates that the *in situ* gelling vehicles acted as drug depots. As the slope of the curves is almost identical in the first 70 min, this indicates that the concentration gradient (regarding the molecularly dissolved drug) should also be very similar between the three formulations. However, after this time point, the control sample profile decreases reaching a plateau, whereas the two formulations sustain the drug permeation. After 300 min, the mass permeated across the surface unit was 18.29 ± 0.33 μg/cm^2 for the CBZ solution, whereas for the nasal gels it was

significantly ($p < 0.05$) higher 38.19 ± 1.19 μg/cm^2 for the P407 22%-P188 5% formulation and 35.92 ± 2.26 μg/cm^2 for the P407 22%-P188 5%-E50LV 0.8% formulation.

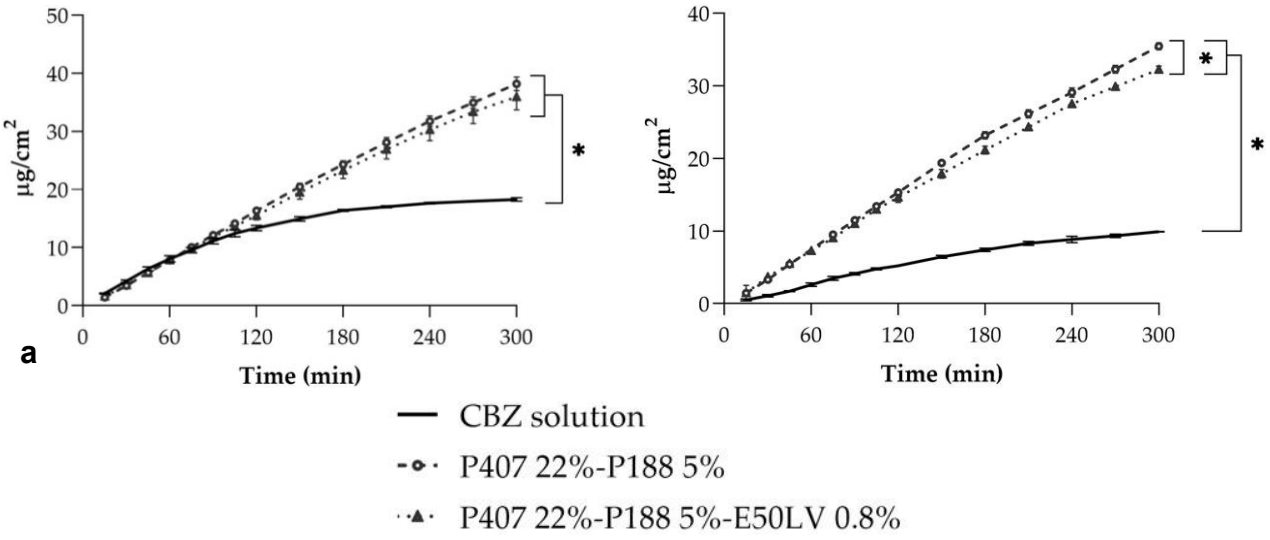

Figure PIII 2.6 Permeation profile of CBZ across a) the Permeapad® barrier, b) the Permeapad® barrier functionalized with a mucin layer. Data are expressed as means ± SD, n =3. Significance indicated by * =$p < 0.05$ between samples indicated by the brackets.

Since the trigeminal neuronal endings are located within the lower regions of the epithelia [14] and that the olfactory bipolar neurons extend their dendritic processes into the mucus layer [9], drug passive diffusion was also investigated using a Permeapad® barrier functionalized with a mucin layer. **Figure PIII 2.6b** depicts the permeation profile of the drug across this enriched membrane. Similarly to the previous diffusion study, the permeation profiles of the nasal gels were characterized by a more extended period of linearity compared to the control, even though their permeation rate started to slightly decrease after 180 min. However, in this case, the slope of the initial part of the profile is greatly higher for CBZ in the two formulations as compared to the control solution. The result could be due to the interaction between the polymer network and mucin, that probably altered drug availability to permeation. Also in this case, the gelling formulation allowed for a greater mass diffusion after 300 min with respect to the CBZ solution (9.93 ± 0.06 μg/cm^2), and a small but significant ($p < 0.05$) difference was noted between the two thermosensitive vehicles. In fact, the plain formulation allowed for the diffusion of 35.44 ± 0.48 μg/cm^2 compared to the mucoadhesive gel, that reached 32.25 ± 0.46 μg/cm^2. This observation could be owed to the higher viscosity of the P407 22%-P188 5%-E50LV 0.8% compared to the plain gel, which contributed to an increased resistance of the polymer matrix, resulting in the slowdown of the diffusion process. It needs to be noted that the presence of the mucus

left the amount of permeation widely unchanged for the two formulations as compared to the plain Permeapad® barrier.

The permeation profiles were also used to determine the drug flux in the different tested conditions, and data are summarized in **Figure PIII 2.7**.

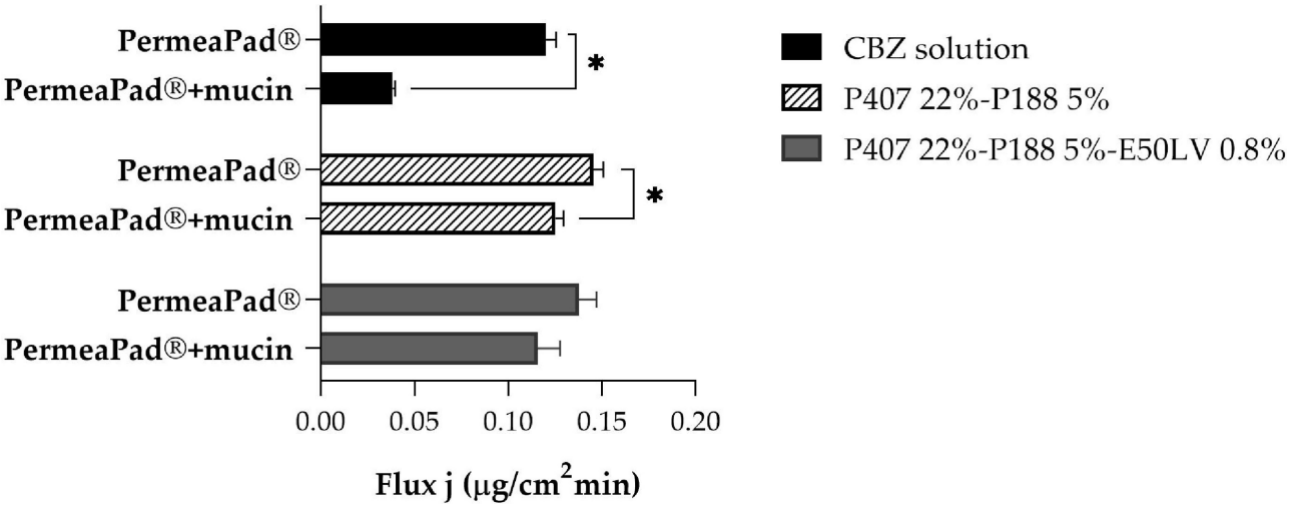

Figure PIII 2.7 Drug flux across the Permeapad® barrier and the Permeapad® barrier functionalized with a mucin layer. Data are expressed as means ±SD, n =3. Significance indicated by * =p < 0.05 between samples indicated by the brackets.

We decided to report the fluxes instead of the apparent permeability as the concentration of the molecularly dissolved drug within the gelling systems was not determined by a direct analytical method. Results clearly pointed out the negative influence of the mucin layer on drug diffusion rate when CBZ was solubilized in ultrapure water: the drug flux notably ($p < 0.05$) decreased from 0.12 ± 0.005 μg/cm^2 min in absence of mucin to 0.04 ± 0.001 μg/cm^2 min in presence of the mucous layer. This was an expected outcome since it is reported that the mucous coating mostly affects the diffusion of lipophilic and charged hydrophilic molecules rather than that of uncharged hydrophilic ones [14]. Moreover, it was in agreement with our previous findings regarding the effect of mucin on hydrocortisone absorption through the nasal mucosa [26]. Concerning the nasal gels, an interesting result was obtained. When CBZ was loaded in the plain formulation, the drug flux across the Permeapad® barrier functionalized with mucin was decreased with respect to standard Permeapad® model, even though j was reduced to a lower extent compared to the control sample. Conversely, any remarkable differences were noted in the drug flux across the different models of the nasal mucosa when the thermoresponsive formulation containing 0.8% (w/v) of E50LV was employed. This effect might be consequence of the improved ability of the P407 22%-P188 5%-E50LV 0.8% formulation to interact with the mucous layer

(see Section 2.3.2) that, as we had already observed for other molecules with bioadhesive properties (Corazza et al., 2022), favored drug diffusion.

2.4. Conclusions

The present work allowed for the development of a thermosensitive formulation capable of undergoing sol-gel transition once in the nasal cavity and intended for nasal and nose-to-brain delivery of CBZ. The candidate vehicle, which is composed of 22% P407, 5% P188 and 0.8% of E50LV, was obtained by means of a very straightforward procedure and using materials characterized by a good safety profile. The low viscosity of the formulation makes it suitable for an easy and comfortable instillation as a nasal spray. Moreover, it shows a $T_{sol-gel}$ comprised between 32-35 °C, undergoes gelation in less than 60 s and is featured by a pH value of 6, thus it presents all the properties required by an *in situ* gelling vehicle for nasal drug delivery. In addition to this, the developed formulation exhibits remarkable mucoadhesive properties, because it can strengthen the interaction with the mucous layer and the *in vitro* studies demonstrated that it is retained on the nasal mucosa for nearly 30 min. The possibility to exploit this optimized formulation as a platform for the delivery of CBZ is further supported by its ability to increase the solubility of the hydrophobic substance, release approximately 50% of the loaded drug in a controlled and sustained manner, as well as to favor CBZ permeation across both Permeapad® based models of the nasal mucosa as compared to a drug solution. Lastly, the outstanding result obtained in this work is that the drug flux across the Permeapad® barrier functionalized with the reconstituted mucin layer is not decreased when the selected gelling system is used. This strongly highlights the importance of bioadhesive agents when tuning the properties of these emerging smart delivery systems to improve drug absorption across mucosal tissues.

2.5. References Paper II

1. Beydoun, A.; DuPont, S.; Zhou, D.; Matta, M.; Nagire, V.; Lagae, L. Current Role of Carbamazepine and Oxcarbazepine in the Management of Epilepsy. Seizure 2020, 83, 251–263, doi:10.1016/j.seizure.2020.10.018.
2. Khan, N.; Shah, F.A.; Rana, I.; Ansari, M.M.; Din, F. ud; Rizvi, S.Z.H.; Aman, W.; Lee, G.-Y.; Lee, E.-S.; Kim, J.-K.; et al. Nanostructured Lipid Carriers-Mediated Brain Delivery of Carbamazepine for Improved in Vivo Anticonvulsant and Anxiolytic Activity. Int. J. Pharm. 2020, 577, 119033, doi:10.1016/j.ijpharm.2020.119033.

3. Liu, S.; Yang, S.; Ho, P.C. Intranasal Administration of Carbamazepine-Loaded Carboxymethyl Chitosan Nanoparticles for Drug Delivery to the Brain. Asian J. Pharm. Sci. 2018, 13, 72–81, doi:10.1016/j.ajps.2017.09.001.
4. Martins, I.L.; Nunes, J.; Charneira, C.; Morello, J.; Pereira, S.A.; Telo, J.P.; Marques, M.M.; Antunes, A.M.M. The First-Line Antiepileptic Drug Carbamazepine: Reaction with Biologically Relevant Free Radicals. Free Radic. Biol. Med. 2018, 129, 559–568, doi:10.1016/j.freeradbiomed.2018.10.408.
5. Ana, R.; Mendes, M.; Sousa, J.; Pais, A.; Falcão, A.; Fortuna, A.; Vitorino, C. Rethinking Carbamazepine Oral Delivery Using Polymer-Lipid Hybrid Nanoparticles. Int. J. Pharm. 2019, 554, 352–365, doi:10.1016/j.ijpharm.2018.11.028.
6. Mawazi; Al-Mahmood; Chatterjee; Hadi; Doolaanea Carbamazepine Gel Formulation as a Sustained Release Epilepsy Medication for Pediatric Use. Pharmaceutics 2019, 11, 488, doi:10.3390/pharmaceutics11100488.
7. Gierbolini, J.; Giarratano, M.; Benbadis, S.R. Carbamazepine-Related Antiepileptic Drugs for the Treatment of Epilepsy - a Comparative Review. Expert Opin. Pharmacother. 2016, 17, 885–888, doi:10.1517/14656566.2016.1168399.
8. Li, H.; Zhang, M.; Xiong, L.; Feng, W.; Williams, R.O. Bioavailability Improvement of Carbamazepine via Oral Administration of Modified-Release Amorphous Solid Dispersions in Rats. Pharmaceutics 2020, 12, 1023, doi:10.3390/pharmaceutics12111023.
9. Cassano, R.; Servidio, C.; Trombino, S. Biomaterials for Drugs Nose–Brain Transport: A New Therapeutic Approach for Neurological Diseases. Materials 2021, 14, 1802, doi:10.3390/ma14071802.
10. Nguyen, T.-T.-L.; Maeng, H.-J. Pharmacokinetics and Pharmacodynamics of Intranasal Solid Lipid Nanoparticles and Nanostructured Lipid Carriers for Nose-to-Brain Delivery. Pharmaceutics 2022, 14, 572, doi:10.3390/pharmaceutics14030572.
11. Berillo, D.; Zharkinbekov, Z.; Kim, Y.; Raziyeva, K.; Temirkhanova, K.; Saparov, A. Stimuli-Responsive Polymers for Transdermal, Transmucosal and Ocular Drug Delivery. Pharmaceutics 2021, 13, 2050, doi:10.3390/pharmaceutics13122050.
12. Cunha, S.; Forbes, B.; Sousa Lobo, J.M.; Silva, A.C. Improving Drug Delivery for Alzheimer's Disease Through Nose-to-Brain Delivery Using Nanoemulsions, Nanostructured Lipid Carriers (NLC) and in Situ Hydrogels. Int. J. Nanomedicine 2021, Volume 16, 4373–4390, doi:10.2147/IJN.S305851.

13. Pires, P.C.; Rodrigues, M.; Alves, G.; Santos, A.O. Strategies to Improve Drug Strength in Nasal Preparations for Brain Delivery of Low Aqueous Solubility Drugs. Pharmaceutics 2022, 14, 588, doi:10.3390/pharmaceutics14030588.
14. Crowe, T.P.; Hsu, W.H. Evaluation of Recent Intranasal Drug Delivery Systems to the Central Nervous System. Pharmaceutics 2022, 14, 629, doi:10.3390/pharmaceutics14030629.
15. Giuliano, E.; Paolino, D.; Fresta, M.; Cosco, D. Mucosal Applications of Poloxamer 407-Based Hydrogels: An Overview. Pharmaceutics 2018, 10, 159, doi:10.3390/pharmaceutics10030159.
16. Schilling, A.L.; Cannon, E.; Lee, S.E.; Wang, E.W.; Little, S.R. Advances in Controlled Drug Delivery to the Sinonasal Mucosa. Biomaterials 2022, 282, 121430, doi:10.1016/j.biomaterials.2022.121430.
17. Russo, E.; Villa, C. Poloxamer Hydrogels for Biomedical Applications. Pharmaceutics 2019, 11, 671, doi:10.3390/pharmaceutics11120671.
18. Yu, Y.; Cheng, Y.; Tong, J.; Zhang, L.; Wei, Y.; Tian, M. Recent Advances in Thermo-Sensitive Hydrogels for Drug Delivery. J. Mater. Chem. B 2021, 9, 2979–2992, doi:10.1039/D0TB02877K.
19. Abdeltawab, H.; Svirskis, D.; Sharma, M. Formulation Strategies to Modulate Drug Release from Poloxamer Based in Situ Gelling Systems. Expert Opin. Drug Deliv. 2020, 17, 495–509, doi:10.1080/17425247.2020.1731469.
20. Zahir-Jouzdani, F.; Wolf, J.D.; Atyabi, F.; Bernkop-Schnürch, A. In Situ Gelling and Mucoadhesive Polymers: Why Do They Need Each Other? Expert Opin. Drug Deliv. 2018, 15, 1007–1019, doi:10.1080/17425247.2018.1517741.
21. Qi, X.-J.; Liu, X.-Y.; Tang, L.-M.-Y.; Li, P.-F.; Qiu, F.; Yang, A.-H. Anti-Depressant Effect of Curcumin-Loaded Guanidine-Chitosan Thermo-Sensitive Hydrogel by Nasal Delivery. Pharm. Dev. Technol. 2020, 25, 316–325, doi:10.1080/10837450.2019.1686524.
22. Wang, Q.-S.; Li, K.; Gao, L.-N.; Zhang, Y.; Lin, K.-M.; Cui, Y.-L. Intranasal Delivery of Berberine via in Situ Thermoresponsive Hydrogels with Non-Invasive Therapy Exhibits Better Antidepressant-like Effects. Biomater. Sci. 2020, 8, 2853–2865, doi:10.1039/C9BM02006C.
23. Singh, R.M.; Kumar, A.; Pathak, K. Mucoadhesive in Situ Nasal Gelling Drug Delivery Systems for Modulated Drug Delivery. Expert Opin. Drug Deliv. 2013, 10, 115–130, doi:10.1517/17425247.2013.746659.

24. Mura, P.; Mennini, N.; Nativi, C.; Richichi, B. In Situ Mucoadhesive-Thermosensitive Liposomal Gel as a Novel Vehicle for Nasal Extended Delivery of Opiorphin. Eur. J. Pharm. Biopharm. 2018, 122, 54–61, doi:10.1016/j.ejpb.2017.10.008.
25. Serralheiro, A.; Alves, G.; Fortuna, A.; Falcão, A. Intranasal Administration of Carbamazepine to Mice: A Direct Delivery Pathway for Brain Targeting. Eur. J. Pharm. Sci. 2014, 60, 32–39, doi:10.1016/j.ejps.2014.04.019.
26. Corazza, E.; Abruzzo, A.; Giordani, B.; Cerchiara, T.; Bigucci, F.; Vitali, B.; di Cagno, M.P.; Luppi, B. Human Lactobacillus Biosurfactants as Natural Excipients for Nasal Drug Delivery of Hydrocortisone. Pharmaceutics 2022, 14, 524, doi:10.3390/pharmaceutics14030524.
27. Wu, I.Y.; Bala, S.; Škalko-Basnet, N.; di Cagno, M.P. Interpreting Non-Linear Drug Diffusion Data: Utilizing Korsmeyer-Peppas Model to Study Drug Release from Liposomes. Eur. J. Pharm. Sci. 2019, 138, 105026, doi:10.1016/j.ejps.2019.105026.
28. Illum, L. Nasal Delivery. The Use of Animal Models to Predict Performance in Man. J. Drug Target. 1996, 3, 427–442, doi:10.3109/10611869609015963.
29. Abruzzo, A.; Crispini, A.; Prata, C.; Adduci, R.; Nicoletta, F.P.; Dalena, F.; Cerchiara, T.; Luppi, B.; Bigucci, F. Freeze-Dried Matrices for Buccal Administration of Propranolol in Children: Physico-Chemical and Functional Characterization. J. Pharm. Sci. 2021, 110, 1676–1686, doi:10.1016/j.xphs.2020.10.033.
30. Huerta, B.; Jakimska, A.; Gros, M.; Rodríguez-Mozaz, S.; Barceló, D. Analysis of Multi-Class Pharmaceuticals in Fish Tissues by Ultra-High-Performance Liquid Chromatography Tandem Mass Spectrometry. J. Chromatogr. A 2013, 1288, 63–72, doi:10.1016/j.chroma.2013.03.001.
31. Huang, W.; Zhang, N.; Hua, H.; Liu, T.; Tang, Y.; Fu, L.; Yang, Y.; Ma, X.; Zhao, Y. Preparation, Pharmacokinetics and Pharmacodynamics of Ophthalmic Thermosensitive in Situ Hydrogel of Betaxolol Hydrochloride. Biomed. Pharmacother. 2016, 83, 107–113, doi:10.1016/j.biopha.2016.06.024.
32. M.A. Fathalla, Z.; Vangala, A.; Longman, M.; Khaled, K.A.; Hussein, A.K.; El-Garhy, O.H.; Alany, R.G. Poloxamer-Based Thermoresponsive Ketorolac Tromethamine in Situ Gel Preparations: Design, Characterisation, Toxicity and Transcorneal Permeation Studies. Eur. J. Pharm. Biopharm. 2017, 114, 119–134, doi:10.1016/j.ejpb.2017.01.008.
33. Cirri, M.; Maestrelli, F.; Nerli, G.; Mennini, N.; D'Ambrosio, M.; Luceri, C.; Mura, P.A. Development of a Cyclodextrin-Based Mucoadhesive-Thermosensitive In Situ Gel for

Clonazepam Intranasal Delivery. Pharmaceutics 2021, 13, 969, doi:10.3390/pharmaceutics13070969.

34. He, Z.; Wang, Z.; Zhang, H.; Pan, X.; Su, W.; Liang, D.; Wu, C. Doxycycline and Hydroxypropyl-β-Cyclodextrin Complex in Poloxamer Thermal Sensitive Hydrogel for Ophthalmic Delivery. Acta Pharm. Sin. B 2011, 1, 254–260, doi:10.1016/j.apsb.2011.10.004.
35. Joshi, S.C. Sol-Gel Behavior of Hydroxypropyl Methylcellulose (HPMC) in Ionic Media Including Drug Release. Materials 2011, 4, 1861–1905, doi:10.3390/ma4101861.
36. da Silva, J.B.; Cook, M.T.; Bruschi, M.L. Thermoresponsive Systems Composed of Poloxamer 407 and HPMC or NaCMC: Mechanical, Rheological and Sol-Gel Transition Analysis. Carbohydr. Polym. 2020, 240, 116268, doi:10.1016/j.carbpol.2020.116268.
37. P. Martin, G.; B. Lansley, A. Nasal Drug Delivery. In Aulton's Pharmaceutics: The Design and Manufacture of Medicines; Elsevier Ltd., 2018; pp. 671–689 ISBN 978-0-7020-7005-1.
38. Ban, E.; Park, M.; Jeong, S.; Kwon, T.; Kim, E.-H.; Jung, K.; Kim, A. Poloxamer-Based Thermoreversible Gel for Topical Delivery of Emodin: Influence of P407 and P188 on Solubility of Emodin and Its Application in Cellular Activity Screening. Molecules 2017, 22, 246, doi:10.3390/molecules22020246.
39. Borisover, M.; Sela, M.; Chefetz, B. Enhancement Effect of Water Associated with Natural Organic Matter (NOM) on Organic Compound–NOM Interactions: A Case Study with Carbamazepine. Chemosphere 2011, 82, 1454–1460, doi:10.1016/j.chemosphere.2010.11.035.
40. Javeer, S.D.; Patole, R.; Amin, P. Enhanced Solubility and Dissolution of Simvastatin by HPMC-Based Solid Dispersions Prepared by Hot Melt Extrusion and Spray-Drying Method. J. Pharm. Investig. 2013, 43, 471–480, doi:10.1007/s40005-013-0092-1.
41. Abouhussein, D.M.N.; Khattab, A.; Bayoumi, N.A.; Mahmoud, A.F.; Sakr, T.M. Brain Targeted Rivastigmine Mucoadhesive Thermosensitive In Situ Gel: Optimization, in Vitro Evaluation, Radiolabeling, in Vivo Pharmacokinetics and Biodistribution. J. Drug Deliv. Sci. Technol. 2018, 43, 129–140, doi:10.1016/j.jddst.2017.09.021.
42. Berben, P.; Bauer-Brandl, A.; Brandl, M.; Faller, B.; Flaten, G.E.; Jacobsen, A.-C.; Brouwers, J.; Augustijns, P. Drug Permeability Profiling Using Cell-Free Permeation Tools: Overview and Applications. Eur. J. Pharm. Sci. 2018, 119, 219–233, doi:10.1016/j.ejps.2018.04.016.

43. Bibi, H.A.; Holm, R.; Bauer-Brandl, A. Use of Permeapad® for Prediction of Buccal Absorption: A Comparison to in Vitro, Ex Vivo and in Vivo Method. Eur. J. Pharm. Sci. 2016, 93, 399–404, doi:10.1016/j.ejps.2016.08.041.
44. Ilie, A.-R.; Griffin, B.T.; Brandl, M.; Bauer-Brandl, A.; Jacobsen, A.-C.; Vertzoni, M.; Kuentz, M.; Kolakovic, R.; Holm, R. Exploring Impact of Supersaturated Lipid-Based Drug Delivery Systems of Celecoxib on in Vitro Permeation across Permeapad® Membrane and in Vivo Absorption. Eur. J. Pharm. Sci. 2020, 152, 105452, doi:10.1016/j.ejps.2020.105452.

3. Lactobacilli cell-free supernatants: potential green and natural enhancers for nose-to-brain delivery of small hydrophilic molecules

Elisa Corazza[1,†], Janik Martin[2,†], Barbara Giordani[1], Beatrice Vitali[1], Martina Rossi[1,3], Angela Abruzzo[1], Federica Bigucci[1], Teresa Cerchiara[1], Massimiliano Pio di Cagno[4], Barbara Luppi[1*], and Katharina Schindowski[2].

[1] Department of Pharmacy and Biotechnology, Alma Mater Studiorum, University of Bologna, Via San Donato 19/2, 40127 Bologna, Italy. elisa.corazza7@unibo.it (E.C.); barbara.giordani4@unibo.it (B.G.); b.vitali@unibo.it (B.V.); martina.rossi12@unibo.it (M.R.); angela.abruzzo2@unibo.it (A.A); federica.bigucci@unibo.it (F.B.); teresa.cerchiara2@unibo.it (T.C.); barbara.luppi@unibo.it (B.L.)

[2] Institute of Applied Biotechnology, University of Applied Science Biberach, Hubertus-Liebrecht Straße 35, 88400 Biberach, Germany. martin@hochschule-bc.de (J.M.); schindowski@hochschule-bc.de (K.S.)

[3] Center for Applied Biomedical Research (CRBA), Alma Mater Studiorum, University of Bologna, Via Massarenti 9, 40126 Bologna, Italy. martina.rossi12@unibo.it (M.R.)

[4] Department of Pharmacy, Faculty of Mathematics and Natural Sciences, University of Oslo, Sem Sælands vei 3, 0371 Oslo, Norway. m.p.d.cagno@farmasi.uio.no (M.P.d.C)

[*] Corresponding author

[†] These authors contributed equally to this work

Manuscript under submission to the International Journal of Pharmaceutics.

Abstract: Concerns about environmental health are driving pharmaceutical industries towards more eco-friendly and biocompatible products. Lactobacilli cell-free supernatants (CFS) are mixtures of soluble factors derived from the microbial growth of beneficial bacteria with the potential to serve as natural and sustainable excipients in emerging formulations. This work aims to verify the usefulness of the CFS obtained from human *L. crispatus* BC5, *L. gasseri* BC9 and BC12 as enhancers in the nose-to-brain absorption of small hydrophilic molecules. CFS influence on cell viability was investigated together with their ability to

increase the diffusion of sodium fluorescein across *in vitro* models of the olfactory epithelium. The enhancing mechanism was studied through differential scanning calorimetry analysis and immunostaining assay of zonula occludens-1. The use of 25% (v/v) of all lactobacilli CFS on porcine olfactory epithelial primary cells was not associated with any cytotoxic effect, but only the CFS obtained from BC5 was pointed out as a permeation enhancer across both the biomimetic membrane PermeaPad®, the porcine olfactory tissue, and the primary cell model. The enhancing mechanism seems to rely on the CFS perturbation effect on lipid membranes that, in the case of the cell-based model, probably also results in an alteration of tight junctions' activity.

Keywords: nose-to-brain; postbiotic; *Lactobacillus*; sustainability; diffusion; enhancer.

3.1. Introduction

Because of their carbon footprint and toxicological impact on organisms and environmental health, pharmaceuticals are regarded as emerging pollutants [1]. Therefore, policy initiatives are going in the direction of shifting the paradigm: the focus should not be exclusively on the standard of bioactive compounds, but a broader look that also includes the nature of excipients as well as the entire production process should be adopted, thus ending up with a pharmaceutical product that is less detrimental to the environment [2,3].

Recently, the application of postbiotics mixtures and individual postbiotics in food and pharmaceutical industries has been reviewed [4]. These can be defined as biological materials containing soluble probiotic-derived metabolites or cell wall-derived components without the presence of viable microorganisms [5]. Examples of postbiotics are cell-free supernatants (CFS), which represent the mixture of metabolites that bacteria secrete in the culture medium during fermentation [6] and that are well established for their beneficial effect on human health [5]. Regardless of being exploited as therapeutic agents, little is known concerning their employment as excipients, even though the presence of organic acids and short-chain fatty acids within their complex composition [5,6] suggests a potential application as pharmaceutical aids to improve bioavailability of drugs. Demonstrating this alternative use of CFS would answer the demand for more eco-friendly products. Indeed, CFS are natural compounds, thus are suggested to feature greater biocompatibility than synthetic substances [3,7], and postbiotic-producing cells can be cultivated using waste substrates derived from agricultural and industrial activities, hence supporting sustainability [8].

The intranasal route appears as a valid delivery strategy for an increasing number of drugs targeting the brain, particularly for those indicated for acute and rapid treatment of neurologic conditions [9]. Despite the growing interest in exploring nose-to-brain delivery as a potential alternative method for administering therapeutics, some formulation constraints remain; among others, the less efficient absorption of hydrophilic and/or high molecular weight molecules compared to small lipophilic drugs [10,11]. Nonetheless, the transepithelial passage of low liposoluble drugs can be improved by using permeation enhancers, which are excipients bearing the ability to modulate membrane structures and/or tight junctions [11].

As the success of a formulation is closely related to the active ingredient's ability to cross the biological barriers it encounters, digging into the enhancing properties of innovative pharmaceutical aids is of paramount importance [12]. When it comes to the early stages of drug development, excised tissues, cell monolayers, and artificial membranes are useful *in vitro* tools to assess membrane permeability, even though each one shows its pros and cons [13]. *Ex vivo* models, specifically those of animal origin, are easily accessible from slaughterhouses and preserve both the structure and composition of the anatomical region from where they were sourced. However, they must be handled within a short post-mortem delay, the isolation process is usually extremely labor-intensive, and they frequently show interindividual differences [14]. Alternatively, different cell lines can be employed to study drug permeation across cell monolayers that resemble the function and morphology of the nasal epithelium, even though this often requires 21 days of *in vitro* cell differentiation [13]. Usually, tumor cell lines are preferred over primary cell models as they are permanent cells, can be easily cultured, and are associated with higher reproducibility, but feature a reduced differentiative capacity [14]. Even though cell-based assays allow for moderate throughput, cell-free biomimetic models are more suitable for routine and screening procedures, they enable the measurements of the passive permeability of compounds cost-effectively, but they are not as physiologically relevant as the *ex vivo* and cell-based models [12]. Being made of lipids soaked in a filter (Nasal-Parallel artificial membrane permeability assay [15]) or enclosed in support membranes (PermeaPad® [16]), they cannot account for relevant interactions that occur in biological systems [17].

Since it has been demonstrated that the biosurfactant, an example of cell-bound metabolite produced by the human *Lactobacillus gasseri* BC9, might be employed as a natural enhancer for hydrocortisone intranasal permeation [18], our question was whether the complex mixture of products derived from the microbial metabolism could itself affect drug

absorption. We answered this question by proving the ability of the CFS produced by the human *L. crispatus* BC5 (BC5-CFS), *L. gasseri* BC9 (BC9-CFS), and *L. gasseri* BC12 (BC12-CFS) to improve the nose-to-brain absorption of fluorescein sodium salt, a small hydrophilic paracellular marker, across a cell-free, a tissue-based and a cell-based model of the olfactory mucosa. Besides, to elucidate the mechanism of action of these potential innovative excipients, differential scanning calorimetry analysis of the treated nasal tissue and immunostaining assay of the tight junction protein zonula occludens-1 were performed.

3.2. Materials and methods

3.2.1. Materials

Fluorescein sodium salt (FSS), sodium chloride (NaCl), and sodium hydroxide (NaOH) were purchased from Sigma-Aldrich (Taufkirchen, Germany). In contrast, phosphate buffer saline pH 7.4 (ROTI®Fair PBS pH 7.4 1000 mL/tablet) and Octenisept® were bought from Carl Roth (Karlsruhe, Germany) and Schülke & Mayr GmbH (Norderstedt, Germany), respectively. Regarding the microbiological part, Man, Rogosa, and Sharpe (MRS) culture medium was supplied by Difco (Detroit, USA) and L-cysteine hydrochloride monohydrate by Merck (Darmstadt, Germany). Concerning cell culturing and biological assays, Dulbecco's Modified Eagle Medium: Nutrient Mixture F12 (DMEM – F12) w/o L-Glutamine w/o HEPES w/o Glucose, Earle's balanced salt solution (EBSS), Minimum essential medium (MEM) w/o phenol red, MEM non-essential amino acids (NEAA) were provided by Gibco (Darmstadt, Germany). The antibiotics gentamycin sulfate and kanamycin sulfate were supplied by Carl Roth (Karlsruhe, Germany), while Penicillin/Streptomycin (PenStrep) (10000 U) was obtained from AppliChem (Darmstadt, Germany). Besides, L-Glutamine (Gln), Fetal Bovine Serum (FBS), debris removal solution, rat tail collagen solution, and AlamarBlue™ HS Cell Viability Reagent Invitrogen were purchased from Gibco (Darmstadt, Germany), Capricorn Scientific (Ebsdorfergrund, Germany), Milteny Biotec (Bergisch Gladbach, Germany), Primacyte (Schwerin, Germany), and Thermo Fisher Scientific (Darmstadt, Germany), respectively. Lastly, the pronase was delivered by Sigma-Aldrich (Taufkirchen, Germany), and the antimycotic amphotericin B was provided by Carl Roth (Karlsruhe, Germany). Methanol, acetone, piperazine-N-N'-bis(2-ethanesulphonic acid) (PIPES), ethylene glycol-bis(2-aminoethylether)-N,N,N,N-tetraacetic acid (EGTA), Tween-20, and bovine serum albumin (BSA) were used for immunofluorescence staining and were purchased from Carl Roth (Karlsruhe, Germany). Magnesium chloride hexahydrate ($MgCl_2$ x $6H_2O$) and ammonium chloride (NH_4Cl) were delivered by Merck (Darmstadt, Germany). 4′,6-

diamidino-2-phenylindole (DAPI) was obtained from Sigma-Aldrich (Taufkirchen, Germany). For embedding of stained transwells mowiol and 1,4 diazabicyclo[2.2.2]octane (DABCO) were purchased from Sigma-Aldrich (Taufkirchen, Germany), whereas glycerol and tris-(hydroxymethyl)-amino methane (TRIS) were purchased from Carl Roth (Karlsruhe, Germany). Hereafter the compositions of the different cultivation media and buffers are described (**Table PIII 3.1**).

Table PIII 3.1 Composition of the different employed media and buffers.

Medium / Buffer	Composition
Pronase medium	EBSS - 1.4 mg/mL pronase - 1:100 PenStrep - 1:100 Gentamycin sulfate - 1:100 kanamycin sulfate - 1:10000 amphotericin B
Primary culture adhesion medium	DMEM: F12 (1:1) – 20% FBS – 2 mM Gln – 1% NEAA – 4.5 g/L Glucose – 1:500 PenStrep – 1:100 gentamycin sulfate – 1:100 kanamycin sulfate – 1:10000 amphotericin B
Primary culture medium	DMEM: F12 (1:1) – 10% FBS – 2 mM Gln – 1% NEAA – 4.5 g/L Glucose – 1:500 PenStrep – 1:100 gentamycin sulfate – 1:100 kanamycin sulfate – 1:10000 amphotericin B
PEM	80 mM PIPES – 5 mM EGTA – 1 mM $MgCl_2$ – 18.5 ml 10 M NaOH – 800 ml H_2O Adjust pH to 7.4 with NaOH and set volume to 1 L with H_2O
PEMT	PEM – 0.2% Tween-20
Quenching buffer	PEM – 50 mM NH_4Cl
Blocking/ staining buffer	PEMT – 0.5% BSA
Mowiol embedding medium	60 g mowiol – 150 g glycerol – 300 ml 0.2 M TRIS (pH 8.5) – 2.5 % DABCO in H_2O

3.2.2. Cell-free supernatant isolation and pH adjustment

The cell-free supernatants (CFS) were obtained from the human *L. crispatus* BC5 (BC5-CFS), *L. gasseri* BC9 (BC9-CFS), and *L. gasseri* BC12 (BC12-CFS), cultured in MRS broth supplemented with 0.05% L-cysteine at 37°C in anaerobic jars containing Gas-Pak EZ

(Beckton, Dickinson and Co., Milan, Italy) [19]. Briefly, overnight lactobacilli cultures were used to inoculate 90 mL of MRS broth at a concentration of 10^6 CFU/mL and allowed to grow for 24 h. After this incubation, bacterial cells were precipitated by centrifugation (10,000 x g for 10 min) (Centrisart G-16C; Sartorius, Göttingen, Germany) and the supernatants were recovered. The latter were subjected to pH measurement (Basic 20 pH meter, Crison Strumenti Spa, Modena, Italy) and adjusted to a pH value of 6 by using NaOH 10% (w/v). Finally, the lactobacilli supernatants were filtered with a polyethersulfone (PES) vacuum filtration unit 0.22 μm pore size (Sartolab®, Sartorius, Goettingen, Germany) to obtain the CFS and to ensure sterility.

3.2.3. Cell culture

3.2.3.1. Olfactory epithelial primary cell isolation

Olfactory epithelial primary cells (OEPC) were isolated from mucosal explants derived from the olfactory region of 4 – 6-month-old slaughterhouse pigs (Metzgerei Joas, Dietenheim, Germany). Tissues were handled within 1.5 h from slaughtering and according to the protocol described by Ladel and co-workers but with slight modifications [20]. The mucosa explants excised from the *regio olfactoria* were disinfected using Octenisept® and washed twice with PBS pH 7.4. The epithelial cells were isolated by incubation for 1 h at 37 °C with pronase medium in a T25 cell-suspension cultivation flask (Cellstar®, Greiner bio-one GmbH, Frickenhausen, Germany). The resulting suspension was collected and centrifuged at 300 x *g* for 10 min at 4°C (Heraeus 4 KR centrifuge, Thermo Scientific). The supernatant was removed and the cell pellet was resuspended in cold PBS and processed for debris removal according to the manufacturer protocol. Lastly, cells were resuspended in appropriate volumes of primary culture adhesion medium and directly seeded in cell culture inserts.

3.2.3.2. Cells seeding and cultivation in air-liquid interface conditions

OEPC were seeded in cell culture inserts (ThinCert™ 24 well polyethylene terephthalate 1 µm, Greiner Bio-one, Frickenhausen, Germany), previously coated with 0.05 mg/mL rat tail collagen solution for 48 h at 37 °C. Cells were seeded at a density of ~10^6 cells/mL and cultivated submerged at standard conditions (37 °C, 5% CO_2, 96% rH) for one day. After 24 h, the apical medium was removed to cultivate cells under ALI (air-liquid interface) conditions for 21 days and the basolateral medium was changed to the primary culture medium. The exchange was necessary to contain fibroblast growth due to reduced serum concentration.

Cells were apically washed with 200 µL PBS and the medium (260 µL/well) was changed every two days.

3.2.4. Cell viability assay

After 21 days of cultivation in ALI conditions, cells were washed with 200 µL PBS, and inserts were moved to a new 24-well plate, which had been previously filled with 260 µL/well of MEM w/o phenol red. CFS's and MRS's cytotoxic effect was investigated at three different volume ratios, 12.5%, 25%, and 50% (v/v). Specifically, cells were treated with 100 µL volume, half of which was represented by the medium and the other half was distributed between MRS or the investigated CFS and normal saline solution (NaCl 0.9% w/v), which was used as diluent. MEM was employed as the negative control (CTRL-), whereas DMSO 50% (v/v) as the positive control (CTRL+). Plates were stored in the incubator at standard conditions for 24 h. Afterward, treatment solutions were removed and 100 µL/well of AlamarBlue™ HS Cell Viability Reagent diluted 1:10 in MEM w/o phenol red were added apically. Plates were stored in the incubator for 5 h before detecting the fluorescence signal at the fluorescence spectrophotometer (Infinite® 200 Pro, TECAN, Männedorf, Switzerland) using the following setup: plate shaking for 2 sec in linear mode with an amplitude of 1 mm and a frequency of 886.9 rpm before the measurement, that was performed at excitation and emission wavelengths of 530 nm and 590 nm, respectively.

3.2.5. Osmolality measurement

As the osmolarity of the applied medium can influence permeability, the investigated CFS, as well as MRS, were tested for their osmolality values before trying out their potential permeation-enhancing effect. The osmolality (mOsm/kg) was measured through a cryoscopic osmometer (Osmomat 030, Gonotec, Berlin, Germany) calibrated with a reference solution of 300 mOsm/kg and MilliQ water as 0 mOsm/kg. The analysis was carried out on samples used at 25% v/v in normal saline solution as it was the concentration employed during the following studies.

3.2.6. In vitro permeation studies

The role of the considered CFS as absorption enhancers was investigated by proving their ability to increase the apparent permeability of fluorescein sodium salt (FSS). Alongside, to obtain a more complete and reliable approach to figuring out their enhancing properties, diffusion studies were performed by combining three different *in vitro* models: the biomimetic

membrane PermeaPad®, the excised porcine olfactory tissue, and the primary cell model (OEPC). Moreover, to ensure that the products of the lactobacilli metabolism were the only ones responsible for the improvement in the drug diffusion, two control samples were considered: the FSS solubilized in normal saline solution in the absence and presence of 25% (v/v) of the lactobacilli culture medium, named as CTRL and MRS respectively.

3.2.6.1. Sample preparation

Samples were prepared by solubilizing FSS at the concentration of 0.67 mg/mL in normal saline solution and filtered with 0.22 μm PES syringe filters (Whatman ™ Puradisc 25 mm, Cytivia, Dassel, Germany) to ensure sterility, which was strictly necessary for the diffusion study across primary cells. For consistency, sterility was also maintained during transport experiments across the other two barriers. Lastly, the FSS solution was mixed with 25% (v/v) of NaCl 0.9% (w/v) for the CTRL sample, or MRS or one of the three CFS, having a final concentration of the paracellular marker equal to 0.5 mg/mL.

3.2.6.2. Biomimetic model

The ready-to-use biomimetic membrane PermeaPad® (Phabioc GmbH, Espelkamp, Germany) was mounted on Franz-type static glass vertical diffusion cells equipped with a V6A Stirrer (PermeGear Inc., Hellertown, PA, USA). The acceptor chamber was filled with 12 mL of MEM w/o phenol red supplemented with 10% FBS (named transport or permeation medium), which was kept under stirring and at the temperature of 37 °C thanks to a surrounding jacket. 200 μL of test solution were loaded in the donor chamber and at predetermined time points (after 30, 60, 120, 180, 240, and 300 min) 200 μL were withdrawn from the sampling port and quickly replaced with an equal volume of permeation medium. Once the diffusion study was completed, the content of both the donor and acceptor compartments was collected, and the membrane was submerged with 2 mL of normal saline solution and then kept under stirring at room temperature for 3 h to release the FSS that eventually accumulated. This sample was then centrifuged at 12,000 x *g* for 15 min (Microspin 12, Biosan, Riga, Latvia) to take apart debris from the supernatant containing FSS.

3.2.6.3. Tissue-based model

The porcine tissue was sourced from a local slaughterhouse (Salumificio Capelli, Bologna, Italy) and processed for the isolation of the nasal olfactory mucosa. The septum was excised, and the *regio olfactoria* was extracted from the nasal cavity using forceps and a

scalpel. Subsequently, the mucosa was separated from the attached cartilaginous tissue and rinsed with a normal saline solution. The biological specimens were then preserved in aluminum foil at -20°C until they were required for use. The permeation study across the tissue-based model was performed following the procedure described for the biomimetic model (see Section 3.2.6.2), but before starting the experiment, the integrity of the mucosa was verified. First, the excised nasal mucosa was clamped between the donor and acceptor compartments, with the latter being filled with 12 mL of NaCl 0.9% (w/v). Then, the Franz cell was repeatedly tilted and the eventual accumulation of saline solution in the donor compartment due to the loss of membrane integrity was checked. Moreover, to ensure that the CFS did not damage the olfactory mucosa, at the beginning and the end of the diffusion study, the electrical resistance was measured (voltage: 100 mV, frequency: 100 Hz; Agilent 4263B LCR Meter, Microlease, I). To do so, both the Franz cell's chambers were loaded with normal saline solution (12 mL for the acceptor and 1 mL for the donor) and each compartment was supplied with an electrode. Only mucosa specimens that did not appear to be leaky and were characterized by unchanged electrical resistance values between the starting and end points were included in the study.

3.2.6.4. Cell-based model

After 21 days in ALI cultivation mode, cells were washed apically with 200 μL/well of PBS pH 7.4 and then processed to ensure the integrity of the cell layer. The transepithelial electrical resistance (TEER) measurement was performed directly in the permeation medium by adding 500 μL and 350 μL of it to the basolateral and apical compartments of the transwell, respectively. Cells were left to equilibrate for 20 min at 37°C and then cooled down at room temperature for 15 min. The TEER was measured employing an EVOM2 epithelial volt ohmmeter and chopstick electrodes (World Precision Instruments, Sarasota, USA). The instrument was calibrated with a control resistor (1000 Ω) and the resistance produced by an insert without cells was determined to serve as a blank. The TEER of each insert was measured in triplicate and the obtained values (already subtracted by the blank) were multiplied by the growth area of the membrane (0.336 cm^2). Because a previously published work pointed out a correlation between permeability and TEER for primary cells (higher TEER resulted in lower flux), only those cell layers exhibiting TEER values equal to or higher than 300 Ωcm^2 were included in the experiment [20]. The transport study was performed in the transwell setup by placing cell inserts in 260 µL of permeation medium and adding 100 µL of a sample (see Section 3.2.6.1 for sample preparation) to the apical

compartment. FSS permeation was studied under atmospheric conditions, in a steady state, and over 5 h. 20 µL were sampled from the basolateral compartment at the usual time points and they were immediately refilled with fresh permeation medium. At the end of the experiment, the apical and basolateral solutions were collected, the cell layer was washed with 200 µL of PBS, and the TEER measurement was repeated as previously described (only cell layers bearing a TEER $\geq$ 300 Ωcm^2 were considered). To calculate the mass balance at the end of the experiment, the support membrane was removed from the insert and placed in 200 µL of Milli-Q water. Subsequently, cells were subjected to three cycles of freeze-thawing (30 min at -80°C followed by 30 min at 37°C), and the obtained suspension was centrifuged at 12,000 x g for 15 min to remove cell debris.

3.2.6.5. Marker quantification and calculations

FSS quantification in the different samples was achieved using the fluorescence spectrophotometer with the following setup: plate shaking for 3 sec in linear mode with an amplitude of 1 mm and a frequency of 886.9 rpm before the measurement, that was performed at excitation and emission wavelengths of 460 nm and 512 nm, respectively. The cumulative amount of drug permeating per unit area (µg/cm^2) versus time (min) was plotted and the slope of the linear portion of the plot was calculated as the flux j (µg/cm^2 min). The lag time was determined by intercepting the linear portion of the cumulative amount of drug permeated versus time with the abscissa. The apparent permeability coefficient (P_{app}) was determined using **Equation PIII 3.1**:

$$P_{app} = \frac{dM}{dt} \times \frac{1}{A \times C_0}$$

Equation PIII 3.1

where dM/dt (µg/s) is the slope at the steady state period, A (cm^2) is the diffusion surface area and C_0 (µg/mL) is the initial drug concentration within samples. Besides, for a better understanding of the permeation-enhancing properties of the tested CFS, the enhancement ratio (ER) was calculated according to **Equation PIII 3.2**:

$$ER = \frac{P_{app}\ with\ CFS\ or\ MRS}{P_{app}\ CTRL}$$

Equation PIII 3.2

3.2.7. Differential scanning calorimetry

Differential scanning calorimetry (DSC) analyses were carried out to investigate a potential interaction between the selected CFS and the lipid components of the olfactory nasal mucosa. The nasal mucosa explant was cut into 5 pieces weighing the same, which were then treated for 5 h with 3 mL of normal saline solution in the absence (CTRL) or presence of 25% v/v of either MRS or one of the three CFS. Once the incubation time had expired, the tissue specimens were washed with MilliQ water and left to dry in a desiccator under vacuum containing $CaCl_2$ for 48 h. DSC analysis was conducted utilizing a Perkin Elmer DSC 6 instrument (Perkin Elmer, Beaconsfield, UK) with nitrogen employed as the purge gas at a flow rate of 20 mL/min. Samples, weighing between 2 and 3 mg, were loaded into an aluminum pan and subjected to a heating process, starting at 30 °C and ending at 180 °C, with a scanning rate of 10 °C/min.

3.2.8. Immunostaining assay of tight junctions

To evaluate the influence of the three CFS on the barrier integrity, immunofluorescence (IF) staining against the tight junction marker zonula occludens-1 (ZO-1) was performed. Therefore, the primary cells were treated as described in section 3.2.6.4. The only difference was that there was no sampling during the 5h permeation. Further, after the last washing step with 200 µL PBS, the cells were fixated by adding 200 µL of a 1:1 methanol/acetone mixture to the apical and 500 µL to the basolateral compartment. Cells were placed at -20°C for 20 min. Afterward, the mixture was removed and replaced with PBS. In PBS cells can be stored for up to 1 week at 4°C until staining is performed. All washing steps were performed by applying 300 µL of the buffer to the apical and 500 µL to the basolateral compartment. Transwells were washed 3 times with PEMT for 5 min. Next, a 5 min washing step with quenching buffer was performed followed by another washing step with PEMT (twice for 5 min each). Afterward, each transwell was blocked by adding 200 µL blocking buffer to the apical compartment for 1 h at room temperature (RT) or overnight at 4°C. After blocking, the blocking buffer was removed and 100 µL of a 1:100 dilution of anti-tight junction protein 1 antibody (Novus Biologicals, #NBP1-85047, Centennial, USA) in blocking buffer was applied overnight at 4°C. Then, the primary antibody was removed and the transwells were washed 4 times for 5 min each using blocking buffer. In the end, 100 µL of a 1:300 dilution of the secondary antibody (F(ab´)2 goat anti-rabbit IgG (H+L) AF Plus 488, Thermo Fisher Scientific, #A48282, Darmstadt, Germany) and DAPI (20 µg/ml) diluted in blocking buffer were added apically. Incubation was performed at RT for 1 h in the dark. To wash away

unbound antibodies, cells were washed 5 times for 5 min each using PEMT. The membranes of the transwells were then separated from the well and embedded in the Mowiol mounting medium on an object slide for imaging using a Keyence BZ-X800 Fluorescence Microscope.

3.2.9. Statistical analysis

The presented results are expressed as mean values along with their corresponding standard deviations (SD). The SD was computed based on data collected from three independent experiments, except for the permeation results obtained with the tissue and the cell-based models, which were derived accordingly from four and ten independent experiments, and for the immunostaining assay, for which 5 replicates were produced. Statistical analysis was carried out for all experimental data using a *t*-test, with significance determined for p-values less than 0.05.

3.3. Results and discussion

3.3.1. Human lactobacilli CFS

The three CFS were obtained through a very straightforward downstream process that consists of two main steps: centrifugation of lactobacilli broth to isolate the supernatant and filtration to remove eventual residual cells and cell debris. CFS were employed in their liquid form and were characterized by both a typical yellowish color, due to the MRS broth components, and an acidic pH. The latter was found to range between 3.60 and 3.83, with BC5-CFS and BC12-CFS featuring the lower and the higher pH values, respectively. The low pH of the isolated CFS agreed with previously published results and was due to the metabolic activity of lactic acid bacteria, which tends to acidify the culture medium [21]. Since the pH can simultaneously affect both the nasal mucosa health and the absorption of molecules across the biological barrier, it is suggested to keep the pH of the formulation close to that of the administering site [22], that is 5.5 – 6.5 [23]. Consequently, the pH of CFS was adjusted to the value of 6, preventing mucosal damage and/or irritation and differences in drug permeation.

3.3.2. CFS influence on cell viability

The potential cytotoxic effect of different volume ratios of BC5-CFS, BC9-CFS, and BC12-CFS on the porcine primary cell model of the olfactory epithelium was verified after 24h treatment and the results are shown in **Figure PIII 3.1**. According to ISO 10993-5:2009, chemicals are to be considered cytotoxic when they cause a decrease in cell viability below

70%; therefore, as it comes clear from the graph, none of the considered samples were found cytotoxic at the tested conditions. This implies that neither the composition of the lactobacilli culture medium (MRS) nor the products of the probiotic metabolism negatively impact cell survival. Wanting to prove the role of the CFS as permeation enhancers and, at the same time, to employ the excipients at reduced concentrations, the intermediate volume ratio of 25% was selected for the following studies, even though none of the tested volume ratios negatively affected cell viability.

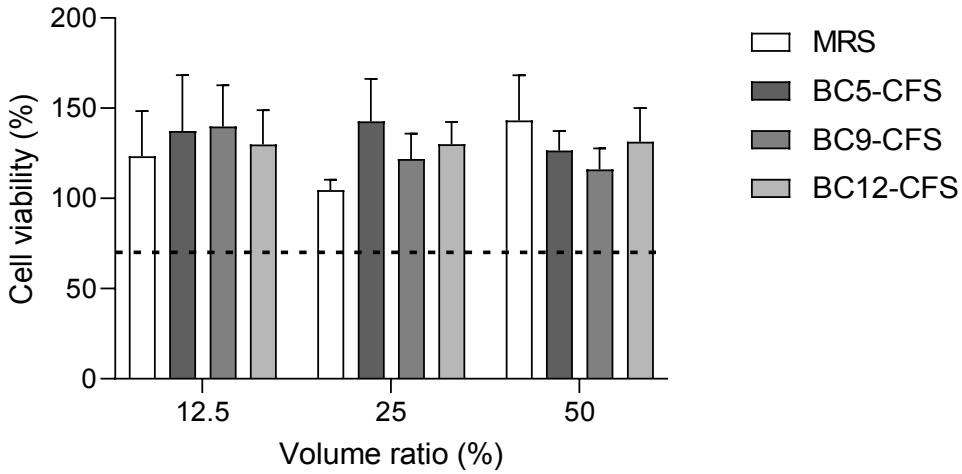

Figure PIII 3.1 CFS influence on porcine olfactory epithelial primary cells viability. Cell viability evaluation was performed after 24h treatment with different volume ratios of either MRS or CFS. The black dotted line indicates 70% cell viability. Data are reported as Mean + SD, n = 6.

3.3.3. CFS influence on osmolality

Similarly to the pH, even osmolality can affect the nasal mucosa [24]. Pujara and co-workers, for example, perfused sodium chloride solutions of increasing osmolalities through the rat nasal cavity and evaluated their potential for cell damage. The authors observed that hypotonic solutions induced cell swelling, with a consequent remarkable release of lactate dehydrogenase (LDH). Differently, isotonic and hypertonic solutions exerted little effect in terms of LDH release, but a 600 mOsm/kg solution determined cell shrinking. Moreover, they noted that the functional mucociliary system was most efficiently maintained at the nasal isosmotic value (280 mOsm/kg [24]) [25]. In this study, NaCl 0.9% (v/v) was chosen as a diluent because of its being isosmotic, and the influence of 25% (v/v) of either MRS or one of three tested CFS was evaluated. **Table PIII 3.2** shows that samples' osmolalities were comprised between 280 mOsm/kg and 370 mOsm/kg, therefore they matched the requirement for being administered in the nasal cavity: they featured osmolality values close

to the physiological one and did not exceed 500 mOsm/kg [26]. These results further support the safety of the investigated CFS, because, apart from not being cytotoxic, they are expected to be non-irritating or harmful to the mucosa. Besides, it has been demonstrated that by altering the osmolarity of a formulation it is possible to increase drug absorption, as cell swelling and shrinking can alter the epithelium paracellular permeability. This was verified for both cell-free and cell-based *in vitro* studies [27–29]. Consequently, the gathered osmolality values guaranteed that tonicity would not influence the subsequent permeation studies.

Table PIII 3.2 Osmolality values of NaCl 0.9% (w/v) in the absence (CTRL) and presence of 25% (v/v) of either MRS or CFS. Data are reported as Mean ± SD, n = 3.

Sample	mOsm/kg	SD
CTRL	280.67	1.15
MRS	313.00	2.00
BC5-CFS	370.00	0.00
BC9-CFS	360.33	1.15
BC12-CFS	355.67	2.08

3.3.4. CFS influence on fluorescein sodium salt permeability

When it comes to the initial stage of drug development, high-throughput screening of different compounds and formulations is highly convenient, but this is impractical with *in vivo* studies. Consequently, there is continuous research in the establishment of rapid and high-performance *in vitro* models to assess the permeability of compounds through the nasal epithelium and mucosa [30]. Therefore, in the present study, different *in vitro* models of the olfactory nasal mucosa were used to screen the selected CFS for their potential activity as enhancers towards FSS nose-to-brain permeation. Specifically, diffusion studies were performed across a cell-free, a tissue-based, and a cell-based model, thus gradually increasing the complexity and the informative level of the assay.

First, *in vitro* transport studies were carried out using the commercially available biomimetic membrane PermeaPad®. The latter features a dry film consisting of soybean phosphatidylcholine S-100, positioned between two low-retention layers of regenerated cellulose, functioning as support sheets. Upon hydration, the dry lipids swell and create a dense layer of vesicles interspersed in an aqueous environment, and this particular arrangement mimics cell organization within a tissue [31]. **Figure PIII 3.2** depicts the permeation profiles of FSS across the PermeaPad® barrier when solubilized in normal

saline solution alone (CTRL) or with 25% (v/v) of either MRS or one of the investigated CFS. At first glance, the CTRL sample stands out as the only one featuring a lag time (t_{lag}), which was quantified in 7.69 ± 2.49 min, a short span but not negligible. Given that the thickness is a constant value (l), according to **Equation PIII 3.3** [32], the lag time is only dependent on the diffusion coefficient of the molecule (D).

$$t_{lag} = \frac{l^2}{6D}$$

Equation PIII 3.3

This means that both CFS and MRS favored FSS diffusivity across the barrier. However, the mass permeated after 300 min was not significantly different between the tested samples (28.99 ± 1.16 μg/cm^2 CTRL; 30.98 ± 0.33 μg/cm^2 MRS; 28.52 ± 1.08 μg/cm^2 BC9-CFS; 30.07 ± 0.61 μg/cm^2 BC12-CFS), with the only exception of BC5-CFS, which enabled the permeation of the higher amount of the marker (35.31 ± 0.88 μg/cm^2). This is due to BC5-CFS's ability to greatly improve FSS flux across the barrier, quantified in 0.14 ± 0.01 μg/cm^{2}min, compared to all the other tested samples, which allowed FSS diffusion at a rate of 0.12 ± 0.01 μg/min each cm^2 of surface. This result has a relevant implication. Hence, considering the definition of the drug flux (J) according to **Equation PIII 3.4** [32]

$$J = -D\frac{dC}{dx}$$

Equation PIII 3.4

it is likely that BC5-CFS also influenced FSS solubility within the membrane, thus increasing the concentration gradient (dC/dx). In addition, the BC5-CFS effect on the marker flux ultimately resulted in an apparent permeability coefficient of 4.59 ± 0.17 10^{-6} cm/s, which was significantly increased compared to both the CTRL (4.03 ± 0.16 10^{-6} cm/s) and MRS (3.94 ± 0.11 10^{-6} cm/s) samples (**Figure PIII 3.3**).

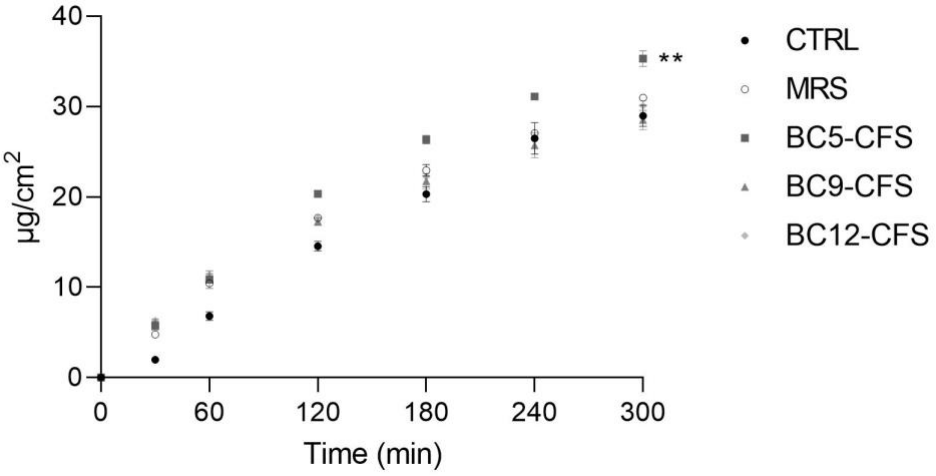

Figure PIII 3.2 Fluorescein sodium salt permeation profiles across the cell-free model (PermeaPad® barrier) in the absence (CTRL) or presence of 25% (v/v) of either the lactobacilli culture medium (MRS) or BC5/BC9/BC12-CFS. Data are reported as Mean ± SD, n = 3. Significance indicated by ** = $p < 0.01$ compared to both CTRL and MRS.

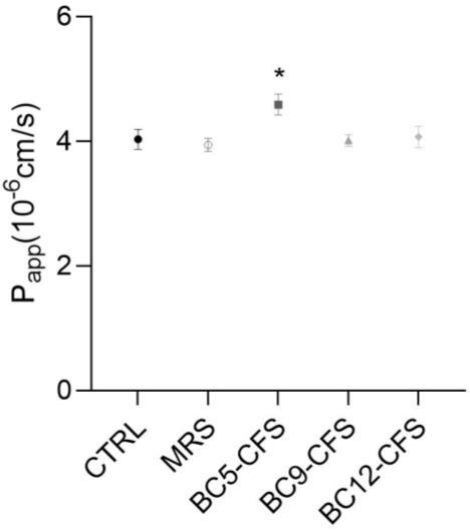

Figure PIII 3.3 Fluorescein sodium salt apparent permeability coefficient (P_{app}) across the cell-free model (PermeaPad® barrier) in the absence (CTRL) or presence of 25% (v/v) of either the lactobacilli colture medium (MRS) or BC5/BC9/BC12-CFS. Data are reported as Mean ± SD, n = 3. Significance indicated by * = $p < 0.05$ compared to both CTRL and MRS.

To perform diffusion studies across a tissue-based system, the porcine model was chosen because of its being considered suitable for nasal permeability studies [33]. As the tissue viability was not maintained because of its storage at -20°C without the use of cryoprotectants, this model is characterized by membrane integrity [34] and a more complex architecture compared to the PermeaPad® barrier but, similarly to the cell-free model, it can only account for molecules' passive diffusion. Interestingly, when testing FSS permeation across the excised olfactory tissue, not only the CTRL but also the MRS-containing sample

displayed a lag time, corresponding respectively to 17.34 ± 7.52 min and 20.41 ± 9.64 min (**Figure PIII 3.4**). Therefore, it can be stated that, because any of the CFS-containing samples showed a lag time, it was the probiotic metabolism that made the difference in terms of diffusivity. Further, the permeation profiles of the CTRL and MRS samples almost overlapped, thus allowing for the diffusion of a similar amount of FSS: 45.11 ± 2.02 μg/cm^2 and 42.31 ± 3.40 μg/cm^2 in the absence and presence of the lactobacilli culture medium, respectively. Instead, the addition of 25% (v/v) of any one of the tested CFS significantly increased the permeated mass compared to both reference samples, but the diffused FSS after 300 min did not differ between the three (52.40 ± 4.26 μg/cm^2 BC5-CFS; 50.51 ± 4.75 μg/cm^2 BC9-CFS; 52.33 ± 2.09 μg/cm^2 BC12-CFS). When it comes to the apparent permeability coefficient (**Figure PIII 3.5**), compared to what was observed with the cell-free model, BC9-CFS (7.37 ± 0.37 10^{-6} cm/s) and BC12-CFS (7.81 ± 0.88 10^{-6} cm/s) showed a tendency to enhance FSS apparent permeability, but differences were deemed significant just with respect to the MRS sample (6.47 ± 0.54 10^{-6} cm/s). This means that the composition of the two CFS did not provide particular advantages compared to an FSS standard solution. Instead, the use of the CFS produced by BC5 demonstrated once more its enhancing properties, as it was able to increase FSS P_{app} from 6.88 ± 0.61 10^{-6} cm/s in the CTRL to 9.23 ± 0.89 10^{-6} cm/s. Again, probably this is the result of a dual effect: BC5-CFS might act on both the molecule diffusion coefficient and solubility in the membrane.

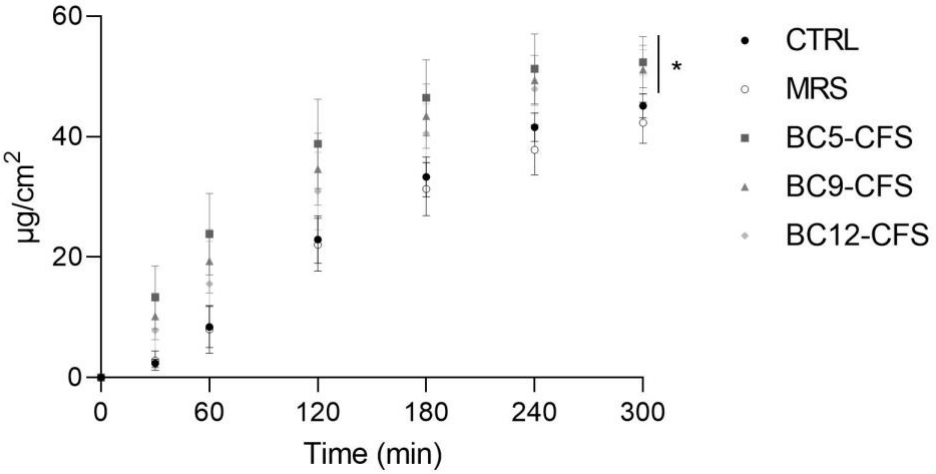

Figure PIII 3.4 Fluorescein sodium salt permeation profiles across the tissue-based model (porcine olfactory mucosa) in the absence (CTRL) or presence of 25% (v/v) of either the lactobacilli culture medium (MRS) or BC5/BC9/BC12-CFS. Data are reported as Mean ± SD, n = 4. Significance indicated by * = $p < 0.05$ between samples on the left side of the black line compared to both CTRL and MRS.

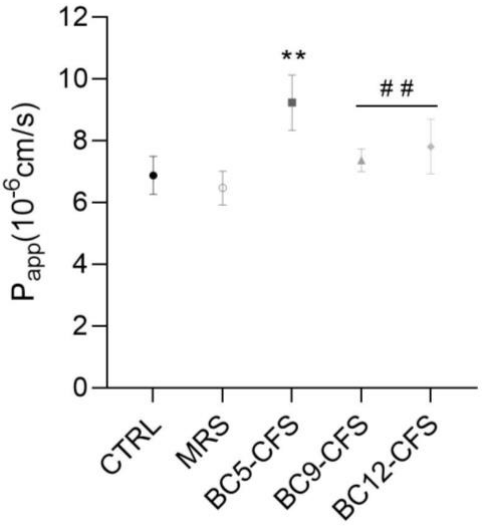

Figure PIII 3.5 Fluorescein sodium salt apparent permeability coefficient (P_{app}) across the tissue-based model (porcine olfactory mucosa) in the absence (CTRL) or presence of 25% (v/v) of either the lactobacilli culture medium (MRS) or BC5/BC9/BC12-CFS. Data are reported as Mean ± SD, n = 4. Significance indicated by ** = $p < 0.01$ compared to both CTRL and MRS; by ## = $p < 0.01$ between the samples under the black line compared to MRS.

The third and last permeation model was the cell-based one. RPMI 2650 is the only immortalized cell line obtained from the nasal cavity of a human being and is regarded as the standard *in vitro* cell-based model to investigate nasal drug permeation [35,36], including the nose-to-brain route [37]. However, we thought that some of the features of the RPMI 2650 model did not fit the purpose of the present study. First of all, the permanent cell line was originally derived from the nasal septum, which belongs to the respiratory region of the nose rather than the olfactory one. Secondly, RPMI 2650 cells have a limited differentiative capacity and thus cannot reproduce the heterogeneous cell type composition of the olfactory mucosa [20]. Moreover, they tend to create a leaky multilayered barrier [20], which could make it difficult to point out the influence of CFS on the permeability of a model molecule such as FSS, which is supposed to permeate through the paracellular pathway. Consequently, we employed the porcine olfactory primary cell model that Ladel and colleagues have recently developed. It consists of a monolayer of porcine olfactory epithelial cells that differentiated over 21 days thereby producing a functional epithelial barrier, with secreted mucins and cilia [20]. **Figure PIII 3.6** displays the permeation profiles across the cell-based model and the most striking difference compared to the aforementioned systems is that all tested samples exhibited a lag time. It must also be said that the lag time measured for the three CFS (78.16 ± 8.14 min BC5-CFS; 42.65 ± 4.94 min BC9-CFS; 55.15 ± 19.55 min BC12-CFS) was higher compared to both the CTRL (20.53 ± 6.35 min) and the MRS (10.51 ± 6.41 min) samples, suggesting that the lactobacilli metabolic products negatively impact the time required to reach the steady state. Nevertheless, only when FSS diffusion

took place in the presence of the CFS, a greater increase in mass permeation was observed, as demonstrated by profiles featuring high slopes. As a result, both the mass permeated after 300 min (m) and flux (j) were remarkably higher in the presence of CFS (m = 23.99 ± 3.31 μg/cm^2 – j = 0.10 ± 0.02 μg/cm^{2}min BC5-CFS; m = 19.66 ± 2.45 μg/cm^2 – j = 0.07 ± 0.01 μg/cm^{2}min BC9-CFS; m = 17.81 ± 4.68 μg/cm^2 – j = 0.07 ± 0.02 μg/cm^{2}min BC12-CFS) compared to both reference samples (m = 9.20 ± 1.18 μg/cm^2 – j = 0.03 ± 0.01 μg/cm^{2}min CTRL; m = 12.78 ± 2.67 μg/cm^2 – j = 0.04 ± 0.01 μg/cm^{2}min MRS). Referring to **Equation PIII 3.4**, in this case, it is not clear whether the increase in the marker flux was the result of the CFS influence on diffusivity or concentration gradient, or both. What is evident is their permeation enhancer activity as demonstrated by P_{app} coefficients in **Figure PIII 3.7**. The apparent permeability of FSS was greatly improved from 1.15 ± 0.18 10^{-6} cm/s and 1.45 ± 0.31 10^{-6} cm/s in the CTRL and MRS samples respectively, to 3.47 ± 0.52 10^{-6} cm/s, 2.68 ± 0.37 10^{-6} cm/s, and 2.42 ± 0.76 10^{-6} cm/s accordingly in BC5-CFS, BC9-CFS, and BC12-CFS. The graph also shows that MRS itself was able to significantly improve the P_{app} of the fluorescent marker, suggesting that there must be some inherent components of the culture medium bearing the ability to enhance small hydrophilic molecule permeation.

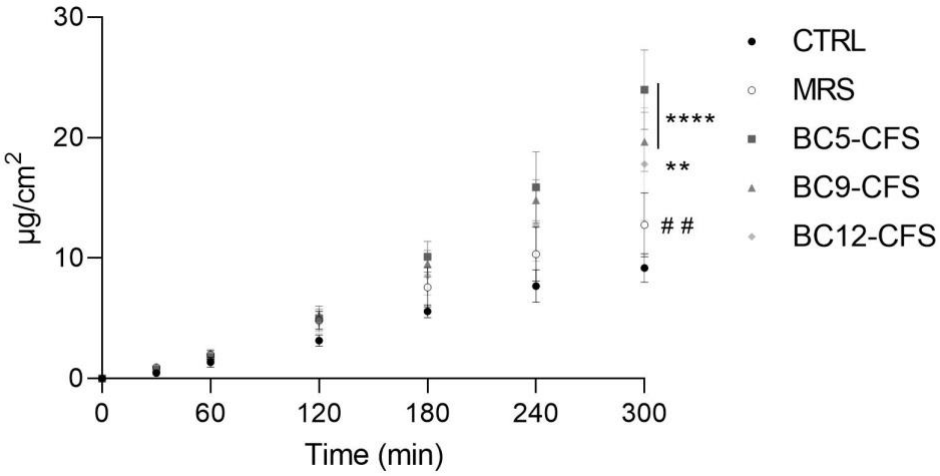

Figure PIII 3.6 Fluorescein sodium salt permeation profiles across the cell-based model (porcine olfactory epithelial primary cell) in the absence (CTRL) or presence of 25% (v/v) of either the lactobacilli culture medium (MRS) or BC5/BC9/BC12-CFS. Data are reported as Mean ± SD, n = 10. Significance indicated by **** = $p < 0.0001$ between samples on the left side of the black line compared to both CTRL and MRS; by ** = $p < 0.01$ compared to both CTRL and MRS; by ## = $p < 0.01$ compared to CTRL.

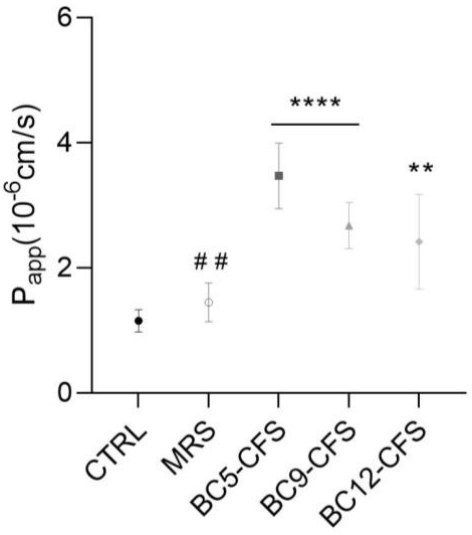

Figure PIII 3.7 Fluorescein sodium salt apparent permeability coefficient (P_{app}) across cell-based model (porcine olfactory epithelial primary cell) in the absence (CTRL) or presence of 25% (v/v) of either the lactobacilli culture medium (MRS) or BC5/BC9/BC12-CFS. Data are reported as Mean ± SD, n = 10. Significance indicated by **** = $p < 0.0001$ between samples under the black line compared to CTRL and MRS; by ** = $p < 0.01$ compared to both CTRL and MRS; by ## = $p < 0.01$ compared to CTRL.

To gain a deeper understanding of the extent to which the investigated CFS improved FSS permeation, we calculated the enhancement ratio. The data presented in **Figure PIII 3.8** highlight the predominant role of BC5-CFS as a permeation enhancer and they also prove the predictive power of the three *in vitro* models, as they ranked the same CFS as the best-performing enhancer. Besides, it must be noted that, when diffusion studies were performed across the cell-based model, also BC9-CFS and BC12-CFS acted as enhancers. Furthermore, it seems that the ER values of the CFS rise with the increase in the barrier system complexity.

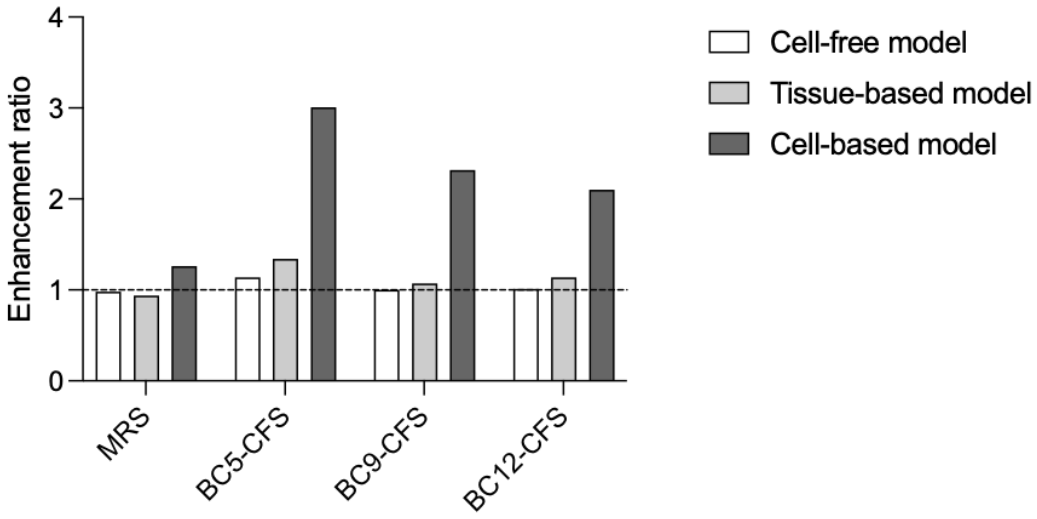

Figure PIII 3.8 Enhancement ratio (ER) of CFS and MRS when tested on the three in vitro barriers: cell-free model (PermePad® barrier), tissue-based model (excised porcine olfactory mucosa), and cell-based model (porcine olfactory epithelial primary cells). Only samples exhibiting ER > 1 (indicated by the black dotted line) are to be considered enhancers.

These observations suggest that the three CFS might improve FSS diffusion because of a preferential interaction with some components of the tested barriers, such as lipids and proteins. Reasonably, the improvement in FSS permeability must be due to the composition of the CFS. Parolin and co-workers described the metabolites present in the cell-free supernatants of different human *Lactobacillus* strains, including those selected in the present study. Even though the CFS composition was strain-specific, the authors observed a common subset of molecules comprising amino acids, organic acids, monosaccharides, ketones, and alcohols [21]. Specifically, what stands out is the presence of some organic acids such as lactic acid, and orotate (mostly represented in BC5-CFS). Organic acids have been previously proven to function as enhancer molecules in transdermal drug delivery, and lactic acid was seen to outperform compared to other related substances [38], thus it might be possible that a similar role is played in nose-to-brain delivery as well. Alongside, in the case of the cell-based model, it cannot be excluded that, apart from paracellular diffusion, some sort of transcellular transport took place. Indeed, on the surface of olfactory epithelial cells different membrane-associated channel proteins have been identified. Aquaporins, for instance, are involved in the bidirectional transport of water, but small solutes and ions can also be transferred through this mechanism [39]. Moreover, amino acids, organic acids, and nucleosides contained in the CFS obtained from BC5, BC9, and BC12 [21] can be the substrates of different SLC (solute carrier) transporters [40].

The use of a small hydrophilic paracellular marker, such as fluorescein sodium salt, which is often exploited to evaluate the tightness and integrity of barriers [41], also allowed us to

gather information regarding membrane suitability for nasal *in vitro* diffusion studies. Comparing the P_{app} of FSS across our barrier systems to that reported in the literature for the RPMI 2650 cell line, the only value that was deemed significantly different was that measured across the cell-based model (**Figure PIII 3.9)**. This is probably due to the primary nasal epithelial cells' tendency to develop an excessive number of tight junctions (TEER values measured 1753.42 ± 557.44 Ω cm^2) compared to both the excised tissue from which they were isolated (TEER values reported for the porcine mucosa 30 – 250 Ω cm^2 [42]) and the immortalized cell line (TEER values reported for RPMI2650 cell line 55 – 75 Ω cm^2 [20]). For this reason, combining studies on different barrier types might represent a more complete and reliable approach to assess the performance of molecules [33]. However, it must be said that the P_{app} measured for FSS across the primary cell model was closer (p = 0.0136) to that reported across the excised human mucosa (3.12 ± 1.99 10^{-6} cm/s [41]).

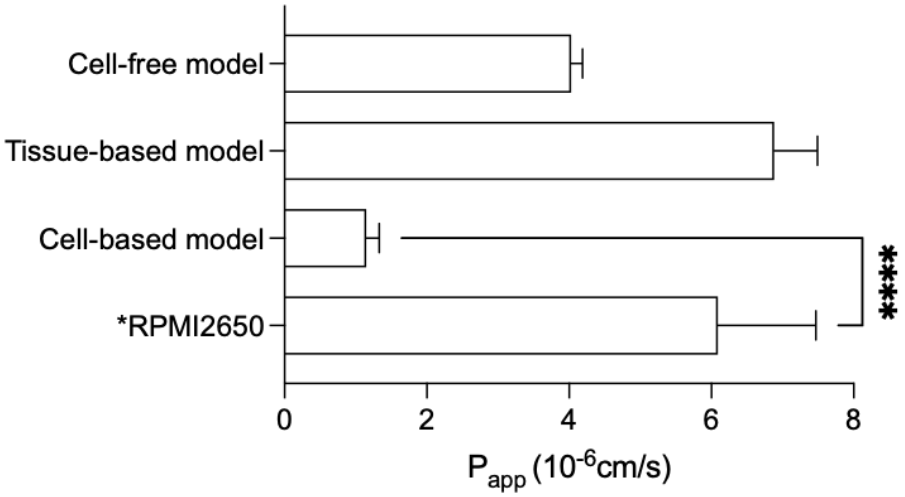

Figure PIII 3.9 Apparent permeability coefficients (P_{app}) of fluorescein sodium salt through the cell-free (PermeaPad® barrier), tissue based (excised porcine olfactory mucosa), and cell-based (porcine olfactory primary epithelial cell) models compared to P_{app} calculated by Wengst and Reichl, 2010 across the RPMI2650 cell line. Data are reported as Mean ± SD, n ≥ 3. Statistical differences between samples are indicated by **** = p < 0.0001.

3.3.5. CFS influence on lipid membranes

We speculated that the increase in the P_{app} of FSS might be the result of an interaction between probiotic metabolites and phospholipid bilayers. Therefore, to better elucidate the mechanism of permeation enhancement operated by CFS, DSC analyses were performed on the excised porcine olfactory mucosa untreated (CTRL) and treated with 25% (v/v) of MRS or one of the CFS under investigation. **Figure PIII 3.10** shows that the CTRL sample was characterized by an endothermic peak at 71.06°C, which is coherent with lipid

transitions, that according to Corbo and co-workers should occur between 70°C and 100°C [43]. However, olfactory mucosa treatment with either MRS or one of CFS determined a shift in the endothermic peak to lower temperatures: 64.31°C, 56.06°C, 59.50°C, and 58.80°C for MRS, BC5-CFS, BC9-CFS, and BC12-CFS respectively. This suggests that lactobacilli's CFS can perturb the lipids within the nasal mucosa, and it is likely that this effect contributes to the increase in membrane permeability. Concerning the work of Parolin et al. [21], there are some molecules present in the CFS of BC5, BC9, and BC12 that catch the eye, in particular, butyrate (only present in BC5-CFS) and ethanol. The first belongs to the family of salts of fatty acids, which are known for their permeation-enhancing properties due to their ability to alter the lipid environment and cause membrane fluidization [44,45]. Ethanol, instead, features an established ability to increase membrane fluidity and pores formations, which has been exploited for example to increase transdermal absorption of drugs [38]. Therefore, these two elements might improve FSS permeation through their interaction with the lipid component of the three tested barriers.

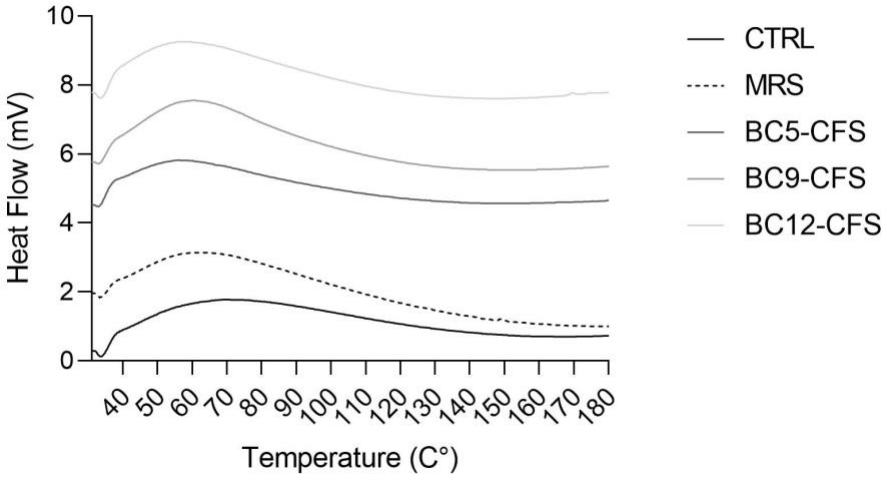

Figure PIII 3.10 Differential scanning calorimetry curves of the excised porcine olfatory mucosa untreated (CTRL) and treated with 25%(v/v) or MRS or BC5/BC9/BC12-CFS.

3.3.6. CFS influence on tight junctions

FSS is a well-established marker of paracellular transport, therefore the observation of an improved permeability, particularly on the primary cell-based model, prompted us to investigate a potential involvement of CFS in tight junction modulation. To do so, olfactory primary cell monolayers were treated with either sodium chloride 0.9% (CTRL), MRS, or the CFS for 5 h, and two data were acquired: the TEER values at the beginning and the end of the experiment, as well as the immunoreactivity against ZO-1, which is a polypeptide that

connects tight junction proteins (i.e. occludin and claudin) to the cytoskeleton [46]. **Figure PIII 3.11** shows the percentage of decrease in TEER between the starting and the end point of the analysis. Interestingly, the CTRL sample itself presents a 44.28 ± 13.72 % reduction, which is probably due to the change in the basolateral medium composition [47]; in fact, the primary culture medium was substituted with MEM without phenol red solely supplemented with 10% FBS. Furthermore, the presence of MRS determined a significant decrease in TEER (65.33 ± 5.14 %) compared to the CTRL sample, which correlates with the enhancing effect observed on the cell-based model and the influence on lipids' endothermic peak. Most notably, the influence on TEER was even greater when primary cells were treated with CFS and, in agreement with the permeation and DSC studies, BC5-CFS demonstrated the highest influence on TEER (81.07 ± 3.66 %).

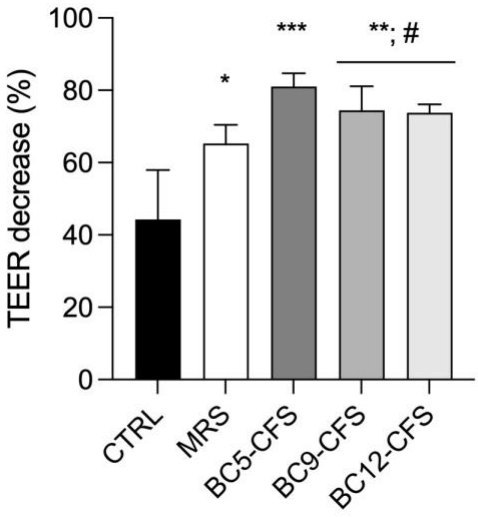

Figure PIII 3.11 Olfactory epithelial primary cells' percentage of TEER decrease after 5 h treatment with 25% (v/v) of either MRS or CFS. Data are reported as Mean ± SD, n = 5. Significance indicated by * = $p < 0.05$ compared to CTRL; by # = $p < 0.05$ between samples under the black line compared to MRS; by ** = $p < 0.01$ between samples under the black line compared to CTRL; by *** = $p < 0.001$ compared to both CTRL and MRS.

The measurement of TEER reduction is often employed as a screening parameter to investigate tight junction modulation ability by permeation enhancers [44], therefore we expected to observe a correlation between TEER decrease and ZO-1 immunostaining distribution. However, as is pointed out in **Figure PIII 3.12**, any difference could be highlighted neither in terms of tight junctions' staining pattern nor in fluorescence intensity. The absence of an evident disruption of cell-cell connections might indicate that CFS influence tight junctions' activity rather than their localization. This outcome is further supported by the work of Chen-Quay et al., who demonstrated the ability of PGPC (1-palmitoyl-2-glutaroyl-*sn*-glycero-3-phosphocholine) to cause a reduction in TEER values

without affecting the structural integrity of tight junctions in EpiAirway tissues [48]. The authors suggested the possibility for their candidate lipid to interact with the lipid rafts where tight junctions' proteins localize, thereby influencing both membrane permeability and electrical resistance [48].

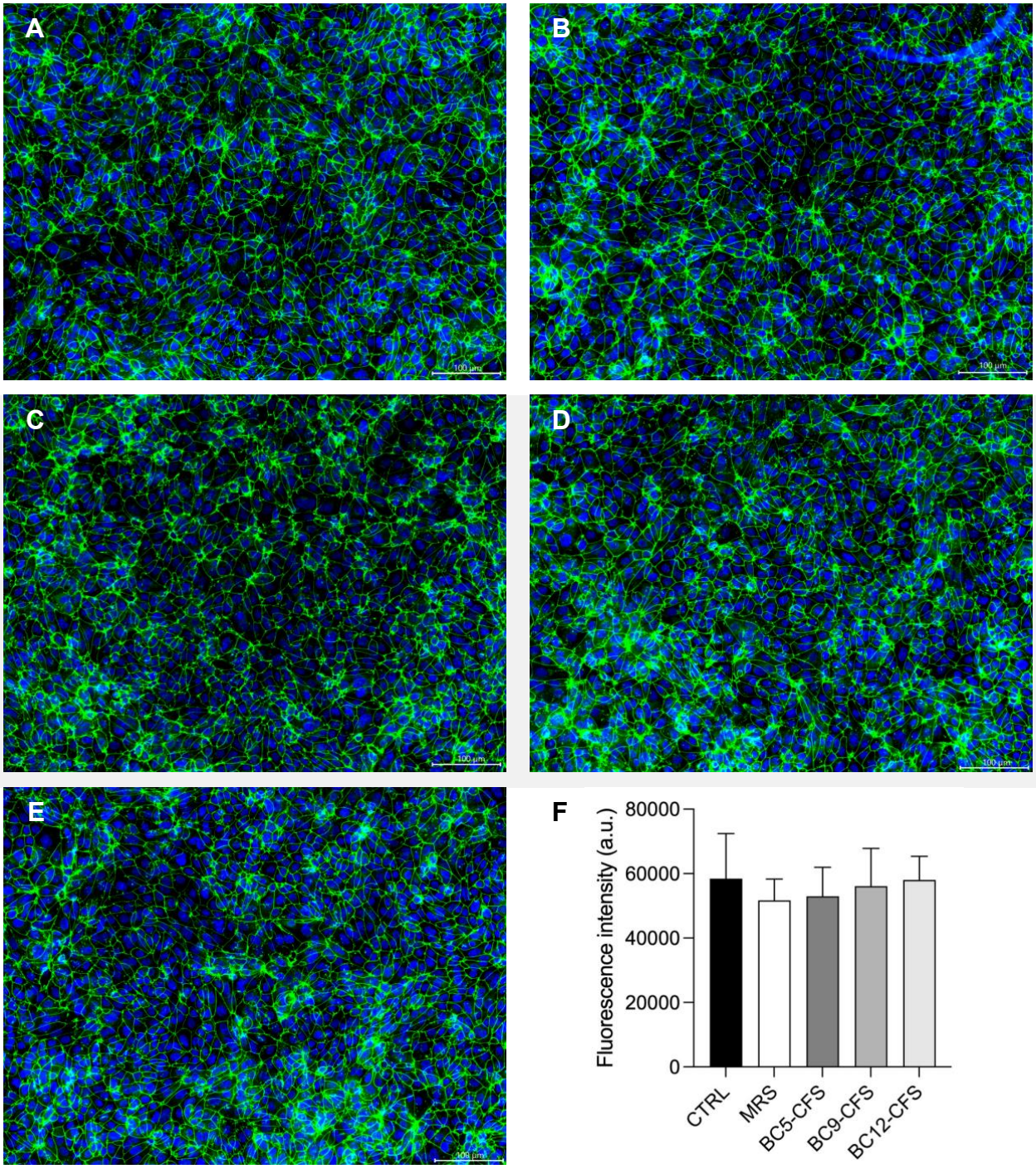

Figure PIII 3.12 Influence of CFS on tight junction integrity. A – E) Staining of the zonula occludens marker ZO-1 in olfactory epithelial primary cells treated for 5 h with either sodium chloride (A), MRS (B), BC5-CFS (C), BC9-CFS (D), or BC12-CFS (E). F) Fluorescence quantification; data are reported as Mean ± SD, n = 5.

3.4. Conclusions

Based on the current information, this is the first attempt to demonstrate the applicability of postbiotics, like CFS, as permeation enhancers in nose-to-brain drug delivery. Moreover, this innovative approach might be of particular interest for the development of more sustainable and less pollutant pharmaceuticals. Indeed, CFS are obtained from naturally occurring and health-promoting human lactobacilli through a simple, easily scalable, and green (extraction using toxic and harmful solvents is not required) procedure. Besides, as CFS are frequently discarded by many food and pharmaceutical industries [49], their use would contribute to the reduction of waste and even the microbial cells could be used to produce probiotic-containing delivery systems [50]. Among the screened CFS in the study, BC5-CFS outperformed as a permeation enhancer and the robustness of the result is supported by the use of three *in vitro* models of the olfactory epithelium. The fact that different barriers highlighted diverse behaviors (the presence of lag time as well as BC9-CFS and BC12-CFS's ability to improve FSS permeability across the cell-based model) suggests that each model should be preferred depending on the scientific need. Specifically, the PermeaPad® barrier is surely a promising tool for a sustainable, less time-consuming, and cost-effective screening of enabling formulations. However, when selecting those excipients and/or drugs to be further optimized during the late stages of the pharmaceutical development process, it might be also useful to rely on more complete models, i.e., cell-based models. The mixture of metabolites present in BC5-CFS likely increases FSS permeation by perturbing the lipid environment within the tested barriers which, in the case of OEPC, seems to exert an effect on tight junctions, as demonstrated by the decrease in TEER values. Nonetheless, this outcome does not affect either barrier integrity or cell viability. Hopefully, these results will encourage the introduction of BC5-CFS as an innovative natural and green excipient in the field of nose-to-brain delivery of small hydrophilic molecules.

3.5. References Paper III

1. Souza, H.D.O.; Costa, R.D.S.; Quadra, G.R.; Fernandez, M.A.D.S. Pharmaceutical Pollution and Sustainable Development Goals: Going the Right Way? Sustain. Chem. Pharm. 2021, 21, 100428, doi:10.1016/j.scp.2021.100428.
2. Puhlmann, N.; Vidaurre, R.; Kümmerer, K. Designing Greener Active Pharmaceutical Ingredients: Insights from Pharmaceutical Industry into Drug Discovery and Development. Eur. J. Pharm. Sci. 2024, 192, 106614, doi:10.1016/j.ejps.2023.106614.

3. Silvério, L.A.L.; Coco, J.C.; Macedo, L.M.D.; Santos, É.M.D.; Sueiro, A.C.; Ataide, J.A.; Tavares, G.D.; Paiva-Santos, A.C.; Mazzola, P.G. Natural Product-Based Excipients for Topical Green Formulations. Sustain. Chem. Pharm. 2023, 33, 101111, doi:10.1016/j.scp.2023.101111.
4. Thorakkattu, P.; Khanashyam, A.C.; Shah, K.; Babu, K.S.; Mundanat, A.S.; Deliephan, A.; Deokar, G.S.; Santivarangkna, C.; Nirmal, N.P. Postbiotics: Current Trends in Food and Pharmaceutical Industry. Foods 2022, 11, 3094, doi:10.3390/foods11193094.
5. Teame, T.; Wang, A.; Xie, M.; Zhang, Z.; Yang, Y.; Ding, Q.; Gao, C.; Olsen, R.E.; Ran, C.; Zhou, Z. Paraprobiotics and Postbiotics of Probiotic Lactobacilli, Their Positive Effects on the Host and Action Mechanisms: A Review. Front. Nutr. 2020, 7, 570344, doi:10.3389/fnut.2020.570344.
6. Liu, C.; Ma, N.; Feng, Y.; Zhou, M.; Li, H.; Zhang, X.; Ma, X. From Probiotics to Postbiotics: Concepts and Applications. Anim. Res. One Health 2023, 1, 92–114, doi:10.1002/aro2.7.
7. Carriço, C.; Ribeiro, H.M.; Marto, J. Converting Cork By-Products to Ecofriendly Cork Bioactive Ingredients: Novel Pharmaceutical and Cosmetics Applications. Ind. Crops Prod. 2018, 125, 72–84, doi:10.1016/j.indcrop.2018.08.092.
8. Duarte, M.; Oliveira, A.L.; Oliveira, C.; Pintado, M.; Amaro, A.; Madureira, A.R. Current Postbiotics in the Cosmetic Market—an Update and Development Opportunities. Appl. Microbiol. Biotechnol. 2022, 106, 5879–5891, doi:10.1007/s00253-022-12116-5.
9. Madden, S.; Carrazana, E.; Rabinowicz, A.L. Optimizing Absorption for Intranasal Delivery of Drugs Targeting the Central Nervous System Using Alkylsaccharide Permeation Enhancers. Pharmaceutics 2023, 15, 2119, doi:10.3390/pharmaceutics15082119.
10. Grassin-Delyle, S.; Buenestado, A.; Naline, E.; Faisy, C.; Blouquit-Laye, S.; Couderc, L.-J.; Le Guen, M.; Fischler, M.; Devillier, P. Intranasal Drug Delivery: An Efficient and Non-Invasive Route for Systemic Administration. Pharmacol. Ther. 2012, 134, 366–379, doi:10.1016/j.pharmthera.2012.03.003.
11. Lofts, A.; Abu-Hijleh, F.; Rigg, N.; Mishra, R.K.; Hoare, T. Using the Intranasal Route to Administer Drugs to Treat Neurological and Psychiatric Illnesses: Rationale, Successes, and Future Needs. CNS Drugs 2022, 36, 739–770, doi:10.1007/s40263-022-00930-4.
12. Yang, W.; Lipert, M.; Nofsinger, R. Current Screening, Design, and Delivery Approaches to Address Low Permeability of Chemically Synthesized Modalities in Drug Discovery

and Early Clinical Development. Drug Discov. Today 2023, 28, 103685, doi:10.1016/j.drudis.2023.103685.

13. Volpe, D.A. Application of Method Suitability for Drug Permeability Classification. AAPS J. 2010, 12, 670–678, doi:10.1208/s12248-010-9227-8.
14. Haasbroek-Pheiffer, A.; Van Niekerk, S.; Van Der Kooy, F.; Cloete, T.; Steenekamp, J.; Hamman, J. In Vitro and Ex Vivo Experimental Models for Evaluation of Intranasal Systemic Drug Delivery as Well as Direct Nose-to-brain Drug Delivery. Biopharm. Drug Dispos. 2023, 44, 94–112, doi:10.1002/bdd.2348.
15. Henriques, P.; Bicker, J.; Silva, S.; Doktorovová, S.; Fortuna, A. Nasal-PAMPA: A Novel Non-Cell-Based High Throughput Screening Assay for Prediction of Nasal Drug Permeability. Int. J. Pharm. 2023, 643, 123252, doi:10.1016/j.ijpharm.2023.123252.
16. Wu, I.Y.; Bala, S.; Škalko-Basnet, N.; di Cagno, M.P. Interpreting Non-Linear Drug Diffusion Data: Utilizing Korsmeyer-Peppas Model to Study Drug Release from Liposomes. Eur. J. Pharm. Sci. 2019, 138, 105026, doi:10.1016/j.ejps.2019.105026.
17. Carrasco-Correa, E.J.; Ruiz-Allica, J.; Rodríguez-Fernández, J.F.; Miró, M. Human Artificial Membranes in (Bio)Analytical Science: Potential for in Vitro Prediction of Intestinal Absorption-A Review. TrAC Trends Anal. Chem. 2021, 145, 116446, doi:10.1016/j.trac.2021.116446.
18. Corazza, E.; Abruzzo, A.; Giordani, B.; Cerchiara, T.; Bigucci, F.; Vitali, B.; di Cagno, M.P.; Luppi, B. Human Lactobacillus Biosurfactants as Natural Excipients for Nasal Drug Delivery of Hydrocortisone. Pharmaceutics 2022, 14, 524, doi:10.3390/pharmaceutics14030524.
19. Parolin, C.; Abruzzo, A.; Giordani, B.; Oliver, J.C.; Marangoni, A.; Luppi, B.; Vitali, B. Anti-Candida Activity of Hyaluronic Acid Combined with Lactobacillus Crispatus Lyophilised Supernatant: A New Antifungal Strategy. Antibiotics 2021, 10, 628, doi:10.3390/antibiotics10060628.
20. Ladel, S.; Schlossbauer, P.; Flamm, J.; Luksch, H.; Mizaikoff, B.; Schindowski, K. Improved In Vitro Model for Intranasal Mucosal Drug Delivery: Primary Olfactory and Respiratory Epithelial Cells Compared with the Permanent Nasal Cell Line RPMI 2650. Pharmaceutics 2019, 11, 367, doi:10.3390/pharmaceutics11080367.
21. Parolin, C.; Marangoni, A.; Laghi, L.; Foschi, C.; Ñahui Palomino, R.A.; Calonghi, N.; Cevenini, R.; Vitali, B. Isolation of Vaginal Lactobacilli and Characterization of Anti-Candida Activity. PLOS ONE 2015, 10, e0131220, doi:10.1371/journal.pone.0131220.

22. Javia, A.; Kore, G.; Misra, A. Polymers in Nasal Drug Delivery: An Overview. In Applications of Polymers in Drug Delivery; Elsevier, 2021; pp. 305–332 ISBN 978-0-12-819659-5.
23. Cirri, M.; Maestrelli, F.; Nerli, G.; Mennini, N.; D'Ambrosio, M.; Luceri, C.; Mura, P.A. Development of a Cyclodextrin-Based Mucoadhesive-Thermosensitive In Situ Gel for Clonazepam Intranasal Delivery. Pharmaceutics 2021, 13, 969, doi:10.3390/pharmaceutics13070969.
24. Campbell, C.; Morimoto, B.H.; Nenciu, D.; Fox, A.W. Drug Development of Intranasally Delivered Peptides. Ther. Deliv. 2012, 3, 557–568, doi:10.4155/tde.12.12.
25. Pujara, C.P.; Shao, Z.; Duncan, M.R.; Mitra, A.K. Effects of Formulation Variables on Nasal Epithelial Cell Integrity: Biochemical Evaluations. Int. J. Pharm. 1995, 114, 197–203, doi:10.1016/0378-5173(94)00238-Z.
26. Bitter, C.; Suter-Zimmermann, K.; Surbera, C. Nasal Drug Delivery in Humans. In Current Problems in Dermatology; Surber, C., Elsner, P., Farage, M.A., Eds.; KARGER: Basel, 2011; Vol. 40, pp. 20–35 ISBN 978-3-8055-9616-9.
27. Dufes, C.; Olivier, J.-C.; Gaillard, F.; Gaillard, A.; Couet, W.; Muller, J.-M. Brain Delivery of Vasoactive Intestinal Peptide (VIP) Following Nasal Administration to Rats. Int. J. Pharm. 2003, 255, 87–97, doi:10.1016/S0378-5173(03)00039-5.
28. Eriksen, J.B.; Barakat, H.; Luppi, B.; Brandl, M.; Bauer-Brandl, A. Modulation of Paracellular-like Drug Transport across an Artificial Biomimetic Barrier by Osmotic Stress-Induced Liposome Shrinking. Pharmaceutics 2022, 14, 721, doi:10.3390/pharmaceutics14040721.
29. Olivier, J.-C.; Djilani, M.; Fahmy, S.; Couet, W. In Situ Nasal Absorption of Midazolam in Rats. Int. J. Pharm. 2001, 213, 187–192, doi:10.1016/S0378-5173(00)00668-2.
30. Barlang, L.-A.; Weinbender, K.; Merkel, O.M.; Popp, A. Characterization of Critical Parameters Using an Air–Liquid Interface Model with RPMI 2650 Cells for Permeability Studies of Small Molecules. Drug Deliv. Transl. Res. 2023, doi:10.1007/s13346-023-01474-w.
31. Berben, P.; Bauer-Brandl, A.; Brandl, M.; Faller, B.; Flaten, G.E.; Jacobsen, A.-C.; Brouwers, J.; Augustijns, P. Drug Permeability Profiling Using Cell-Free Permeation Tools: Overview and Applications. Eur. J. Pharm. Sci. 2018, 119, 219–233, doi:10.1016/j.ejps.2018.04.016.

32. Selzer, D.; Abdel-Mottaleb, M.M.A.; Hahn, T.; Schaefer, U.F.; Neumann, D. Finite and Infinite Dosing: Difficulties in Measurements, Evaluations and Predictions. Adv. Drug Deliv. Rev. 2013, 65, 278–294, doi:10.1016/j.addr.2012.06.010.
33. Sosnik, A. Tissue-Based in Vitro and Ex Vivo Models for Nasal Permeability Studies. In Concepts and Models for Drug Permeability Studies; Elsevier, 2016; pp. 237–254 ISBN 978-0-08-100094-6.
34. Nicolazzo, J.A.; Reed, B.L.; Finnin, B.C. The Effect of Various In Vitro Conditions on the Permeability Characteristics of the Buccal Mucosa. J. Pharm. Sci. 2003, 92, 2399–2410, doi:10.1002/jps.10505.
35. Gerber, W.; Svitina, H.; Steyn, D.; Peterson, B.; Kotzé, A.; Weldon, C.; Hamman, J.H. Comparison of RPMI 2650 Cell Layers and Excised Sheep Nasal Epithelial Tissues in Terms of Nasal Drug Delivery and Immunocytochemistry Properties. J. Pharmacol. Toxicol. Methods 2022, 113, 107131, doi:10.1016/j.vascn.2021.107131.
36. Gonçalves, V.S.S.; Matias, A.A.; Poejo, J.; Serra, A.T.; Duarte, C.M.M. Application of RPMI 2650 as a Cell Model to Evaluate Solid Formulations for Intranasal Delivery of Drugs. Int. J. Pharm. 2016, 515, 1–10, doi:10.1016/j.ijpharm.2016.09.086.
37. Deruyver, L.; Rigaut, C.; Gomez-Perez, A.; Lambert, P.; Haut, B.; Goole, J. In Vitro Evaluation of Paliperidone Palmitate Loaded Cubosomes Effective for Nasal-to-Brain Delivery. Int. J. Nanomedicine 2023, Volume 18, 1085–1106, doi:10.2147/IJN.S397650.
38. Ren, C.; Fang, L.; Li, T.; Wang, M.; Zhao, L.; He, Z. Effect of Permeation Enhancers and Organic Acids on the Skin Permeation of Indapamide. Int. J. Pharm. 2008, 350, 43–47, doi:10.1016/j.ijpharm.2007.08.020.
39. Gänger, S.; Schindowski, K. Tailoring Formulations for Intranasal Nose-to-Brain Delivery: A Review on Architecture, Physico-Chemical Characteristics and Mucociliary Clearance of the Nasal Olfactory Mucosa. Pharmaceutics 2018, 10, 116, doi:10.3390/pharmaceutics10030116.
40. Anand, U.; Parikh, A.; Ugwu, M.C.; Agu, R.U. Drug Transporters in the Nasal Epithelium: An Overview of Strategies in Targeted Drug Delivery. Future Med. Chem. 2014, 6, 1381–1397, doi:10.4155/fmc.14.77.
41. Wengst, A.; Reichl, S. RPMI 2650 Epithelial Model and Three-Dimensional Reconstructed Human Nasal Mucosa as in Vitro Models for Nasal Permeation Studies. Eur. J. Pharm. Biopharm. 2010, 74, 290–297, doi:10.1016/j.ejpb.2009.08.008.

42. Wadell, C.; Björk, E.; Camber, O. Nasal Drug Delivery – Evaluation of an in Vitro Model Using Porcine Nasal Mucosa. Eur. J. Pharm. Sci. 1999, 7, 197–206, doi:10.1016/S0928-0987(98)00023-2.
43. Corbo, D.C.; Liu, J.-C.; Chien, Y.W. Characterization of the Barrier Properties of Mucosal Membranes. J. Pharm. Sci. 1990, 79, 202–206, doi:10.1002/jps.2600790304.
44. Ghadiri, M.; Canney, F.; Pacciana, C.; Colombo, G.; Young, P.M.; Traini, D. The Use of Fatty Acids as Absorption Enhancer for Pulmonary Drug Delivery. Int. J. Pharm. 2018, 541, 93–100, doi:10.1016/j.ijpharm.2018.02.027.
45. Katdare, A.; Thakkar, S.; Dhepale, S.; Khunt, D.; Misra, M. Fatty Acids as Essential Adjuvants to Treat Various Ailments and Their Role in Drug Delivery: A Review. Nutrition 2019, 65, 138–157, doi:10.1016/j.nut.2019.03.008.
46. Lemmer, H.J.; Hamman, J.H. Paracellular Drug Absorption Enhancement through Tight Junction Modulation. Expert Opin. Drug Deliv. 2013, 10, 103–114, doi:10.1517/17425247.2013.745509.
47. Srinivasan, B.; Kolli, A.R.; Esch, M.B.; Abaci, H.E.; Shuler, M.L.; Hickman, J.J. TEER Measurement Techniques for In Vitro Barrier Model Systems. SLAS Technol. 2015, 20, 107–126, doi:10.1177/2211068214561025.
48. Chen-Quay, S.; Eiting, K.T.; Li, A.W. -A.; Lamharzi, N.; Quay, S.C. Identification of Tight Junction Modulating Lipids. J. Pharm. Sci. 2009, 98, 606–619, doi:10.1002/jps.21462.
49. Raknam, P.; Balekar, N.; Teanpaisan, R.; Amnuaikit, T. Thermoresponsive Sol–Gel Containing Probiotic's Cell Free Supernatant for Dental Caries Prophylaxis. J. Oral Microbiol. 2022, 14, 2012390, doi:10.1080/20002297.2021.2012390.
50. Vitali, B.; Abruzzo, A.; Parolin, C.; Palomino, R.A.Ñ.; Dalena, F.; Bigucci, F.; Cerchiara, T.; Luppi, B. Association of Lactobacillus Crispatus with Fructo-Oligosaccharides and Ascorbic Acid in Hydroxypropyl Methylcellulose Vaginal Insert. Carbohydr. Polym. 2016, 136, 1161–1169, doi:10.1016/j.carbpol.2015.10.035.

4. Conclusions and final considerations

The achievements reported in this Ph.D. thesis represent a contribution to the current research in nasal drug delivery. On the one end, they provide relevant insights concerning strategies to address the main downsides of this alternative route of administration, always keeping an eye on the attributes of excipients, namely safety, natural origin, and sustainable production. On the other end, they prove the usefulness of *in vitro* tools during permeation studies in the early stages of the drug development process, when screening procedures and understanding of the underlying transport mechanisms are required.

Paper I describes the utility of the biosurfactant (BS) produced by the human *Lactobacillus gasseri* strain BC9 (BC9-BS) as an excipient for improving the intranasal delivery of hydrocortisone (HC). The BC9-BS shows attributes that are common to some well-established surfactants, but what makes it an attractive pharmaceutical aid is its bacterial origin. Therefore, it is a natural molecule obtainable from renewable resources. Moreover, at the concentration half of its critical micellar concentration, the BC9-BS alone can improve both the solubility and the apparent permeability of HC, and interact with the mucus layer covering the nasal epithelium. To get a broader view of the applicability of this BS, it would be of great interest to investigate its enhancing properties also towards molecules that differ from HC in terms of lipophilicity and molecular weight. Besides, it must be underlined that microbial biosurfactants will not be easily introduced in the drug delivery field unless their yield of production is improved. Based on the promising results that have been obtained, it is worth trying to tackle this issue by modifying the bacteria culturing conditions (e.g. substrates of growth), designing new protocols for the isolation of both the cell-free and the cell-bound fraction of BS, or editing the bacteria genome to get higher yields.

Paper II, instead, illustrates the possibility of addressing solubility and nasal permeability issues with poloxamer-based *in situ* gelling systems rather than with permeation enhancer molecules. Apart from exploiting the poloxamers' micelles to increase the apparent solubility of carbamazepine (CBZ), the main topic is the influence of gelling formulations and mucoadhesive polymers on intranasal and nose-to-brain permeation of the antiepileptic drug. Thermoresponsive gelling vehicles have the inherent ability to increase their viscosity upon administration in the nasal cavity, thus slowing down mucociliary clearance, which ultimately results in the absorption of a higher amount of drug. Furthermore, the inclusion of a bioadhesive polymer, such as hydroxypropylmethylcellulose, strengthens the interaction between the *in situ* gelling vehicle and the nasal mucosa, hence prolonging the contact time. However, this is not the only implication. The optimization of the cell-free biomimetic model

PermeaPad® with a layer of reconstituted mucin, which is used to mimic as closely as possible the *in vivo* conditions, highlights that the perturbation of the mucus layer operated by the adhesive polymer improves CBZ diffusion as well. This is particularly interesting since the absorption of lipophilic molecules is mainly hampered by the presence of the hydrophilic gel layer of mucus rather than by the epithelium. The thermosensitive and mucoadhesive *in situ* gelling system developed shows all the properties required for the intranasal and nose-to-brain delivery of CBZ, but its applicability should be also demonstrated in *in vivo* models. Alongside, given that it is obtained through a straightforward procedure and since, in theory, it should be suitable for both hydrophilic and lipophilic molecules, it would be useful to test whether it can be exploited as a platform for the delivery of different local, systemic or central nervous system acting drugs.

Lastly, Paper III is a proof-of-concept study, that demonstrates the involvement of microbial metabolites, in the form of liquid cell-free supernatants (CFS), in drug diffusion across the olfactory nasal mucosa. The permeation-enhancing effect of the CFS obtained from three human *Lactobacillus* spp. is verified through diffusion studies of fluorescein sodium salt across the cell-free model PermeaPad®, the non-living porcine tissue, and the porcine olfactory epithelial primary cells. The results collected confirm the usefulness of these *in vitro* models of the olfactory mucosa as substitutes for human tissue and point out the ability of each model to provide slightly different insights depending on their composition. Despite their different architecture and constituents, the barrier models reveal that the CFS obtained from the fermentation of *Lactobacillus crispatus* BC5 (BC5-CFS) is the best-performing molecular enhancer. Based on the conducted investigations, the improved paracellular permeability of the fluorescent tracer is attributed to the superior capability of BC5-CFS to interact with and potentially disturb lipids within *in vitro* membranes. Like Paper I, also this study ends up identifying an innovative excipient bearing the qualities (natural and green) to suit the current pharmaceutical goal, i.e. the development of less pollutant medicinal products. Nevertheless, some aspects might be further explored. First, the immunoreactivity of the nasal-associated lymphoid tissue against the complex composition of CFS and a deeper understanding of the kind of interactions that occur between the microbial metabolites and lipids. Second, it would be of great relevance to investigate whether the CFS activity is only limited to small hydrophilic molecules and whether they can be included in more complex pharmaceutical dosage forms.